

**Microencapsulation of isocyanate compounds for  
autoreactive, monocomponent adhesive**

**Mahboobeh Attaei**

Thesis to obtain the Master of Science Degree in

**Materials Engineering**

Supervisor: Prof. Ana Clara Lopes Marques

**Examination Committee**

Chairperson: Prof. José Paulo Sequeira Farinha

Supervisor: Prof. Ana Clara Lopes Marques

Member of the Committee: Prof. Henrique Anibal Santos de Matos

Member of the Committee: Eng. Isabel Pinho Lima

**November 2017**

To my husband Dr. Eshagh Movahed

## **Acknowledgements**

This thesis has been a valuable experience for me because of the opportunity to work with valuable persons, who transferred their knowledge, gave their endless support, helped to do this work, and I would like to acknowledge them here.

First of all, I would like to thank Instituto Superior Técnico (IST) and Professor João Bordado for the laboratory facilities.

I would like to express a deep sense of gratitude towards my supervisor Prof. Ana Clara Lopes Marques, for giving me this opportunity, for valuable ideas, for technical discussions and for availability all the time to answer my questions.

I wish to express my warmest thank to my colleagues at IST, namely Mónica Loureiro, Mário Vale, José Condeço and David Duarte for helping me in the characterization of microcapsules (MCs) and for their availability to answering my questions and for all their kind support.

I am thankful to Eng. Isabel Pinho from CIPADE's for kindly providing primary materials and information related to those materials and their hospitality during my visit to the company.

This thesis is dedicated to my husband, Dr. Eshagh Movahed, for his constant support throughout my master study, it was not easy, I know! Thank you for your patience and understanding, for supporting my choices and for always being there for me when I needed. I couldn't have made this far without you by my side.

Mahboobeh Attaei

## Table of contents

Acknowledgements .....	iii
Abstract .....	i
Resumo .....	ii
Figure index .....	iii
Table index.....	vi
List of Abbreviations .....	viii
1 Introduction .....	1
1.1 Motivation .....	1
1.2 Thesis Outline .....	1
1.3 Isocyanate based adhesives .....	2
1.3.1 Isocyanate health risks .....	3
1.3.2 Chemistry of isocyanate and its chemical reactions .....	4
1.4 Microencapsulation.....	9
1.4.1 Definition and classification of microcapsules.....	9
1.4.2 Purpose of encapsulation.....	11
1.4.3 Microencapsulation techniques .....	12
1.4.4 State of the art on isocyanate microencapsulation .....	19
2. Microemulsion and interfacial polymerization as a strategy for this work .....	21
2.1 Emulsion formation.....	22
2.2 Microcapsules' shell formation .....	23
2.3 Microcapsules washing, collecting and drying .....	24
2.4 Factors affecting microcapsules formation .....	24
2.4.1 Factors related to primary materials .....	24
2.4.2 Factors related to synthesis parameters .....	27
2.4.3 Factors affecting microcapsules size.....	28
3 Experimental Part.....	29
3.1 Primary materials.....	29
3.2 General steps to perform the syntheses.....	34
3.3 Testing and characterization.....	36
3.3.1 Physical testing and characterization .....	36
3.3.2 Chemical testing and characterization .....	38
4 Main studies: Results and discussion.....	38
4.1 Study of the synthesis parameters .....	38
4.1.1 Effect of concentration of surfactant on the droplets' size and emulsion stability.....	40
4.1.2 Effect of variation of emulsification speed in the droplets' size .....	41
4.1.3 Effect of changing the synthesis temperature in the duration of the synthesis and efficiency of encapsulation .....	42
4.1.4 Effect of variation of mechanical stirring rate on the encapsulation efficiency .....	46
4.2 History of the syntheses .....	48

4.2.1 Group 1.....	48
4.2.2 Group 2.....	50
4.2.3 Group 3.....	56
4.2.4 Group 4.....	59
4.2.5 Group 5&6 .....	62
4.2.6 Groups 7, 8, 9, 10 .....	66
4.2.7 Group 11.....	68
4.3 Peeling strength test .....	73
5 Summary and main conclusions .....	76
5.1 Main Conclusions .....	77
5.1.1 Conclusions related to primary materials .....	77
5.1.2 Conclusions related to physical parameters of synthesis .....	78
5.2 Future work .....	78
Bibliography .....	80
Appendix A-FTIR spectra .....	85
Appendix B-History of the syntheses .....	89
Appendix C-Quantitative information of the syntheses .....	89

## Abstract

The objective of this thesis is the microencapsulation of isocyanate based adhesive material used in footwear industries with the idea of reducing the risk of handling of toxic isocyanate. The interfacial polymerization method was the one selected to produce microcapsules (MCs), with a shell of polyurea (PUa) and/or polyurethane (PU) and containing in their core different isocyanate compounds e.g. isophorone diisocyanate (IPDI), toluene diisocyanate (TDI) and mixtures of monomeric and polymeric species of methylene diphenyl diisocyanate (MDI).

In this work, a general processing method was carried out by: i) formation of an oil-in-water emulsion; ii) formation of PU and/or PUa shell at the interface of the oil-water domains; iii) filtration and washing of MCs to remove the excess of reactants; iv) drying at room temperature (RT).

Fourier transformed infrared spectroscopy (FTIR) and thermogravimetric analysis (TGA) were employed to characterize the MCs in what concerns the presence of free -NCO groups and, therefore, the successful encapsulation of isocyanate compounds. Scanning electron microscopy (SEM) was used to study the morphology of the MCs, i.e. to check if they exhibit a core-shell structure.

Several studies were carried out for understanding the effect of changing the synthesis' parameters e.g., temperature, emulsification rate, stirring rate and quantity of surfactant, on the shape, size and encapsulation efficiency of isocyanate compounds. Moreover, a series of reagents and polymers were added to the syntheses with the objective of changing the morphology and properties of the MCs shell. Finally, peeling strength tests were carried out at different conditions of temperature and pressure, to study the interaction of MCs with the polyol-based component and the MCs behaviour, in terms of isocyanate release.

**Keywords:** Microencapsulation; Interfacial polymerization; Adhesive material; Isocyanate

## Resumo

O objetivo da presente tese é a microencapsulação de compostos à base de isocianato para adesivos a utilizar na indústria do calçado, com o propósito de reduzir o risco associado ao manuseamento de isocianato. O método de polimerização interfacial foi o selecionado para a síntese de microcápsulas (MCs) com parede de poliureia (PUa) e/ou poliuretano (PU), contendo no seu interior diferentes tipos de isocianatos, como por exemplo isoforona de diisocianato (IPDI), diisocianato de tolueno (TDI) e misturas de espécies monoméricas e poliméricas de diisocianato de difenil metano (MDI).

No decorrer deste trabalho foi desenvolvido um método de processamento das MCs com as seguintes etapas: i) formação de uma emulsão óleo em água; ii) formação de uma parede de PU e/ou PUa na interface dos domínios óleo-água; iii) filtração e lavagem das MCs de modo a remover o excesso de reagentes; iv) secagem a temperatura ambiente (RT).

As técnicas de espectroscopia no infravermelho por transformada de Fourier (FTIR) e análise termogravimétrica (TGA) foram utilizadas para caracterizar as MCs no que respeita à presença de grupos –NCO livres e, deste modo, confirmar o sucesso da encapsulação das espécies de isocianato. A técnica de microscopia eletrónica de varrimento (SEM) foi utilizada para estudar a morfologia das MCs, i.e. confirmar se estas têm uma estrutura mono-nucleada (“*core-shell*”).

Foram realizados diversos estudos de modo a perceber o efeito dos diversos parâmetros de síntese, como por exemplo a temperatura, taxa de agitação e quantidade de tensioactivo na forma e tamanho das MCs e na eficiência de encapsulação de espécies de isocianato. Ainda, vários reagentes e polímeros foram adicionados à síntese com o objetivo de modificar a sua morfologia, espessura e propriedades da parede. Por fim, foram realizados testes de resistência à delaminação (“*peeling*”) a diferentes condições de temperatura e pressão, com o objetivo de estudar a interação das MCs com o componente à base de polioliol, assim como o comportamento das MCs no que respeita à libertação de isocianato.

**Palavras-Chave:** Microencapsulação; Polimerização interfacial; Material adesivo; Isocianato

## Figure index

Figure 1.1 Mechanism of typical covalent bond between the PU adhesive and a polar substrate (adapted from (Paiva, 2015)) .....	3
Figure 1.2 Reaction of isocyanate with water, amine and OH group (Kaushiva, 1999) .....	4
Figure 1.3 Resonance in Isocyanate (Zafar, 2012) .....	5
Figure 1.4 Resonance in aromatic Isocyanate (Zafar, 2012) .....	5
Figure 1.5 Primary addition reactions of isocyanate with (a) amine, (b) water, .....	6
Figure 1.6 Secondary addition reactions of isocyanate with .....	7
Figure 1.7 Self-addition reactions of isocyanate (Zafar, 2012).....	7
Figure 1.8 Isocyanate reaction in the absence of a catalyst (Zafar, 2012) .....	8
Figure 1.9 Tertiary amine catalysed reaction (Zafar, 2012) .....	8
Figure 1.10 Metal salts catalysed reaction (Zafar, 2012) .....	9
Figure 1.11 Types of MCs (Silva, 2014).....	10
Figure 1.12 Principal release mechanism of MCs ( Hu , 2017) .....	11
Figure 1.13 New adhesives with improved properties, obtained by microencapsulation technology (adapted from ( Aranais, 2012)) .....	12
Figure 1.14 Major methods of microencapsulation (adapted from (Loureiro, 2016)) .....	13
Figure 1.15 Micro TEE (Li, 2011) .....	14
Figure 1.16 Microfluid device (Polenz, 2014) .....	14
Figure 1.17 Pressure versus temperature phase diagram for pure substances (Silva, 2014) .....	14
Figure 1.18 Simplified scheme of the anti-solvent technique ( Silva, 2014) .....	15
Figure 1.19 Schematic representation of microencapsulation by solvent evaporation technique ( Dubey, 2009) .....	18
Figure 1.20 Schematic representation of direct encapsulation routes of aqueous glycerol in silica MCs (adapted from (Marques, 2017)) .....	18
Figure 2.1 General scheme of the interfacial polymerization and some possible reactions (adapted from (Latnikova, 2012)).....	22
Figure 2.2 Schematic representation of surfactant molecule (Som, 2012) .....	23
Figure 2.3 Molecular structure of a) DETA, b) EDA, c) 0.0 G PAMAM, d) TETA .....	25
Figure 2.4 Particle size and size distribution of PUa MCs from different amines (a) DETA, (b) TETA, and (c) PAMAM (Tatiya, 2016) .....	26
Figure 2.5 General steps of microencapsulation of an organic phase by interfacial polymerization .....	29
Figure 3.1 Schematic representation of synthesis, (adapted (Tatiya, 2016)) .....	35
Figure 3.2 Different steps of MCs preparation in laboratory a) 1st step, b) 2nd step, c) 3rd step, d) 4th step, e) 5th step .....	35



Figure 3.3 Optical microscopy image (a) in the early stage of the emulsion formation, (b) after 1 hour of mechanical stirring; the shell has already been formed, but it is still a thin and fragile polymeric layer, (c) MCs right after filtration (d) Image from Canon camera, MCs right after filtration, (e) SEM image of MC's broken shell, exhibiting a core-shell morphology .....36

Figure 3.4 Failure types of adhesive joints, (adapted from <http://theadhesivesexpt.com>,22/8/2017) ...37

Figure 4.1 Schematic representation of the varied synthesis parameters, considering the different studies involved. ....39

Figure 4.2 a) Instability in emulsion (droplet coalescence), after 3 mins of high shear stirring, using surfactant Tween -20 b) Droplet coalescence formed after 5 mins of high shear stirring, using surfactant DC 193. ....40

Figure 4.3 Effect of changing the emulsification rate on the size of droplets a) 3200 rpm, b) 5000 rpm, c) 7200 rpm, d) 9000 rpm .....42

Figure 4.4 SEM photomicrograph, IP-130, Scalebar=100µm .....43

Figure 4.5 SEM photomicrograph, IP-64, Scalebar=100µm .....44

Figure 4.6 SEM photomicrograph, IP-64 Scalebar=10µm .....44

Figure 4.7 SEM photomicrograph, IP-73, Scalebar=100µm .....44

Figure 4.8 SEM photomicrograph, IP-73, Scalebar=10µm .....44

Figure 4.9 SEM photomicrograph, IP-126, Scalebar=100µm .....44

Figure 4.10 SEM photomicrograph, IP-126, Scalebar=10µm .....44

Figure 4.11 Typical FTIR spectrum of the MCs developed, showing the peaks involved in the area calculation for the relative encapsulation yield (Y) determination. ....45

Figure 4.12 SEM photomicrograph, IP-73, Scalebar=10µm .....46

Figure 4.13 SEM photomicrograph, IP-121, Scalebar=100µm .....47

Figure 4.14 SEM photomicrograph, IP-121, Scalebar=10µm .....47

Figure 4.15 SEM photomicrograph, IP-74, Scalebar=100µm .....47

Figure 4.16 SEM photomicrograph, IP-123, Scalebar=100µm .....47

Figure 4.17 SEM photomicrograph, IP-123, Scalebar=10µm .....47

Figure 4.18 SEM photomicrograph of IP-27, Scalebar=100µm .....49

Figure 4.19 SEM photomicrograph of IP-33, Scalebar=100µm .....49

Figure 4.20 SEM photomicrograph of IP-33, Scalebar=100µm .....49

Figure 4.21 SEM photomicrograph of IP-64, Scalebar=100µm .....51

Figure 4.22 SEM photomicrograph of IP-64 Scalebar=10µm .....51

Figure 4.23 Optical microscope image a) MCs before tearing of shell by needle, b) The same image after breaking the shell .....51

Figure 4.24 SEM photomicrograph of IP-66, Scalebar=100µm .....52

Figure 4.25 SEM photomicrograph of IP-66, Scalebar=10µm .....52

Figure 4.26 TGA for IP-64 & IP-66 .....54

Figure 4.27 SEM photomicrograph of IP-67, Scalebar=100µm.....	56
Figure 4.28 SEM photomicrograph of IP-67, Scalebar=10µm.....	56
Figure 4.29 SEM photomicrograph of IP-67, Scalebar=10µm.....	57
Figure 4.30 TGA for IP-67 .....	57
Figure 4.31 SEM photomicrograph of IP-83, Scalebar=100µm.....	60
Figure 4.32 SEM photomicrograph of IP-83, Scalebar=10µm.....	60
Figure 4.33 SEM photomicrograph of IP-84, Scalebar=10µm.....	60
Figure 4.34 SEM photomicrograph of IP-84, Scalebar=10µm.....	60
Figure 4.35 SEM photomicrograph of IP-84, Scalebar=10µm.....	60
Figure 4.36 TGA for IP-84 .....	61
Figure 4.37 SEM photomicrograph of IP-102, Scalebar=100µm .....	64
Figure 4.38 SEM photomicrograph of IP-102, Scalebar=10µm.....	64
Figure 4.39 SEM photomicrograph of IP-91, Scalebar=100µm.....	64
Figure 4.40 SEM photomicrograph of IP-91, Scalebar=10µm.....	64
Figure 4.41 SEM photomicrograph of IP-114, Scalebar=100µm.....	65
Figure 4.42 SEM photomicrograph of IP-114, Scalebar=10µm.....	65
Figure 4.43 TGA for IP-113 .....	67
Figure 4.44 SEM photomicrograph of IP-90, Scalebar=100µm.....	70
Figure 4.45 SEM photomicrograph of IP-90, Scalebar=10µm.....	70
Figure 4.46 SEM photomicrograph of IP-88, Scalebar=100µm.....	70
Figure 4.47 SEM photomicrograph of IP-88, Scalebar=10µm.....	70
Figure 4.48 SEM photomicrograph of IP-112, Scalebar=100µm.....	70
Figure 4.49 SEM photomicrograph of IP-112, Scalebar=10µm.....	70
Figure 4.50 SEM photomicrograph of IP-109, Scalebar=100µm.....	71
Figure 4.51 SEM photomicrograph of IP-109, Scalebar=10µm.....	71
Figure 4.52 SEM photomicrograph of IP-119, Scalebar=100µm.....	71
Figure 4.53 SEM photomicrograph of IP-119, Scalebar=10µm.....	71
Figure 4.54 Addition of MCs to the polyol based component.....	73
Figure 4.55 Step (ii) of peeling strength test .....	73
Figure 4.56 Steps (iii) & (iv) of peeling strength test.....	74
Figure 4.57 Step (vii) of peeling strength test, exhibiting mostly a structural type of failure of the adhesive joint .....	74

## Table index

Table 1.1 The chemical groups with active hydrogen atoms that can react with isocyanates (adapted from (Langenberg, 2010)) .....	2
Table 3.1 List of primary materials used in this work.....	30
Table 3.2 List of isocyanate sources used in this work .....	31
Table 3.3 List of surfactants used in this work.....	32
Table 3.4 List of active hydrogen sources used in this work .....	33
Table 3.5 List of solvents used in this work .....	34
Table 4.1 Effect of GA concentration on the stability of the emulsion and size of droplets .....	40
Table 4.2 Variation of droplets size for different rotation speed in the emulsification process .....	41
Table 4.3 Variation of synthesis time due to temperature change .....	43
Table 4.4 Summary of results, due to stirring speed changing .....	46
Table 4.5 Selected syntheses from group 1 .....	48
Table 4.6 Group 1, summary of results .....	50
Table 4.7 Primary materials used in the best syntheses of group 2 .....	51
Table 4.8 Some of the temperature ranges and related phenomena, for TGA analyses .....	53
Table 4.9 TGA results for IP-66 .....	54
Table 4.10 TGA results for IP-64 .....	55
Table 4.11 Group 2, summary of results .....	55
Table 4.12 Primary material used in the best synthesis of group 3 .....	56
Table 4.13 Summary of TGA results for IP-67 .....	58
Table 4.14 Summary of synthesis results for IP-67 .....	58
Table 4.15 Primary material used in the best synthesis of group 4.....	59
Table 4.16 Summary of TGA results for IP-84 .....	61
Table 4.17 Summary of characterization results for IP-83 & IP-84.....	62
Table 4.18 Primary materials used in the selected syntheses of group 5&6 .....	63
Table 4.19 Summary of characterization results for Group 5&6 .....	63
Table 4.20 Primary materials used in syntheses of groups 7, 8, 9, 10 .....	66
Table 4.21 Summary of characterization results for the selected MCs from Groups 7, 8, 9, 10 .....	67
Table 4.22-Summary of TGA results for IP-113.....	67
Table 4.23 Primary materials used in the best syntheses of group 11 .....	69
Table 4.24 Summary of characterization results for Group 11.....	72
Table 4.25 Peeling strength test parameters and relative results (type of failure) .....	75

Table 5.1 The best syntheses, according to the relative encapsulation yields achieved .....	77
Table 5.2 The best combination of active hydrogen source and solvent for each isocyanate compound in this work.....	78

## List of Abbreviations

DCM	Dichloromethane
DETA	Diethylenetriamine
DSC	Differential Scanning Calorimetry
DMF	Dimethylformamide
EDA	Ethylenediamine
FTIR	Fourier Transformed Infrared Spectra
GA	Gum Arabic
HLB	Hydrophilic-Lipophilic Balance
IPDI	Isophorone Diisocyanate
MCs	Microcapsules
MDI	Methylene Diphenyl Diisocyanate
MEK	Methyl Ethyl Ketone
Ongronat	Ongronat 2500
PA	Polyamide
PUa	Polyurea
PU	Polyurethane
RT	Room Temperature
SEM	Scanning Electron Microscopy
SCF	Supercritical Fluid
TDI	Toluene diisocyanate
TEOS	Tetraethyl Orthosilicate
TETA	Triethylenetetramine
TGA	Thermogravimetric Analysis
TPI	3-(Triethoxysilyl) propyl isocyanate
Y	Relative encapsulation yield

# 1 Introduction

## 1.1 Motivation

High quality, strong and long-lasting adhesives used in the footwear, automobile and aerospace industries are typically isocyanate-based to provide high strength joints. These adhesives are supplied in two components, one being isocyanate and the other being polyol based, to be mixed at the certain proportion by the user. High toxicity of isocyanate-based compound is restricting their use in the industry, based on current legislation. Companies in the adhesive sector, are therefore willing to offer a safe adhesive solution to these industries, but still based on isocyanate chemistry due to its high adhesive efficiency (ECOBOND, 2016).

This thesis was carried out in the framework of a project from Portugal 2020, named ECOBOND (started in 2016) whose Co-promoters are Instituto Superior Técnico, Instituto Politécnico do Cávado e Ave and CIPADE– Industry and Research of Adhesive Products, S.A. The goal of this project is the development of new monocomponent, eco-friendly and highly effective adhesive material by encapsulation of isocyanate and its addition to the polyol based component of glue.

The current thesis was defined as a part of the effort to encapsulate different chemical compounds of isocyanate by micro emulsion technique, combined with interfacial polymerization. New developed MCs will contain isocyanate which is covered by the thin layer of PU and/or PUa to protect the isocyanate from reaction with surrounded (polyol rich) environment and to protect the user from the toxicity of isocyanate compounds. Current commercial adhesives are bicomponent (2K), i.e. they are composed by two components, an adhesive and a crosslinker. The encapsulation of isocyanate (crosslinker) enables the production of one component adhesive (1K), an advancement in the adhesive technology and an improvement in the productivity and quality of the footwear industry in Portugal, and other relevant industries (ECOBOND, 2016; Paiva, 2015).

## 1.2 Thesis Outline

Chapter 1 of this dissertation includes introductory notes on isocyanate based adhesives, isocyanate risks and related chemistry, as well as on microencapsulation aspects, including a description of the state of art on isocyanate microencapsulation. Chapter 2 describes the strategy employed in this Master work and the factors affecting MCs formation. In Chapter 3, Experimental Part, primary materials used in this work are introduced and explained, followed by the description of the general procedure used for synthesizing the MCs and the testing and characterization methods, which were employed to evaluate the MCs properties. Chapter 4 regards the results from the main studies carried out during this work and corresponding discussion. The results of systematic studies related to synthesis parameters are reported. Also, the most important syntheses are classified into several groups, according to primary materials

employed, and their results are discussed. Finally, results obtained from peeling strength tests are reported at the end of this chapter. This is an on-going activity and only the first set of results, from some of the samples with best encapsulation yield, will be presented in this dissertation. Chapter 5, the last one, includes the main conclusions achieved and future work perspectives.

### 1.3 Isocyanate based adhesives

An adhesive material is formulated by mixing different kind of chemical compounds such as polymers, reactive monomers, solvents, catalysts, etc. These chemical compounds, their formulation and their quantity determine the final specific properties of adhesives and allow designing adhesives with the suitable properties for the target applications (Aranais, 2012).

Isocyanate based adhesives have been used for over 60 years since their discovery by Bayer in the late 1930s. They belong to PU family which is a polymer characterized by having an urethane interunit linkage in its chain. The formation of PUs occurs by the reaction of polyisocyanate (having NCO groups) with polyol (having OH groups). The isocyanate chemical group is extremely reactive and can form a chemical bond with any chemical group that contains an active hydrogen atom. Table 1.1 lists some of the functional chemical groups which can react with –NCO groups (Langenberg, 2010).

Table 1.1 The chemical groups with active hydrogen atoms that can react with isocyanates (adapted from (Langenberg, 2010))

Active Hydrogen Compound	Typical Structure
Aliphatic amine	R-NH <sub>2</sub>
Secondary aliphatic amine	R <sub>2</sub> -NH
Primary aromatic amine	Ar-NH <sub>2</sub>
Primary hydroxyl	R-CH <sub>2</sub> OH
Water	H-O-H
Carboxylic acid	R-CO <sub>2</sub> H
Secondary hydroxyl	R <sub>2</sub> CH-OH
Urea proton	R-NH-CO-NH-R
Tertiary hydroxyl	R <sub>3</sub> C-OH
Urethane proton	R-NH-CO-OR
Amide	R-CO-NH <sub>2</sub>

Moreover, isocyanates are very soluble in many solvents, due to their low molecular weight, and they can easily wet and penetrate inside the porous structures to form strong mechanical interlocks, following by the formation of covalent bonds with substrates that have active hydrogen atoms on the surface, so these features make them excellent for adhesives Figure 1.1 (Paiva, 2015).

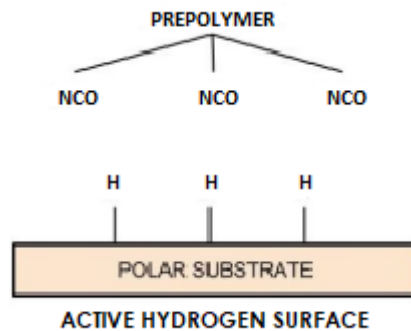


Figure 1.1 Mechanism of typical covalent bond between the PU adhesive and a polar substrate (adapted from (Paiva, 2015))

Generally, isocyanate compounds with two NCO groups per molecule are used to produce isocyanate-based adhesives. The two most important diisocyanates are methylene diphenyl diisocyanate (MDI) and toluene diisocyanate (TDI) and their reaction with polyols can lead to a large number of adhesive systems and a large number of possible formulations, according to chemical reactivity of isocyanate group (Langenberg, 2010). Considerable interest to employ isocyanate based adhesives is justified by very fast curing at significantly low temperature, which allows high productivity. The high strength of isocyanate-based adhesives, can reduce the product rejection rate by increasing the quality. Also, high temperature resistance of isocyanate based adhesives can increase the product durability (Paiva, 2015; Langenberg, 2010; Loureiro, 2016; Serineu, 2014).

### 1.3.1 Isocyanate health risks

There are several potential occupational health risks and safety issues in using isocyanate-based adhesives, due to exposure to isocyanate which, like other chemicals, can be divided in four different mechanisms:

1. Inhalation via dust, aerosols or gas vapours
2. Ingestion via the mouth
3. Absorption through the skin
4. Implantation through punctured skin such as cuts

**Inhalation:** Isocyanates can be considered as a highly irritant chemical, which affects badly the respiratory tract in relatively high concentrations. Some people may become sensitised to isocyanates, even at



very low levels. This sensitization may cause the development of asthma-like symptoms such as coughing, wheezing, chest tightness and breath shortness. These attacks can occur several hours after being exposed. Asthmatic people have more tendency to sensitisation and workers with a history of asthma should not be exposed to isocyanates.

**Skin:** Isocyanates are skin irritants. Sensitization might occur after repeated or long-time contact with MDI or TDI.

**Eyes:** Isocyanates are irritants to the eyes. Splashes of MDI or TDI can cause severe chemical conjunctivitis.

Other health effects that have been reported include liver and kidney dysfunction ( Langenberg, 2010). However, it is possible to reduce significantly the risks by minimizing exposure to isocyanate, usually by

- Elimination or substitution and process modification to eliminate or reduce the need to use isocyanate;
- Application of isocyanate in an enclosed environment with good ventilation to ensure that atmospheric concentrations are maintained at low level of exposure;
- Employment of policies and procedures for the safe handling and use of isocyanates;
- Wearing personal protective equipment when handling isocyanate;

Isocyanate microencapsulation appears as a new strategy to avoid its direct contact, and therefore the associated risks.

### 1.3.2 Chemistry of isocyanate and its chemical reactions

Microencapsulation of isocyanate compounds occurs by formation of PUa or PU shell due to reaction of isocyanate with water or polyol respectively i.e. the reaction of NCO groups with water to form an amine, reaction with an amine group to form urea and reaction with -OH groups to form urethane as it shown in Figure 1.2. (Gogoi, 2014; Kaushiva, 1999)

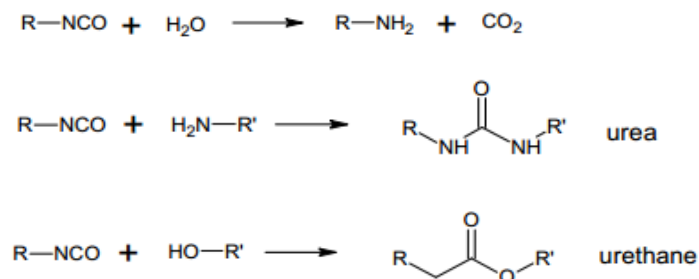


Figure 1.2 Reaction of isocyanate with water, amine and OH group (Kaushiva, 1999)

The isocyanate group possesses cumulated double bond  $R-N=C=O$ , where the positive character of the carbon atom controls the reactivity of isocyanate, so it has tendency to be attacked by nucleophiles, and oxygen and nitrogen by electrophiles, as shown in Figure 1.3. If R is an aromatic group, the negative charge gets delocalized into R, as shown in Figure 1.4, so, the aromatic isocyanates are more reactive, than the aliphatic ones. In case of aromatic isocyanates, the nature of the substituent also affects the reactivity, i.e., electron attracting substituents in ortho or para position increase the reactivity and electron donating substituents lower the reactivity of isocyanate group. In diisocyanates, the presence of the electron attracting second isocyanate increases the reactivity of the first isocyanate, Para substituted aromatic diisocyanates are more reactive than their ortho analogues. The reactivities of the two -NCO groups in isocyanate compounds also differ with respect to each other, depending on the position of -NCO groups. For example, the two -NCO groups in isophorone diisocyanate (IPDI) differ in their reactivity due to the difference in the point of location of -NCO groups (Bayer, 2005; Gogoi, 2014; Zafar, 2012).

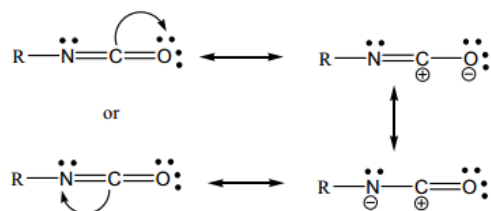


Figure 1.3 Resonance in Isocyanate (Zafar, 2012)

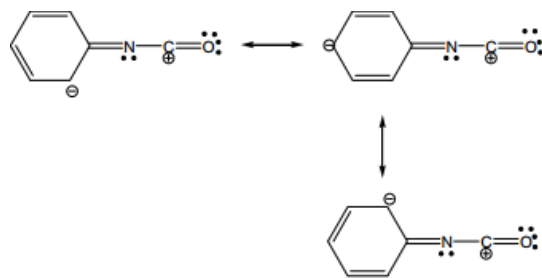


Figure 1.4 Resonance in aromatic Isocyanate (Zafar, 2012)

Generally, the isocyanate reactions are divided into three main groups of reactions: i) primary addition reaction with reagents containing active hydrogen, ii) secondary addition, iii) self-addition reactions. Figures 1.5, 1.6 and 1.7 show a schematic representation of these three groups.

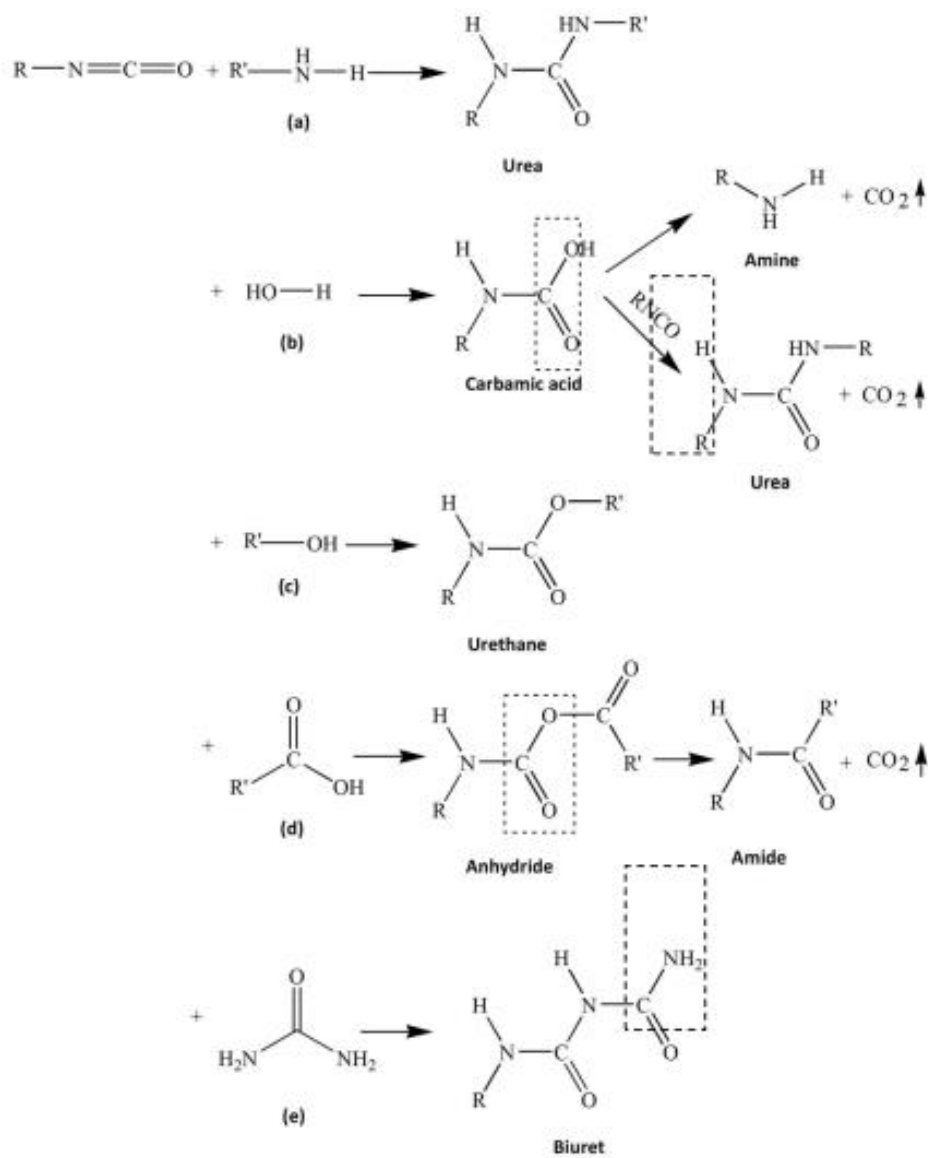


Figure 1.5 Primary addition reactions of isocyanate with (a) amine, (b) water, (c) alcohol, (d) carboxylic acid, (e) urea (Zafar, 2012)

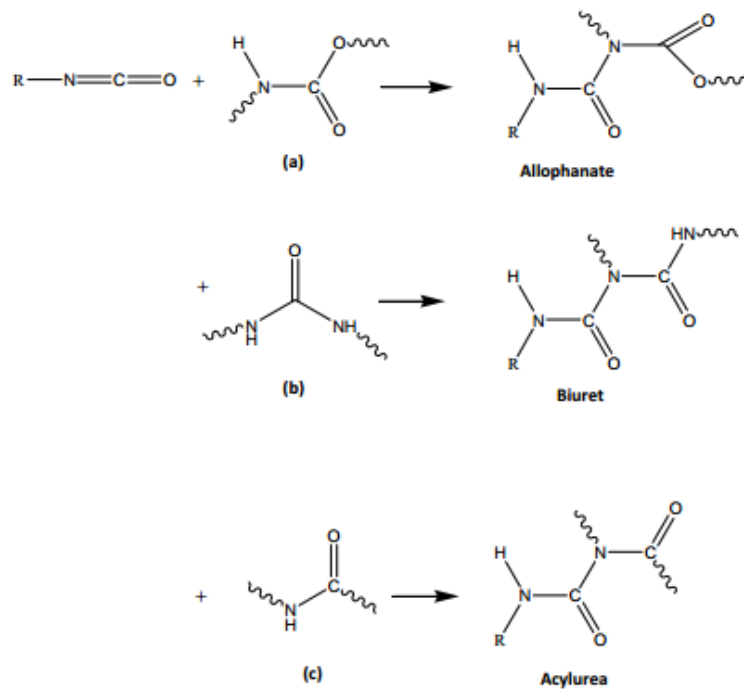


Figure 1.6 Secondary addition reactions of isocyanate with (a) PU, (b) PUa and (c) PA (Zafar, 2012)

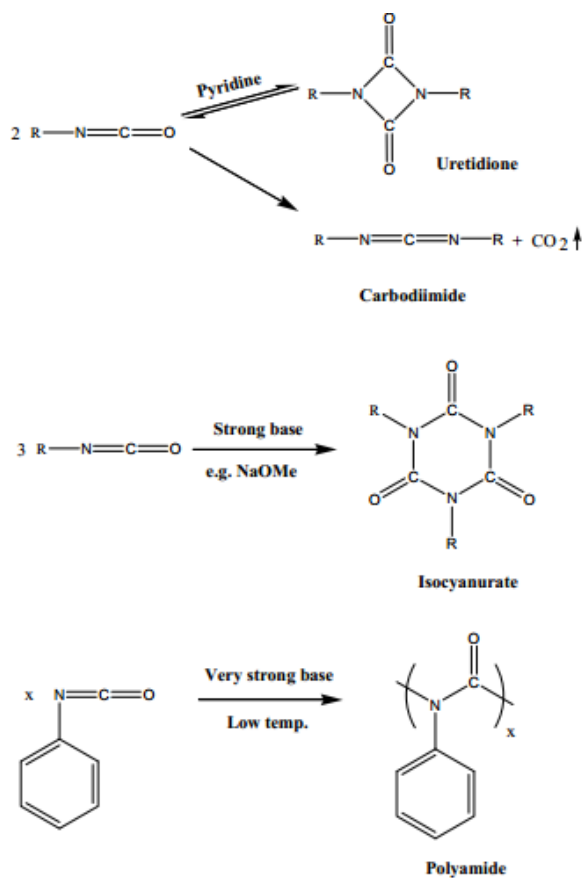


Figure 1.7 Self-addition reactions of isocyanate (Zafar, 2012)

The reaction of an isocyanate with active hydrogen compounds is performed with or without a catalyst. Without any catalyst, the electrophilic carbon of the isocyanate is attacked by the nucleophilic centre of the active hydrogen compound, then hydrogen is added to –NCO group. The reactivity of the –NCO groups is increased due to the presence of the electron reception groups, and decreases by the electron donating groups. While the aromatic isocyanates are more reactive than the aliphatic isocyanates, steric hindrance at –NCO or HXR' groups reduce the reactivity.

The order of reactivity of active hydrogen compounds with isocyanates in uncatalyzed systems is as follows: Aliphatic amines > aromatic amines > primary alcohols > water > secondary alcohols > tertiary alcohols > phenol > carboxylic acid > urea > amides > urethanes. Figure 1.8 shows schematic representation of isocyanate reaction in absence of catalyst.

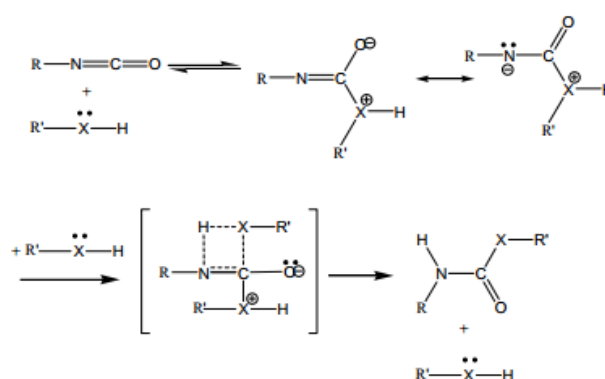


Figure 1.8 Isocyanate reaction in the absence of a catalyst (Zafar, 2012)

Isocyanate reactions may be carried out in the presence of a catalyst, being tertiary amines and, metal compounds like tin compounds the most used. The mechanisms are similar to the uncatalyzed reaction. Figures 1.9 and 1.10 show the reactions of isocyanate in presence of tertiary amines and metallic catalyst, respectively (Zafar, 2012).

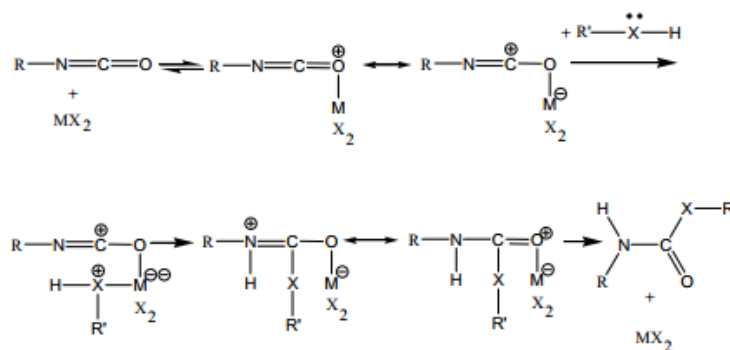


Figure 1.9 Tertiary amine catalysed reaction (Zafar, 2012)

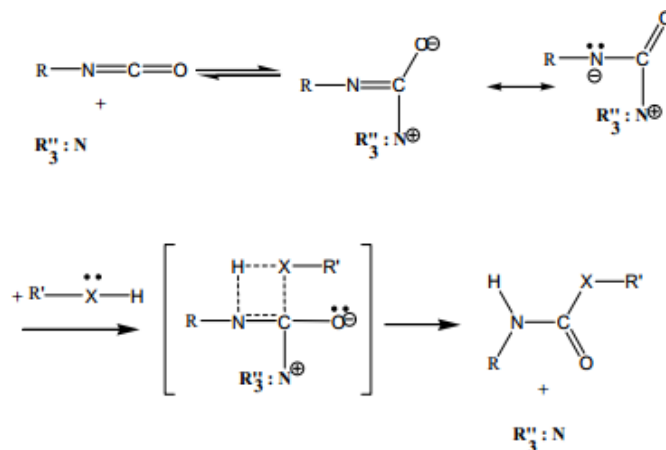


Figure 1.10 Metal salts catalysed reaction (Zafar, 2012)

## 1.4 Microencapsulation

### 1.4.1 Definition and classification of microcapsules

Microencapsulation can be defined as a way of coating small particles, liquid droplets or gas bubbles with a thin film or shell material, which protects or isolates the core material from the surrounding environment. The protection should be somehow to maintain activity of core during storage and consumption, being the resultant product called capsules, which can be classified based on their size and morphology. MCs are also classified as mononuclear, polynuclear and matrix types according to their morphology, as it is shown in Figure 1.11. Mononuclear or core-shell MCs contain the shell around the core, where the active agents are designed as the core material and the less active material forms the shell. Polynuclear capsules have many cores enclosed within the shell, while the matrix type MCs display a core homogeneously integrated within the matrix of the shell material. In addition to these three basic morphologies, MCs can also be mononuclear with multiple shells (“multi-wall”), or they may form clusters of MCs, displaying irregular, complex shapes. The different techniques for formation of MCs will be discussed in section 1.4.3 (Silva, 2014; Hu, 2017; Dubey, 2009; Aranais, 2012).

The terms core material, internal phase, active agent have been used to describe the content of MCs, while the terms of membrane, wall or shell have been used to describe the material of the outer part of MCs. For the sake of consistency, the terms “core” and “shell” will be used throughout this thesis. The morphology of MCs depends on many factors, among them the core materials, the process by which they are formed and other reagents added to the synthesis to functionalize the shell (Latnikova, 2012).

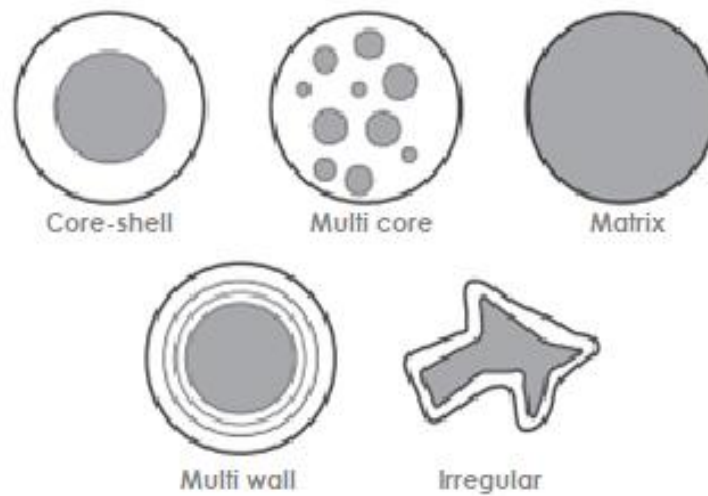


Figure 1.11 Types of MCs (Silva, 2014)

MC's shell can be divided in three main groups i) impermeable; ii) permeable; iii) semipermeable; which can release the core content by dissolution, rupture or diffusion, as shown in Figure 1.12.

Dissolution or melting of the shell happens when the shell dissolved in water or other solvents or when the temperature is such that the shell melts, gradually releasing the core material, while rupture of the shell may happen by pressure applied or by crack propagation due to some triggering mechanisms. Diffusion mechanism has its utilization typically in the pharmaceutical industry, where slow and sustained dosage of medicine needs to be released.

Several parameters determine the selection of the shell type for a certain application e.g., core material, matrix where MCs will be incorporated and core release (triggering) mechanism. For instance, semipermeable shell can be good choice when encapsulated material and matrix have relatively large molecular weight or when gradually release of core material is the objective of encapsulation, again impermeable shell will be good option when the core has low molecular weight or when zero leaching is demanded. The parameters listed above should be considered for engineering the MC's shell ( Dubey, 2009; Aranias, 2012; Hu, 2017).

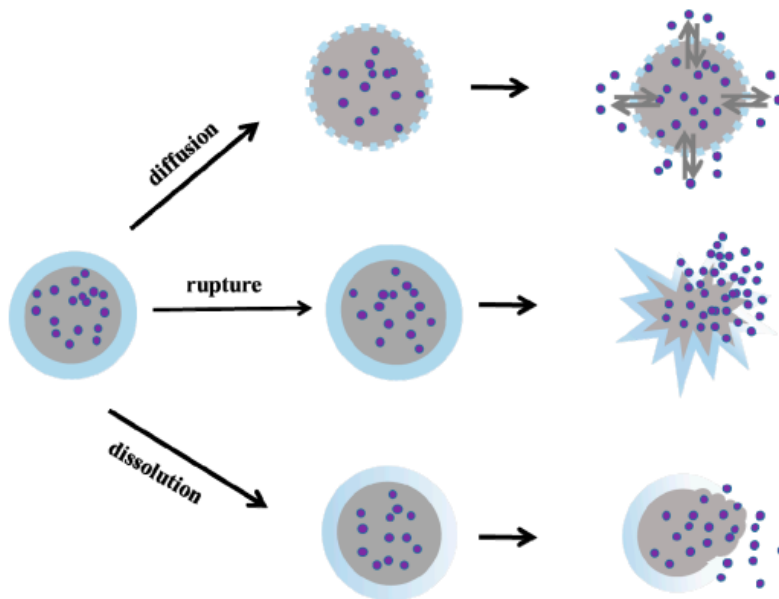


Figure 1.12 Principal release mechanism of MCs ( Hu , 2017)

#### 1.4.2 Purpose of encapsulation

Many different active materials like drugs, enzymes, vitamins, pesticides, flavours, and catalysts have been successfully encapsulated inside the shells made from a variety of polymeric and non-polymeric materials, depending on the end use of encapsulated products. The technology has been used in several fields including pharmaceutical, agriculture, food, printing, cosmetic, textile, defence, gas and oil and adhesives. The main purpose of encapsulation is listed here: (ECOBOND, 2016; Silva, 2014; Dubey, 2009; Aranais, 2012)

- Separation of incompatible components;
- Conversion of liquids to free-flowing solids;
- Increasing the stability or protection of the encapsulated materials against oxidation or deactivation due to reaction with environment;
- Masking of odour, taste;
- Protection of environment, human beings, or organisms;
- Controlled release of active compounds (sustained or delayed release);
- Targeted release of encapsulated materials;
- Combining the properties of different types of material which will be difficult to achieve by different methods;

Figure 1.13 shows some improved properties obtained by microencapsulation of adhesives.



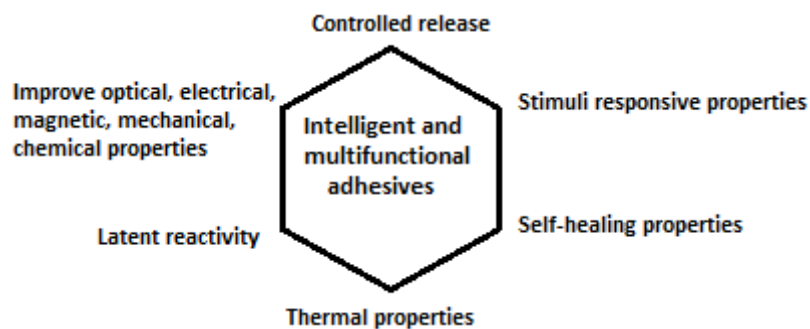


Figure 1.13 New adhesives with improved properties, obtained by microencapsulation technology (adapted from ( Aranaís, 2012))

### 1.4.3 Microencapsulation techniques

Microencapsulation techniques are divided in two main groups;

- Chemical techniques in which chemical reactions are involved in the formation of MCs. Generally, in this method starting primary materials are monomers or prepolymers;
- Physical/mechanical methods in which no chemical reaction is involved in the MCs formation process. Starting materials here are typically in the polymeric phase; ( Dubey, 2009)

Figure 1.14 shows the most common microencapsulation methods. The following pages attempt to describe the most applicable methods of microencapsulation, although in some cases the classification may be slightly different from that of the flow diagram. Selection of a certain microencapsulation technique is strongly depended on the nature of the active reagent to be encapsulated, so appropriate combination of primary material and techniques shall be selected to produce a wide variety of MCs with different characteristics (Azagheswari, 2015).

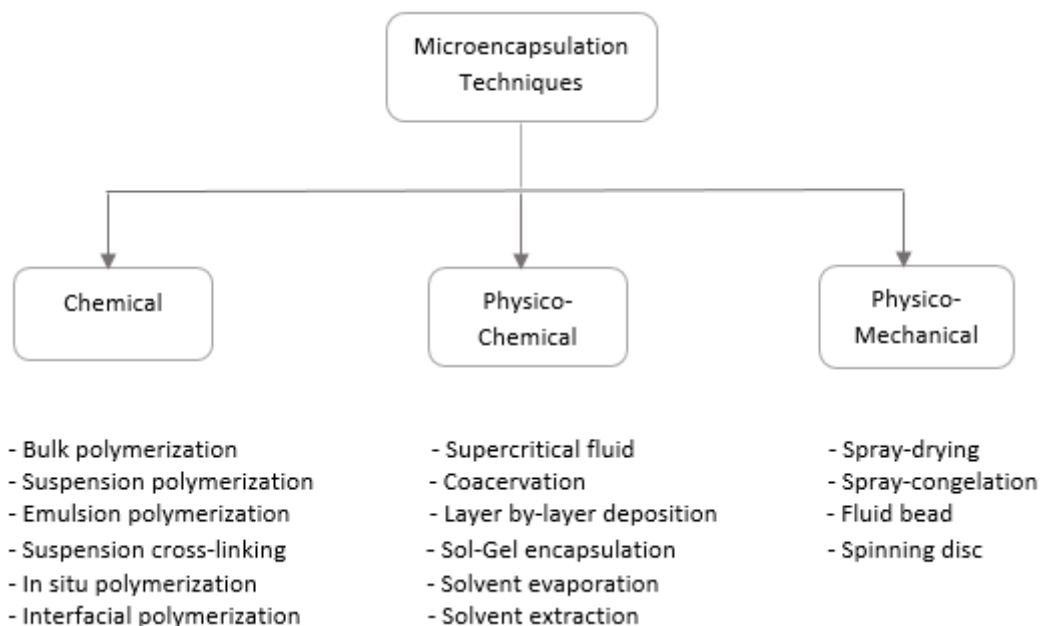


Figure 1.14 Major methods of microencapsulation (adapted from (Loureiro, 2016))

### Physical microencapsulation techniques

#### Spray drying and spray congealing

This technique is a low-cost process, which is mostly used for the encapsulation of drugs, perfumes, oils and flavours. In this process, an emulsion is prepared by dissolution of a polymer (as a shell material) in the solvent such as dichloromethane (DCM) or acetone, then the solid core material is dispersed into the polymer solution by high shear rate homogenizer. The resulting emulsion is atomized to droplets by pumping the slurry through a rotating disc into the heated chamber of a spray drier, where the solvent of emulsion is evaporated, yielding dried capsules containing core material. In the case of spray congealing method, solution is cooled to form (coagulated) MCs. As an example, lycopene has been microencapsulated inside gelatine MCs by using this technique (Shukla, 2006; Azagheswari, 2015; Dubey, 2009).

#### Fluid bead or Co-extrusion

In this process, a dual fluid stream of liquid core and shell materials are pumped through concentric tubes and form droplets under the influence of vibration. Then, solvent evaporation or cross-linking are approaches that help to achieve a mature shell. Another strategy consists of a “microfluidic device” employed to produce MCs with quite narrow size distribution and well-defined structure. Interfacial polymerization is used to assist the production of a mature shell. Figures 1.15 and 1.16 show two different designs of microfluidic devices. Ascorbic acid has been microencapsulated in polymethacrylate as well as

ethyl cellulose by using fluid bead technique and hepatocytes have been encapsulated by polyacrylonitrile by the co-extrusion technique ( Polenz, 2014; Li, 2011; Azagheswari, 2015; Dubey, 2009).



Figure 1.15 Micro TEE (Li, 2011)

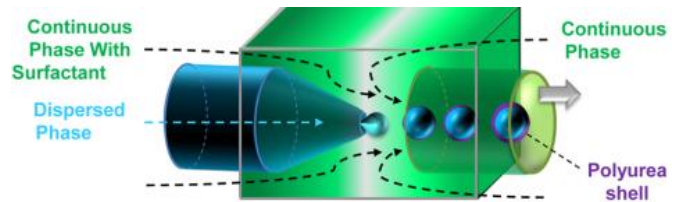


Figure 1.16 Microfluid device (Polenz, 2014)

### Supercritical fluids

Encapsulation assisted by supercritical fluids is based on the solubilization of core and shell materials in supercritical fluids. A supercritical fluid is defined as a substance above its critical temperature and critical pressure and the critical point represents the highest temperature and pressure at which the substance can exist as a vapor and liquid in equilibrium (Figure 1.17).

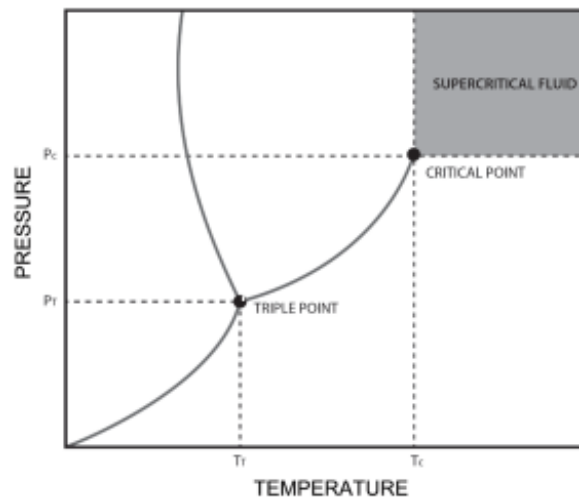


Figure 1.17 Pressure versus temperature phase diagram for pure substances (Silva, 2014)

One of the most widely used supercritical fluids is CO<sub>2</sub>, due to its low critical temperature value (74 bar, 31°C), non-toxicity and non-flammability properties. It is also readily available, highly pure and cost effective. It exhibits liquid-like densities, but gas-like diffusivities and no surface tension, which has made it useful as a renewable solvent for the extraction of ingredients from natural materials and an interesting medium to

be explored for encapsulation. It can act as a drying medium, an anti-solvent or a solute. The main variables that affect the ability to form the encapsulates are the CO<sub>2</sub> density, which influences the solvent capacity of CO<sub>2</sub>, the droplet size and particle formation.

Figure 1.18 depicts a schematic representation of microencapsulation (matrix-type) assisted by supercritical fluids. Felodipine medication has been encapsulated successfully in poly (ethylene glycol) by using this technique (Azagheswari, 2015; Silva, 2014; Dubey, 2009; Shukla, 2006).

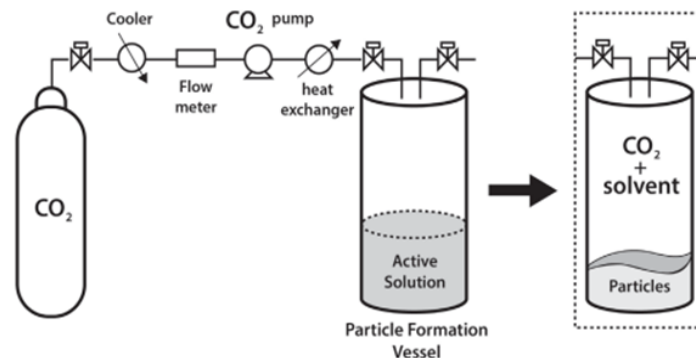


Figure 1.18 Simplified scheme of the anti-solvent technique ( Silva, 2014)

### Spinning disc

In this method, the microencapsulation of suspended core (solid) materials is performed by using a rotating disc. Core particles are poured into the liquid shell material to form a suspension which is then poured into a rotating disc and due to the spinning action of the disc, the core particles become coated with the shell material. The coated particles with the excess shell material are then streamed from the edge of the disc by centrifugal force, the shell material is solidified by external assistance usually cooling. Paraffin micro beads have been synthesized by using this technique (Azagheswari, 2015; Dubey, 2009).

### Coacervation

Coacervation or phase separation is widely used for the preparation of gelatine e.g. or gelatine-acacia MCs and cellulose derivatives as well as synthetic polymers. The process is divided in two subgroups i) simple coacervation; ii) complex coacervation. Simple coacervation involves the use of a single polymer such as gelatine or ethyl cellulose while, complex coacervation involves two oppositely charged polymeric materials (complementary polyelectrolyte) such as gelatine and Gum Arabic (GA), which are soluble in aqueous phase. In both cases, coacervation or formation of colloidal polymer aggregates happens by gradual segregation of the fully solvated polymer molecules by changing temperature or pH. Microencapsulation by coacervation is carried out by preparing an aqueous polymer solution, followed by addition of core material (hydrophobic) which can be solid or liquid. A suitable stabilizer may also be added

to the mixture to avoid aggregation of the final MCs. Segregation (coacervation) agent is gradually introduced to the mixture, which is responsible to form partially segregated polymer molecules, following by their precipitation on the surface of the core particles. The coacervation mixture is cooled to about 5-20°C, followed by the addition of a crosslinking agent e.g. formaldehyde to harden the MC's shell, formed around the core particles. Protein, polysaccharides, ethyl cellulose have been encapsulated successfully by this technique (Dubey, 2009; Shukla, 2006).

### **Layer by-layer deposition**

In this process polyelectrolyte multilayers are prepared by sequentially immersing a substrate in positively and negatively charged polyelectrolyte solutions in a cyclic procedure. Core-shell particles with tailored size and properties are prepared using colloidal particles as the core material which are used as a substrate for fabrication of multilayers. Hollow capsules of organic, inorganic or hybrid shell can be obtained by dissolving the core material. Size of MCs and their properties can be controlled by varying the total number of deposited layers. As an example, glucose oxidase has been microencapsulated by alternate deposition of polyallylamine and polystyrene sulfonate layers (Dubey, 2009).

### **Chemical or Polymerization Techniques**

Polymerization techniques are widely used for the MC's shell or matrix formation in microencapsulation processes. It is possible to divide polymerization techniques in two main groups: i) normal polymerization, including bulk polymerization, suspension polymerization and emulsion polymerization; ii) interfacial polymerization (Azagheswari, 2015). As discussed before in some references the classification is different so that all emulsion polymerization, suspension polymerization, dispersion polymerization, interfacial polycondensation/polyaddition, and *in situ* polymerization are grouped as interfacial polymerization.

In suspension polymerization, the monomer is heated with active agents as droplets dispersion in continuous phase, where the droplets may contain an initiator and other additives. Polystyrene [PCM] encapsulated by employing this technique to use in textile industry (Azagheswari, 2015; Dubey, 2009). In emulsion polymerization, the monomer is added dropwise to the stirred aqueous medium containing core material and surfactant, resulting in the formation of the MCs. Generally lipophilic materials are more suitable to be encapsulated by this technique. Insulin loaded poly (alkyl cyanoacrylate) nanocapsules have been synthesised by using this technique (Dubey, 2009). Suspension crosslinking is the best method for encapsulation proteins, enzymes, polyamines and polysaccharides. It requires dispersion of an aqueous solution of the polymer containing core material in an immiscible organic solvent in the form of small droplets, which are hardened by covalent crosslinking and are directly converted to the corresponding MCs. The crosslinking process is performed either thermally (at >500°C) or using a crosslinking

agent (formaldehyde, terephthaloyl chloride, diisocyanate, etc). The reaction is quite slower than interfacial polymerization and generally pH adjusting is necessary. Employing right crosslinker can control the shell thickness and shell permeability, so that high reactive crosslinker such as diacid chloride react very quickly with water leading to thin shell, while less reactive crosslinker like diisocyanate could migrate further from the interface to react with polymer function leading to thicker shell. As an example, albumin nanocapsules containing doxorubicin and magnetite particles have been synthesised by using this technique (Poncelet, 2013; Dubey, 2009). By in situ polymerization, the reactants, either monomers or oligomer, are in one single phase and the polymerization occurs in the continuous phase. The formed polymer migrates and deposits on the dispersed phase (droplets surface) to form the MCs. TiO<sub>2</sub> as an electrophoretic ink has been encapsulated successfully by this method (Duan, 2016).

### **Solvent Evaporation/Extraction**

In these method, the capacity of the continuous phase is not sufficient to dissolve all dispersed phase solvents. The technique is like suspension crosslinking, but in this case the polymer is usually hydrophobic polyester and is dissolved in an organic solvent like dichloromethane (DCM) or chloroform, also containing the core material. This organic mixture solution is added dropwise to a stirring aqueous solution containing a surfactant or stabilizer like poly vinyl alcohol (PVA) to form small polymer droplets containing the core material. The hardening process of these droplets is carried out by the removal of the solvent through solvent evaporation (applying heat or reduced pressure), or by solvent extraction (with a third liquid which is a precipitant for the polymer and miscible with both water and solvent). Encapsulation efficiency and MCs' morphology depends on the solvent removal technique. E.g. under reduced pressure conditions, MC's shell shows porous and rough morphology (Verma, 2011). Also, solvent extraction produces MCs with higher porosities than those obtained by solvent evaporation (Dubey, 2009). Figure 1.20 shows a schematic representation of microencapsulation by solvent evaporation technique. This technique is suitable for the preparation of drug loaded MCs based on biodegradable polyesters. DCMU (3-(3,4-dichlorophenyl)-1,1-dimethylurea) has been encapsulated using polystyrene by Fan et al. using this technique (Fan, 2017; Verma, 2011; Nikkola, 2014).

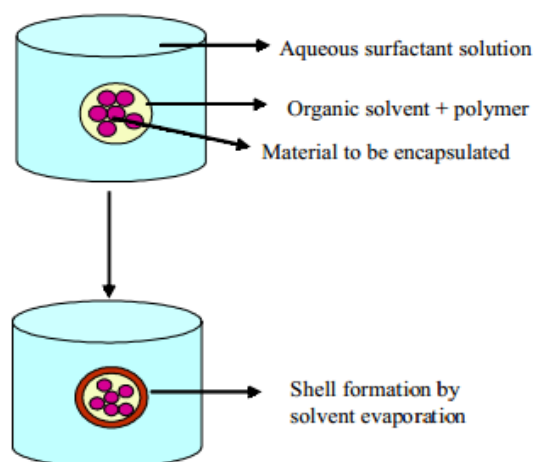


Figure 1.19 Schematic representation of microencapsulation by solvent evaporation technique ( Dubey, 2009)

### Sol-Gel technique

The sol-gel technique (a chemical-physical process) performs in five steps: hydrolysis, condensation, gelation, aging and drying. As the name suggests, the process begins with the formation of a “sol “or colloidal suspension of solid particles in a liquid, which leads to a posterior formation of a “gel”. The precursors, to prepare the colloidal solution, consist of a metal or metalloid element surrounded by ligands. Metal alkoxides that have the general formula  $M(OR)_z$ , are the most commonly used class of precursors, because they react readily with water, which facilitates the hydrolysis reactional step. The alkoxide most thoroughly studied is tetraethyl orthosilicate (TEOS) with  $Si(OC_2H_5)_4$  chemical formula. To achieve microencapsulation, the sol-gel technique is combined with microemulsion technique, so that the sol-gel derived material is formed at the interface of the water-oil, or oil-water phase, leading to encapsulation of the core material. Figure 1.21 shows the schematic diagram of direct encapsulation routes of aqueous glycerol in silica MCs as an example of microencapsulation via sol-gel technique ( Ciriminna, 2011; Galgali, 2011; Loureiro, 2016; Marques, 2017).

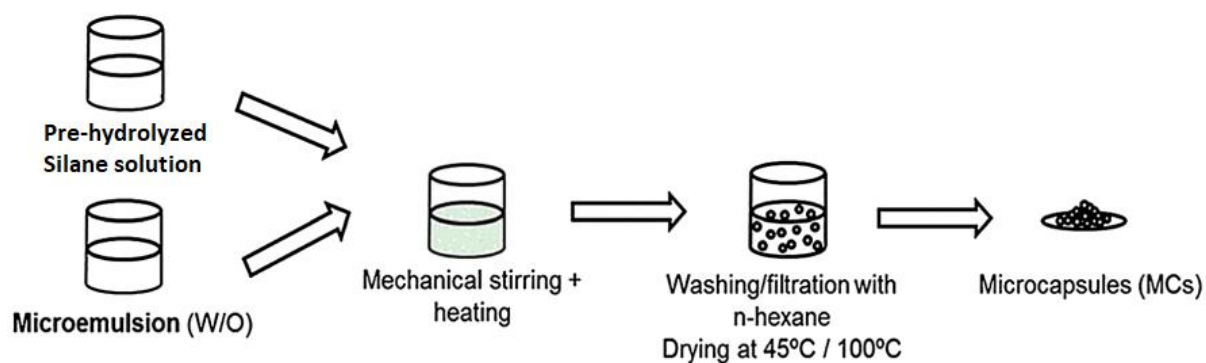


Figure 1.20 Schematic representation of direct encapsulation routes of aqueous glycerol in silica MCs (adapted from (Marques, 2017))

#### 1.4.4 State of the art on isocyanate microencapsulation

Isocyanates have been widely used in the field of coatings and adhesives and, because of their high reactivity, they also have been used for self-healing purposes. A review of the literature shows that the major efforts for microencapsulation of isocyanate compounds, belongs to encapsulation of IPDI as a healing agent. Yang *et al.* in 2008 for the first time, have reported successful microencapsulation of liquid isocyanate compound (IPDI) as a healing agent via interfacial polymerization. They prepared Toluene 2,4-diisocyanate (TDI) prepolymer by dissolution of TDI into cyclohexanone, followed by further addition of 1,4-Butanediol at 80 °C. The solution of this prepolymer in chlorobenzene, as a higher reactive isocyanate compound, was used as shell former component and it was added to the IPDI (core material). The mixture then, was added to an aqueous phase of GA solution in water, together with 1,4-butanediol, which acts as a chain extender. They reported a microencapsulation yield at 70 wt % for stirring rates ranging from 500 to 1500 rpm ( Yang, 2008; Silva, 2017). Most of the other reports look to be significantly similar to the work of Yang. and co-workers. In 2008 J. Li *et al.* prepared MCs containing a mixture of aromatic and aliphatic isocyanates by dissolving isocyanate compounds in p-xylene and dispersing this mixture as an organic phase in the aqueous solution of poly vinyl alcohol (PVA). Interfacial polymerization was carried out to form the MCs shell at different temperatures and the shell formation mechanism, as well as the shell morphologies were studied (Li, 2011). D. Sondari *et al.* in 2010 reported the successful encapsulation of IPDI as a self-healing agent by using glycerol as a polyol. The work structure is pretty similar to the work of Yang *et al.* (Sondari, 2010). M. Huang *et al.* described the successful microencapsulation of hexamethylene diisocyanate (HDI) as core materials in PU shell via interfacial polymerization by reaction of commercial methylene diphenyl diisocyanate (MDI) prepolymer and 1,4-butanediol in an oil-in-water emulsion. The resultant MCs have diameters of 5–350 µm with the shell thickness of 1–15 µm. The obtained MCs showed encapsulation efficiency at 60 -70 wt%, by varying the reaction conditions (Yang, 2011). In 2013 Wang *et al.* reported the microencapsulation of IPDI by poly(urea–formaldehyde), PUF, pre-treated carbon nanotubes embedded, to improve the micromechanical properties of the MCs shell. Quantification of the IPDI core content was not performed, and distinction was not possible between the infrared isocyanate signal, ascribed to the core material on the one hand and the pendant isocyanate groups attached to the solid shell on the other hand ( Nguyen, 2014).

B. Di Credico *et al.* have described an efficient method to encapsulate IPDI with different shells, namely PU, PUF and bi-layer polyurethane/poly (urea–formaldehyde) PU/PUF. The synthesis of PU/PUF MCs was carried out by interfacial polymerization using Desmodur L-75, followed by in situ PUF microencapsulation. The second outer layer was fabricated from urea–formaldehyde resin. It was concluded that only about 49 wt% of IPDI was encapsulated as a core material within the PU MCs and 68 wt% within the PU/PUFMCs (Credico, 2013). T. Nguyen *et al.* in 2014 reported a facile approach for the encapsulation of the liquid hexamethylene diisocyanate isocyanurate trimer (HDI-trimer) in polyurea MCs, formed via the oil-in-water interfacial reaction. HDI-trimer was selected as the encapsulated material because of its high isocyanate functionality and very low vapor pressure compared to other common diisocyanate monomers, such as IPDI which, makes it a useful healing agent. Uretonimine-modified methylene diphenyl diisocyanate (MDI-trimer) was mixed with HDI-trimer in an oil phase. Because of the higher reactivity of MDI-trimer, at the oil-water interface, MDI-trimer reacted primarily with the triaminopyrimidine (TAP) tri-amine, soluble in the water phase, to form a stable polyurea shell. MCs then were



functionalized by addition of 2-ethylhexylamine, 3,4-difluorobenzylamine, perfluorodecylamine + 2-ethylhexylamine, 3,4-difluorobenzylamine + 2ethylhexylamine and hexamethyldisilazane (HMDS). A core content between 48 to 76 wt% was reported for non-functionalized MCs and for MCs functionalized by HMDS, respectively (Nguyen, 2014). D. Sun *et al.* in 2015, synthesised successfully double-layered polyurea MCs containing HDI with outstanding shell tightness via interfacial polymerization reaction in an oil-in water by employing Suprasec 2644 as a shell former. GA was used as a surfactant and triethylenetetramine (TETA) was added to start formation of the shell. The MCs efficiency was reported in the range of 50-56 wt% (Sun, 2015). H. Yehaneh *et al.* in 2015, reported microencapsulation of bulky isocyanate molecules as a fast curing healing agent, instead of the low molecular weight monomeric analogous. They synthesized isocyanate-terminated prepolymer based on IPDI and the isocyanate-terminated prepolymer based on TDI as shell. They used GA as a surfactant and 1,4-butanediol and 2-ethyl-2-hydroxy methyl-1,3-propanediol (TMP), as chain extenders, and dibutyltin dilaurate (DBTL), N-methyl-2-pyrrolidone (NMP). Chlorobenzene (CB) was employed as a solvent to dissolve the prepolymers. They reported 43.3- 48.7 wt% of encapsulation efficiency which was reduced to 36-44 wt% respectively after 10 months (Yeganeh, 2016).

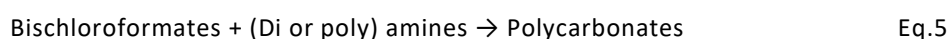
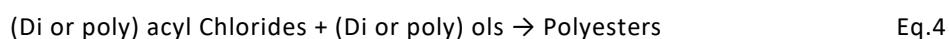
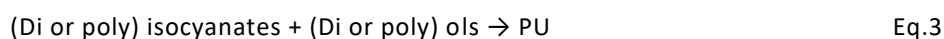
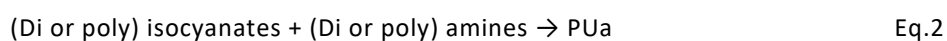
Again, microencapsulation of IPDI MCs via interfacial polymerization of PU was reported by P. Kardar in 2015. MCs were manufactured using different polyols including 1,4-butanediol, 1,6-hexanediol and glycerol. The structure of this work also is pretty similar to the work of Yang's group in 2008. As a result, the utilization of 1,4 butanediol and 1,6-hexanediol as polyol monomer for PU MCs shell is recommended by author due to higher encapsulation efficiency when compared to MCs obtained from addition of glycerol to the synthesis (Kardar, 2015). Y. Ming in 2016 reported the encapsulation of IPDI in Polyurea (PUa) /melamine formaldehyde (MF) double-layered self-healing MCs with high and stable core fraction. The core yield was reported at around 78 wt% (Ming, 2016). In most recent work in 2017, Y. Ma *et al.* reported microencapsulation of polyaryl polymethylene isocyanates (PAPI). They employed PAPI as core materials, which react with small molecules containing active hydrogen i.e. 1,4-butanediol, ethylene glycol, 1,2-diaminoethane, etc. The reaction products of PAPI and active hydrogen would form a shell by interfacial polymerization reaction in an oil-in-water emulsion. Smooth spherical MCs of 70 -180  $\mu\text{m}$  in diameter were produced by controlling the stirring rate at the range of 600 -1200 rpm and a high yield of 80 wt% was reported as the encapsulation efficiency (Ma, 2017). The strategy in the present thesis has been inspired from the work of Yang. and co-workers and P. Kardar, but the novelty here is the optimization studies in terms of active hydrogen sources and the combination of low and high reactivity isocyanate compounds to provide a more efficient encapsulation. Moreover, other commercial isocyanate compounds are encapsulated, such as high reactivity commercial MDI and TDI pre-polymers, within the framework of project ECOBOND, as it will be explained in more detail in chapter 3.

## 2. Microemulsion and interfacial polymerization as a strategy for this work

Among the several methods previously described, microemulsion followed by interfacial polymerization will be described in more details, as almost all the syntheses in this thesis are performed by this approach. Interfacial polymerization was developed at the end of 1960's and its application in microencapsulation technology backs to mid-1970's (Hu, 2017).

The key feature in this process is diffusion of two different reagents to the interface. Generally, both phases (aqueous solution and oil based solution) contain a reactive monomer which come in contact together at the interface and react there to form a polymeric shell (Hu, 2017).

Below equations illustrate the main polymer and reactant system to make MCs by interfacial polymerization:



The mechanism of MC formation comprises four typical steps: (1) Formation of microemulsion, (2) Initial polymerization at the interface, (3) Formation of membrane around the droplets, (4) Membrane growth to form shell or matrix (Arshady, 1998; Duan, 2016).

Figure 2.1 shows the schematic illustration of interfacial polymerization of isocyanate in aqueous solution and the possible reactions which may happen to form several types of shells.

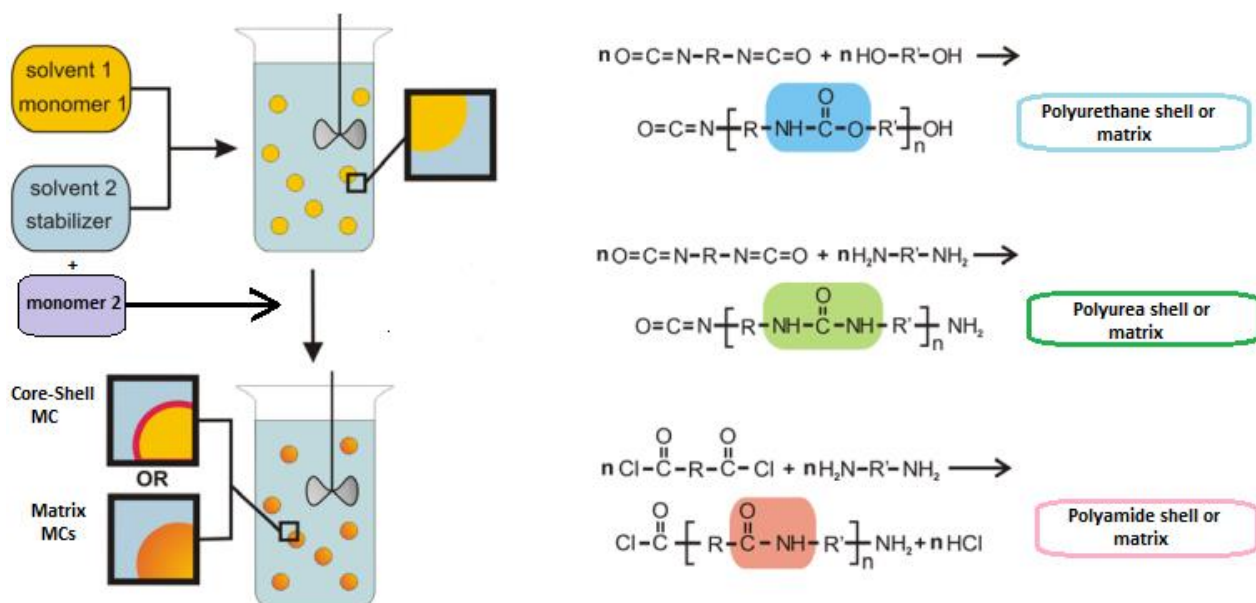


Figure 2.1 General scheme of the interfacial polymerization and some possible reactions (adapted from (Latnikova, 2012))

## 2.1 Emulsion formation

Emulsions, in this work, are a category of dispersed system, which include, two immiscible liquids. In fact, the liquid droplets, in this case organic phase are dispersed in the continuous liquid phase, in this case aqueous solution. Oil in water (O/W), water in oil (W/O) and oil in oil (O/O) are three main groups of emulsions, where the last class (O/O) can be a dispersion of polar oil in nonpolar oil or vis versa. To disperse two immiscible phases other class of material, namely emulsifier and /or surfactant is needed. Surfactants are molecules with an amphiphilic structure e.g., with both a hydrophilic and a hydrophobic group in the structure. Usually, the hydrophobic group consists of a long hydrocarbon chain, while the hydrophilic portion is composed by an ionic or highly polar group. On an emulsion system, the hydrophobic part of the surfactant molecules orients themselves with the hydrophobic phase, i.e. the oil phase, while the hydrophilic part orients toward the hydrophilic phase, i.e. water. Surfactant can form a variety of structures with different functional properties depending on their molecular structure and/or their concentration in the solution. According to the nature of the hydrophilic group, surfactants can be classified as: anionic, cationic, amphoteric, and non-ionic. Figure 2.2, shows schematic representation of different types of surfactant molecules. The presence of a surfactant helps to stabilize the emulsion. The triple system including an organic phase, an aqueous phase and surfactant are transformed to emulsion through high shear rate mixing (Tadros, 2013; Duan, 2016; Yang, 2011).

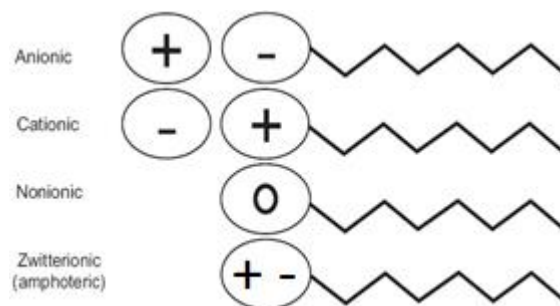


Figure 2.2 Schematic representation of surfactant molecule (Som, 2012)

An important surfactant characteristic is the hydrophilic-lipophilic balance (HLB). The HLB of a surfactant represents the affinity of the surfactant to the aqueous or organic phases. The value is expressed as a ratio between the hydrophilic and lipophilic groups of the amphiphilic surfactant molecule and calculates according to the equation 6. A HLB value higher than 10 indicates hydrophilicity of the surfactant, and when HLB value is lower than 10 it indicates lipophilicity. Thus, in general, surfactants with low HLB value, between 3 and 8, are incorporated into the organic phase. While, surfactants with high HLB value, between 8 and 18, are added into aqueous solutions. However, HLB value only gives information about the emulsifying characteristics of the surfactant, not its efficiency (Loureiro, 2016; Madaan, 2014).

$$HLB = 7 + \Sigma (\text{hydrophilic groups}) - \Sigma (\text{lipophilic groups}) \quad \text{Eq-6}$$

Since emulsions are thermodynamically unstable systems they begin to lose their structure and tend to breakdown over time. The factors which affect an emulsion's stability include: the particle size and distribution of emulsified oil droplets, viscosity and total solid content of the emulsion (if it is the case), type and concentration of the shell material, ratio of core to the shell material, the type of emulsifier, which allows for control of interfacial properties like charge, thickness, rheology, and response to environmental stresses such as pH, ionic strength, temperature and the homogenization temperature, pressure, and time (Avramenko, 2013).

## 2.2 Microcapsules' shell formation

MCs' shell forms in two steps,.during the 1<sup>st</sup> step initial shell forms by deposition of oligomers on the surface of oil droplets. The 2<sup>nd</sup> step will be the increase of the shell thickness by continuation of polymerization towards organic phase, the polymerization is controlled by diffusion, so shell growth's speed will decrease as the shell thickness increases. The reduction of polymerization rate significantly affects the morphology and thickness of the shell. Several factors can control the shell morphology and shell formation process, namely i) type of aqueous soluble monomer, ii) type of organic phase, iii) solubility of amine groups in the organic and aqueous phase, iv) type of solvent, v) synthesis temperature and vi)

stirring rate, which will be discussed in more details later on (Duan, 2016; Salaüna, 2011; Kardar, 2015; Polenz, 2014).

### **2.3 Microcapsules washing, collecting and drying**

To collect the produced MCs, first a washing process should be performed to remove the excess of reactants. Vacuum filtration may be employed by using the proper vacuum pump to avoid the breaking and loss of MCs. MCs are washed out using the proper solvent like distilled water, ethanol, toluene, n-hexane, etc. Finally, MCs can be dried at RT or in the oven at 45°C during 24 hours.

### **2.4 Factors affecting microcapsules formation**

This chapter will explain briefly the most important parameters which can affect the MCs formation processes and thus their morphology. These factors can be divided into two main categories. First category includes factors related to primary materials, their chemical structure, and their concentration. The second group are synthesis parameters, like emulsification speed, synthesis temperature, synthesis time and mechanical stirring rate.

#### **2.4.1 Factors related to primary materials**

##### **Active hydrogen sources solubility**

As it was discussed before, NCO groups of isocyanates react with OH groups or amino groups and form urea or urethane moieties, and their polymerization results in the MC's shell material. The active hydrogen in the syntheses may be provided by amines (NH groups) or polyols (OH groups). They may have different chain length and different chemical structure, with different steric hindrance and reactivity. They are normally soluble in aqueous phase and strongly influence the shell thickness as well as the shell morphology of MCs. Amine and polyol solubility in organic phase and aqueous phase can be defined as their partitioning coefficient  $K_{OW} = \frac{[Amine]_o}{[Amine]_w}$  where the  $[amine]_o$  and the  $[amine]_w$ , are the equilibrium concentration of amine in the oil and aqueous phase, respectively. The same coefficient can be defined for polyols. The shell thickness tends to increase when  $K_{ow}$  increases. This can be explained by higher diffusion rate of amine or polyol molecules toward organic phase than toward aqueous phase, during the shell formation (Polenz, 2014). This factor also can affect the minimum reaction time (Ma, 2017).

### Chemical structure of active hydrogen sources

The different chemical structures of amines and polyols can significantly determine the shell morphology of MCs. Somehow, chemical compounds with more NH or OH groups, tend to produce a crosslinked network structure in the shell and, therefore, higher rigidity. On the other hand, active hydrogen sources with linear structure lead to lower mechanical strength shell and, therefore, MCs with wrinkled shell structure when observed at the SEM. Active hydrogen groups with spatial arrangement of molecular structure, tend to produce thicker shell when compared with those derived from reactants with less hydrogen active groups. For instance, addition of 0.0 G polyamidoamine (PAMAM) results into MCs with better shell morphology than in the presence of DETA and TETA, where thinner and wrinkled shell is revealed at the SEM observation. This could be due to the higher NH functionality in PAMAM, which results in more crosslinking. Figure 2.3 shows the molecular structure of DETA, EDA, TETA and 0.0 G PAMAM (Kardar, 2015; Tatiya, 2016).

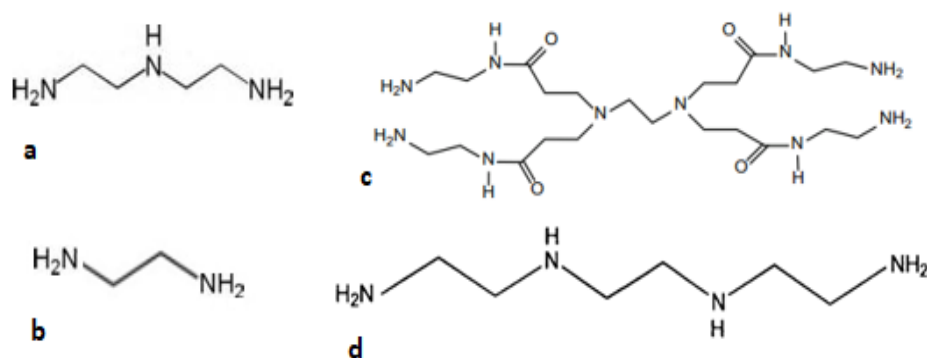


Figure 2.3 Molecular structure of a) DETA, b) EDA, c) 0.0 G PAMAM, d) TETA

In what regards EDA and DETA, it has been reported that EDA tends to diffuse more rapidly, due to its short molecular chain, destroying somehow the stability of the emulsion, resulting in a thick and coarse shell and a nonuniform size of the obtained MCs. As for DETA, its diffusion is slower due to its longer chain. Moreover, a branched polymer can also be generated during reaction with isocyanate compound, which also increases the stability of the emulsion. The number of hydrophilic segments in amine also has an important role in the microstructures of MCs. (Zhang, 2009). Mean diameters and particle size distributions of the MCs also are affected by the chemical structures and properties of active hydrogen sources, so that more NH or OH groups in the molecule and higher molecular weight result in larger MCs size and higher average particle size. Figure 2.4 shows change in the size and size distribution of MCs by using three different types of amines DETA, TETA and PAMAM (Tatiya, 2016).

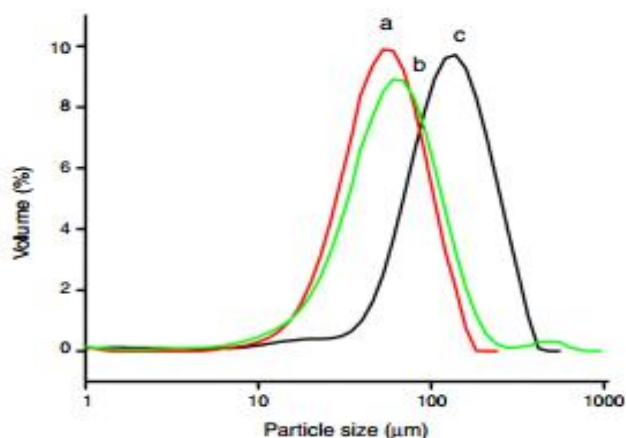


Figure 2.4 Particle size and size distribution of PUa MCs from different amines (a) DETA, (b) TETA, and (c) PAMAM (Tatiya, 2016)

### Concentration of active hydrogen sources

The shell thickness tends to increase with increasing the amine or polyol concentration and also, in less extent, with the increase of the isocyanate concentration. This finding suggests that a threshold amount of the isocyanate is required for the shell to fully form (Polenz, 2014).

### Surfactant

The presence of the right quantity of surfactant gives stability to the emulsion and prevents agglomeration of MCs during the process. Higher concentration of surfactant reduces the droplet size and narrow down the size distribution, and in some cases, can improve the stability of emulsion (Duan, 2016; Yang, 2011)

### Organic phase structure

Aromatic or aliphatic structure of the isocyanate compounds, on one hand, and linear or branched structure, on the other hand, can affect the porosity and permeability of the MC's shell. Moreover, multifunctional polymers can improve the thermal and mechanical stability of MCs by formation of three-dimensional cross-linked polymer. For PUa and PU MCs, polymeric isocyanates are preferred, due to formation of less permeable shells. The reason behind this fact can be explained by competition between interfacial polymerization and hydrolysis reaction, due to limitation in hydrolysis of isocyanate groups followed by reduction of CO<sub>2</sub> release and, therefore, less shell porosity (Duan, 2016).

### Solvent

The solvent has influence on the capsules formation by changing the interfacial tension of the medium. So, it affects the diameter and surface morphology of resulting MCs. In particular, the MCs' diameter

drastically decreases when the solvent quantity is increased. The fact can be explained by the reduction of the viscosity of isocyanate compounds, by addition of solvent. So, the higher solvent concentration formed smaller oil droplets in an oil-in-water emulsion, and as a result, smaller MCs will be produced. Also, solvent influences the contact area between isocyanate compounds and active hydrogen sources and tends to lead for inhomogeneous reaction kinetics. The solvent evaporation in drying stage also affects the MCs morphology (Ma, 2017).

Moreover, an organic solvent can accelerate or decelerate the reactions by changing the diffusivity of the monomers towards their complementary phases. Some organic solvents like toluene and chloroform can be employed to improve the diffusivity, while n-Hexane can decrease the diffusivity (Duan, 2016; Polenz, 2014).

#### **$C_{\text{Core}}/C_{\text{Shell}}$ ratio**

This ratio defines the quantity of core material to be encapsulated and the quantity of material which is added to form the shell, if this is the case. This ratio not only decides the shell thickness of MCs but also the effectiveness of encapsulation process. Some references indicate that the best  $C_{\text{core}}/C_{\text{shell}}$  ratio is 77/23 in terms of higher encapsulation yield content (Salaüna, 2011; Tsuda, 2011). Other reference mentions that, with the decrease of the  $C_{\text{core}}/C_{\text{shell}}$  ratio, the size of the MCs tends to increase (Tan, 1991). An outward diffusion mechanism was considered to explain the phenomenon. This model suggested that the isocyanates (organic phase) migrate outward through the formed shell and part of them react with water to form amines, which then react with additional isocyanates and accumulate PUa on the shell surface. As the process continues, the shell becomes thicker and the MCs size increases (Duan, 2016).

### **2.4.2 Factors related to synthesis parameters**

#### **Reaction temperature**

Higher temperature of the synthesis can accelerate the formation of the shell by increasing the diffusion rate of monomers, as well as increasing the materials reactivity (Duan, 2016). The reaction temperatures have been also investigated and evaluated in terms of core fraction of MCs and thermal resistance by Sun et.al. The same work was mentioned that higher reaction temperatures lead to formation of denser shells and more thermally stable MCs (Sun, 2014).

#### **Emulsification rate and time**

The first stage in the formation of MCs is the creation of a stable emulsion. The properties of O/W emulsions can be manipulated by varying the emulsifiers used, as well as the components that are present in



the aqueous phase. Several works have confirmed the reduction of the MCs diameter with increasing the emulsification rate (Zhuo, 2004; Ramos, 2005; Tsuda, 2011). The influence of emulsification time on the resultant MCs was investigated and evaluated in terms of core fraction of MCs. As a result, the core fraction of MCs decreased from 52.8% to 32.6% with an increase of emulsification time from 15 min to 75 min, respectively. The greater consumption of core material by water for a longer emulsification time contributes to this phenomenon (Sun, 2014).

### **Stirring rate**

Several works about microencapsulation of a liquid agent in PU or PUa shell have confirmed the effect of changing the stirring rate in the size of the MCs, thickness of the shell, as well as yielding of encapsulation (Brochu, 2012; Yang, 2011). W. Brochu et al. showed that, by increasing the stirring rate from 350 rpm to 1100 rpm, the average diameter of MCs decreased from 222  $\mu\text{m}$  to 74  $\mu\text{m}$ , and MCs shell thickness decreased from 6.3  $\mu\text{m}$  to 1.6  $\mu\text{m}$ , respectively. The same work has shown that the core content has decreased from 58% to 46%, when the stirring rate increased from 350 rpm to 1100 rpm. The reduction in yield of MCs by increasing the stirring rate can be explained by two main reasons: firstly, more MCs after formation might be destroyed due to higher shear force under faster stirring; secondly, during the MCs collection, many tiny MCs may not be collected in the process of filtration. As a result, the core fraction in the final MCs will be lower at higher stirring rate (Yang, 2011).

### **Droplet size**

Each small droplet can be considered as a tiny reactor and, since the interfacial polymerization happens at the surface, smaller droplet size mean higher reactivity or shorter synthesis duration, as the surface area increases with the decrease of the droplets' diameter (Duan, 2016).

#### **2.4.3 Factors affecting microcapsules size**

As explained before, several factors influence the size of MCs, including emulsification rate, the geometry of the mixing device, the chemical structures and properties of active hydrogen sources, viscosity of the reaction media, surfactant concentration, stirring rate, temperature, etc. However, the average diameter of MCs is primarily controlled by the emulsification rate after all other parameters were optimized (Yang, 2011). MCs size distribution and core /shell ratio are also affected by changing the type of active hydrogen sources.

Figure 2.5 shows the sample flow diagram of different steps of the microencapsulation process by micro emulsion and interfacial polymerization for encapsulation of isocyanate compound.

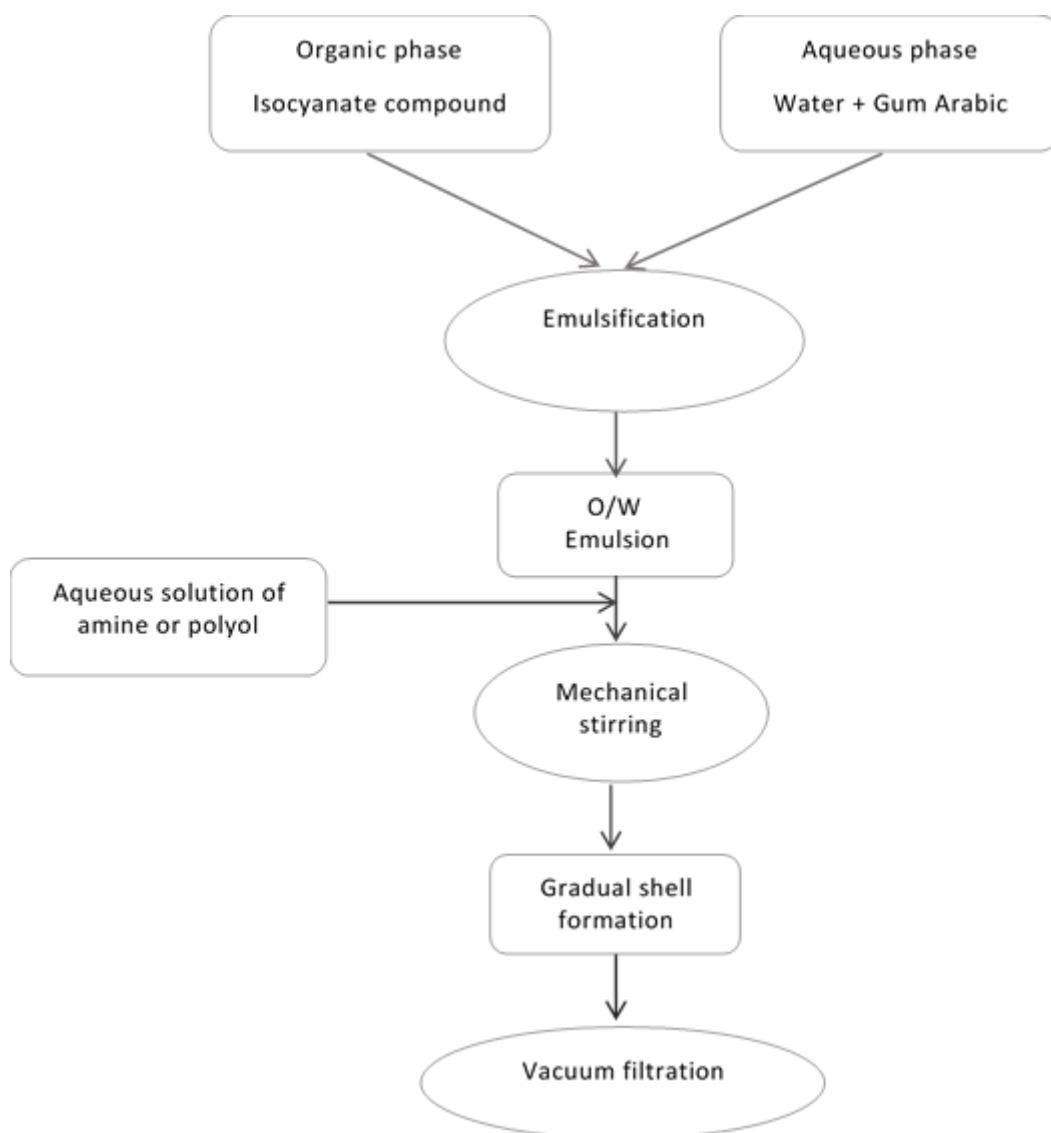


Figure 2.5 General steps of microencapsulation of an organic phase by interfacial polymerization

### 3 Experimental Part

#### 3.1 Primary materials

The primary materials used, together with some of their physical and chemical properties, are listed in Tables 3.1., 3.2, 3.3, 3.4. and 3.5. Four main groups of materials were used to perform the synthesis, namely isocyanate compounds as a core material and / or shell forming materials, polyols or amines as a source of active hydrogen, surfactants acting as emulsifiers and/or stabilizers and finally solvents.

Table 3.1 List of primary materials used in this work

Name	Type	Density (g/ml)	Viscosity @ RT	Purity (%)	Other	Brand
Distilled water	solvent	1	1.002 cP	99	---	MilliQ
Dabco <sup>®</sup> DC 193	Surfactant	1.07	260 cSt		HLB =12	Dow Corning
Gum Arabic	Surfactant	NA	NA	NA	HLB =13.5	LABCHEM
Tween -20	Surfactant	1.1	250-450 cP	99.5	HLB =16.7	SIGMA-ALDRICH
3-(Triethoxysilyl) propyl isocyanate (TPI)	Silane coupling agent	0.999	----	95	----	ALDRICH Chemistry
1,6-Hexanediol	Polyol	NA	NA	99	----	ALDRICH Chemistry
Glycerine	Polyol	1.225	58 cP	87		VWR Chemicals
Ethylenediamine (EDA)	Amine	0.899	1.7 cP	99.5	----	Fluka
Diethylenetriamine (DETA)	Amine	0.95		99	----	Alfa Aesar
3-(2-Aminoethylamino) propyltrimerthoxysilane (Aminosilane)	Amine	0.88	1.499 cP	90	----	VWR Chemicals
Polystyrene (PS)	Polymer	NA	NA	----	Average M <sub>w</sub> =192000	ALDRICH Chemistry
Tetraethyl orthosilicate (TEOS)	Silane	0.93	0.72 cSt	99	----	VWR Chemicals
Polycaprolactone (PCL)	Polymer	NA	NA	----	Average M <sub>w</sub> =45000	ALDRICH Chemistry
PEARLSTICK <sup>®</sup> 45-50/18	Polyol	1.19	NA	---	Hydroxyl No. 0.1	Lubrizol
Isophorone diisocyanate (IPDI)	Isocyanate compound	1.049	15 cP	98	-----	Bayer
Toluene diisocyanate (TDI-TX)	Isocyanate compound	1.22	2.5 cSt	-----	-----	DOW VORANATE
Ongronat <sup>®</sup> 2500	Isocyanate compound	1.24	520 cP	----	NCO value (wt%) =30-32	BorsodChem
Suprasec 2234	Isocyanate compound	1.13	2500 cP	-----	NCO value (wt%) =15.9	HUNTSMAN Chemistry
Desmodur <sup>®</sup> RC	Isocyanate compound	1.01	3 cP	----	NCO value (wt%) =7.0	Covestro
2-Butanone (MEK)	Solvent	0.805	0.43 cP	99.5	Boiling point 80 °C	SIGMA-ALDRICH
n-Hexane	Solvent	0.65	0.3 cP	95	Boiling point 69 °C	VWR Chemicals
Toluene	Solvent	0.87	0.590 cP	99.8	Boiling point 111 °C	CARLO ERBA
Dimethylformamide (DMF)	Solvent	0.948	0.92 cP	99.8	Boiling point 153 °C	Fisher Scientific
Dichloromethane (DCM)	Solvent	1.3266	0.43 cP		Boiling point 39.6 °C	SIGMA-ALDRICH

Table 3.2 List of isocyanate sources used in this work

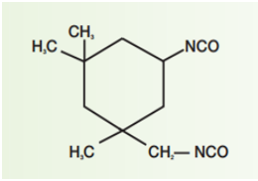
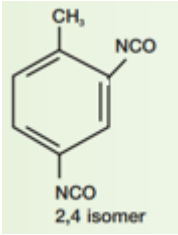
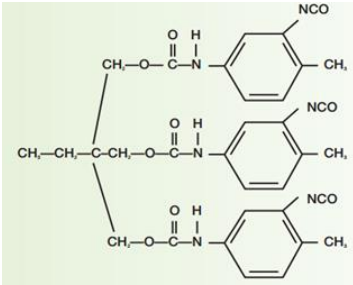
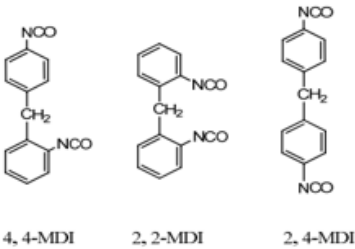
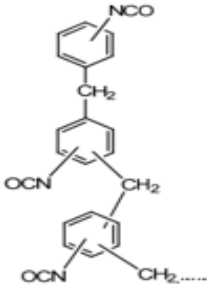
Name	Chemical formula	Molecular structure	Description
Isophorone diisocyanate (IPDI)	$C_{12}H_{18}N_2O_2$		Aliphatic diisocyanate displaying two -NCO groups, which differ in their reactivity due to the difference in their point of location. IPDI has the potential to be applied in a free catalyst self-healing system because of its reactivity with water.
Toluene diisocyanate (TDI)	$CH_3C_6H_3(NCO)_2$		Aromatic diisocyanate. The 4-position is approximately four times more reactive than the 2-position. 2,6-TDI is a symmetrical molecule and thus has two -NCO groups of similar reactivity, like the 2-position on 2,4-TDI. However, since both isocyanate groups are attached to the same aromatic ring, reaction of one isocyanate group will cause a change in the reactivity of the second isocyanate group.
Desmodur	-----		Aromatic polyisocyanate (prepolymer) produced from TDI. Two different types of Desmodur are available: Desmodur L polyisocyanate is a TDI-trimethylolpropane (TMP) adduct, which is available in several solvent blends. Desmodur IL polyisocyanate is the isocyanurate trimer of TDI.
Methylene diphenyl diisocyanate (MDI)	-----		Aromatic diisocyanate. Three isomers are common, varying by the positions of the isocyanate groups around the rings 2,2'-MDI, 2,4'-MDI, and 4,4'-MDI. The 4,4' isomer is the most widely used.
Ongronat <sup>®</sup> 2500 Suprasec 2234	-----		Mixtures of monomeric and polymeric isocyanate species, i.e. oligomeric MDI with increased functionality.

Table 3.3 List of surfactants used in this work

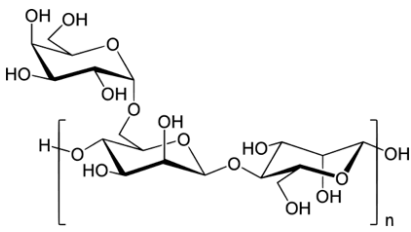
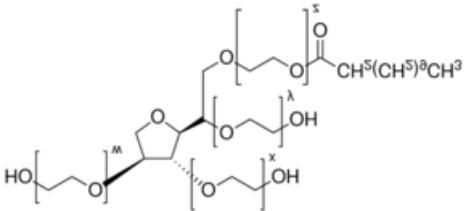
Name	Chemical formula	Molecular structure	Description
DC 193	-----	$  \begin{array}{c}  \text{Me} \quad \text{Me} \\    \quad   \\  \text{Me}_3\text{SiO}(\text{SiO})_x(\text{SiO})_y\text{SiMe}_3 \\    \quad   \\  \text{Me} \quad (\text{CH}_2)_3 \\    \\  \text{O} \\    \\  (\text{CH}_2\text{CH}_2\text{O})_m \\    \\  (\text{CHCH}_3\text{CH}_2\text{O})_n \\    \\  \text{R}  \end{array}  $	<p>It is a water soluble to water dispersible silicone polyether. A silicone surfactant structure with a complex distribution, since it is the reaction product of two polymeric raw materials each one having a different molecular weight distribution.</p>
Gum Arabic	-----		<p>Macromolecules with high proportion of carbohydrate, whose chemical composition may vary slightly depending on the origin.</p>
Tween -20	C <sub>26</sub> H <sub>50</sub> O <sub>10</sub>		<p>Non-ionic surfactant, miscible in water, alcohol and displaying a HLB value of 16.7. Tween 20 is sensitive to light and temperature.</p>

Table 3.4 List of active hydrogen sources used in this work

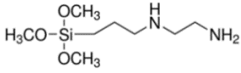
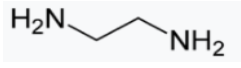
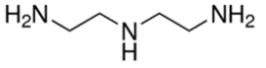

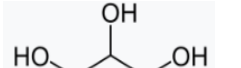
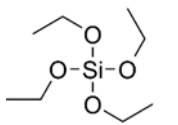
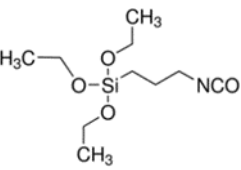
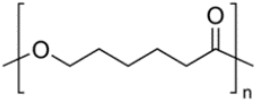
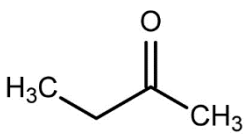
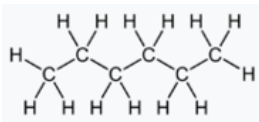
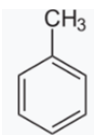
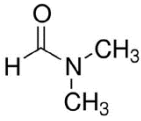
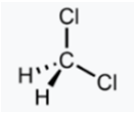
Name	Chemical formula	Molecular structure	Description
3-(2-Aminoethylamino) propyltrimethoxysilane (Aminosilane)	$(\text{CH}_3\text{O})_3\text{Si}(\text{CH}_2)_3\text{NHCH}_2\text{CH}_2\text{NH}_2$		This silane has amino groups, which can react with -NCO groups of organic phases, giving better strength to the shell.
Ethylenediamine (EDA)	$\text{C}_2\text{H}_4(\text{NH}_2)_2$		A liquid, colourless organic compound with an ammonia-like odor and strongly basic. EDA when used as a monomer, soluble in water, tends to diffuse to the organic phase, forming a shell. Due to its short molecular chain, the stability of the emulsion might be destroyed by the fast diffusion and might result in a thick shell.
Diethylenetriamine (DETA)	$\text{HN}(\text{CH}_2\text{CH}_2\text{NH}_2)_2$		A liquid colourless, hygroscopic organic compound, which is soluble in water and polar organic solvents and has longer chain when compare to EDA, so its diffusion is slower. DETA can generate branched polymer in reaction with organic phase and can increase the stability of emulsion.
1,6 Hexanediol	$(\text{HOCH}_2(\text{CH}_2)_4\text{CH}_2\text{OH})$		Colourless crystalline solid that melts at 42 °C and boils at 250 °C. It is soluble in water and acts as a chain extender in the synthesis of the MCs.
Glycerol	$\text{C}_3\text{H}_8\text{O}_3$		Glycerol is a simple polyol compound. It is a colorless, odourless and a viscous liquid.
Tetraethyl orthosilicate (TEOS)	$\text{Si}(\text{OC}_2\text{H}_5)_4$		A colourless liquid that is not stable in water (tends to hydrolyse and condensate). It is the ethyl ester of ortho silicic acid, $\text{Si}(\text{OH})_4$ . It is the most typical alkoxide of silicon.
3-(Triethoxysilyl) propyl isocyanate (TPI)	$\text{C}_{10}\text{H}_{21}\text{NO}_4\text{Si}$		Silane that contains double functionality: —NCO and —OCH <sub>2</sub> CH <sub>3</sub> . Due to the high reactivity of these functional groups, it has been often used as a crosslinking reagent in the synthesis reactions and self-assembling agent in hybrid materials.
Polycaprolactone (PCL)	-----		A semi-crystalline polymer having glass transition temperature of -60 °C and melting point ranging between 59 and 64 °C.
Pearlstick® 45-50/18	-----	-----	An elastic, linear, aromatic polyurethane prepolymer formulation for adhesives, supplied in the form of white spherical granules with an extremely high crystallization rate and a medium-low thermoelectricity level. It has hydroxyl No.= 0.1%

Table 3.5 List of solvents used in this work

Name	Chemical formula	Molecular structure	Description
2-Butanone (MEK)	$\text{CH}_3\text{C}(\text{O})\text{CH}_2\text{CH}_3$		Organic solvent compound. This colourless liquid ketone has a sharp, sweet odour reminiscent of butterscotch and acetone, with boiling point around 79.64 °C.
n-Hexane	$\text{C}_6\text{H}_{14}$		Alkane of six carbon atoms. It is a colourless liquid at RT, odourless when pure, with boiling points between 50 and 70 °C. It is widely used, being a cheap, relatively safe, largely unreactive, easily evaporated, and non-polar solvent.
Toluene	$\text{C}_6\text{H}_5\text{CH}_3$		Clear, water-insoluble liquid with the typical smell of paint thinners. It is an aromatic hydrocarbon that is widely used as an industrial feedstock and as a solvent with boiling point around 111 °C.
Dimethylformamide (DMF)	$(\text{CH}_3)_2\text{NC}(\text{O})\text{H}$		Colourless liquid which is miscible with water. It is an organic compound with boiling point between 152 to 154 °C.
Dichloromethane (DCM)	$\text{CH}_2\text{Cl}_2$		Liquid, colourless, volatile organic compound with a moderately sweet aroma

### 3.2 General steps to perform the syntheses

The general procedure to prepare the MCs is described below. The synthesis can be performed in the glass reactors, as it is shown in Figure 3.1, or in common plastic containers, as it shown in Figure 3.2.

**1<sup>st</sup> Step**-Preparation of aqueous solution by addition of GA, as a surfactant, to Milli-Q water and mixing by mechanical stirring or shaking well to achieve a homogeneous solution without any solid particles.

**2<sup>nd</sup> Step**-Preparation of organic phase by addition of solvent (if applicable) to the isocyanate and stirring for several minutes with a glass rod.

**3<sup>rd</sup> Step**-Preparation of emulsion by addition of organic phase to aqueous phase, following by high shear mixing at a stirring speed of 3200 rpm with Ultra-Turrax IKA T25, during 10 min at room temperature (RT), to obtain a stable emulsion.

**4<sup>th</sup> Step**-Stirring of the emulsion at 400 rpm by using a mechanical stirrer (Heidolph RZR 2051 control, or Jank &Kunel IKA-Werk RW 20 DZM). Addition, dropwise, of another aqueous solution containing active hydrogen sources, while the temperature will be increased gradually from RT to the synthesis temperature (55-77°C). Heating by a hot plate (Nahita-blue 692). The process should continue during several hours until the MCs shell attains enough maturity to tolerate filtration pressure.

**5<sup>th</sup> Step**-Vacuum filtration in a Buchner funnel by using proper filter paper and washing with water or other solvents.

**6<sup>th</sup> Step**-Drying in atmospheric pressure at RT during 24hr.

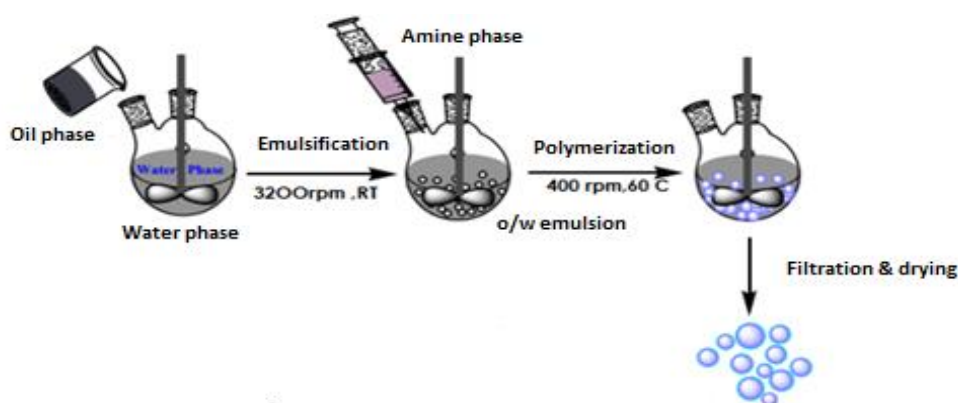


Figure 3.1 Schematic representation of synthesis, (adapted from (Tatiya, 2016))

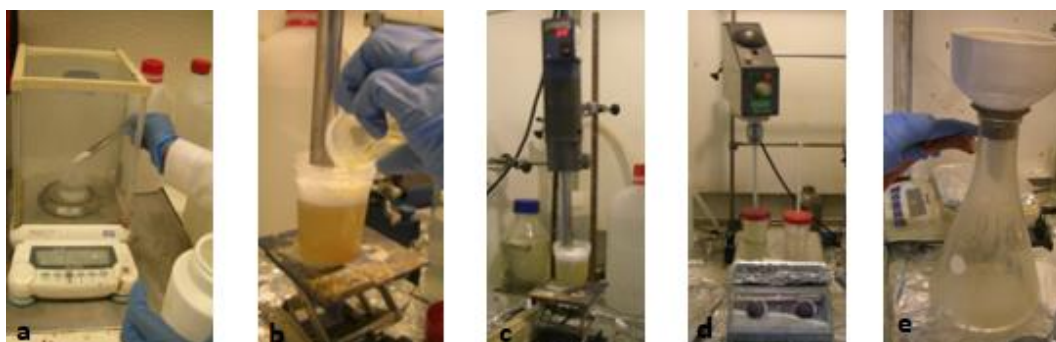


Figure 3.2 Different steps of MCs preparation in laboratory a) 1st step, b) 3rd step, c) 3rd step, d) 4th step, e) 5th step

From the early moment of the 3<sup>rd</sup> step of the synthesis until the last minutes of the 4<sup>th</sup> stage, continuous monitoring of the emulsion quality by means of optical microscopy is necessary, to control the stability of the emulsion, to check the size and shape of the droplets, as well as the maturity degree of the shell. Figures 3.3 (a, b, c) show pictures (from optical microscopy) of the droplet/MCs, from the early moment



of emulsion formation to the end of the synthesis process (after filtration and washing), while Figures 3.3 (c , e) show the typical powdery appearance of the MCs after the synthesis process and SEM photomicrograph of a broken microcapsule respectively.

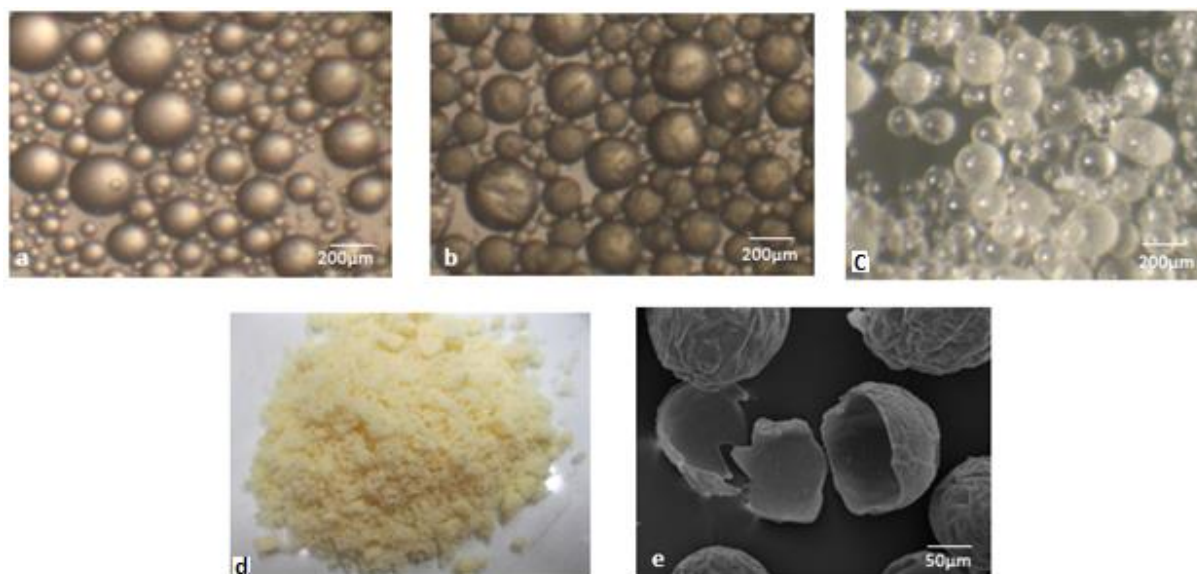


Figure 3.3 Optical microscopy image (a) in the early stage of the emulsion formation, (b) after 1 hour of mechanical stirring; the shell has already been formed, but it is still a thin and fragile polymeric layer, (c) MCs right after filtration (d) Image from Canon camera, MCs right after filtration, (e) SEM image of MC's broken shell, exhibiting a core-shell morphology.

### 3.3 Testing and characterization

The main physical characterization and testing methods employed in this work include optical microscopy, scanning electron microscopy (SEM), as well as peeling strength test, to evaluate the features, morphology, shape and performance of the MCs, as well as their interaction with the polyol based component. Regarding chemical characterization techniques, Fourier transformed infrared spectroscopy (FTIR) and thermogravimetric analysis (TGA) were the ones employed.

#### 3.3.1 Physical testing and characterization

##### Characterization by Optical Microscopy

Characterization and evaluation of the emulsions and MCs were performed right after starting the synthesis by continuous sampling and observation using optical microscope, to evaluate the stability of emulsion, size of droplets and maturity of MCs' shell. The microscope used was a Kruss, MSZ 5600 optical microscope. Moreover, after collection and drying the MCs, optical microscopy was employed to evaluate them in terms of size, shape and aggregation state. The microscope used, was a Nikon microscope OPTIPHOT2-POL.

### Characterization by Scanning Electron Microscope (SEM)

SEM analysis was employed to evaluate the morphology of the MCs. The SEM analysis was performed to evaluate almost 40% of all the obtained MCs batches, by employing a JEOL JSM7001F with FEG (field emission gun) microscope.

### Peeling strength test

The peeling strength test was performed with the purpose of confirming the successful release of the MCs core content and its reaction with the surrounding environment (polyol based component), in response to certain stimuli, such as temperature and pressure. This is critical to evaluate the adhesive effectiveness in the bonding process. Figure 3.4 shows a graphical representation of the three basic ways in which an adhesive bonded joint may fail: i) in one of the adherents outside the joint (structural failure), ii) by fracture of the adhesive layer (cohesive failure), iii) interfacial failure, between the adhesive and one of the adherents (adhesion failure).

Typically, cohesive failure results from the fracture of the adhesive and is characterised by the clear presence of adhesive material on the matching faces of both adherents. Failure happens, usually by shear, or peel stresses, or by a combination of them.

Adhesive failure is typically characterised by the absence of adhesive on one of the bonding surfaces. It occurs along the interface between the adhesive layer and the adherents and it is due to the lack of chemical or physical bonds, which form the link between the adhesive and the surface. In the case of structural failure, both adhesive and chemical or physical bonds between adhesive and substrate are strong enough and the failure tends to occur within the substrate. This latter one is our target in terms of failure of the adhesive joint.

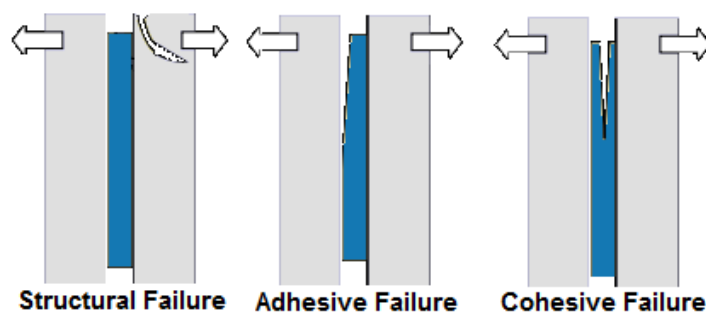


Figure 3.4 Failure types of adhesive joints, (adapted from <http://theadhesivesexpt.com>,22/8/2017)

In this test, a certain quantity of MCs was mixed with polyol. The mixture was then applied on the surface of a paper substrate by using a “Wet film thickness applicator”. This will be discussed in more detail in chapter 3.7. Additional equipment used to perform these tests are a hot plate (Thermaplate JAME H HELA) to apply a controlled temperature without any load and a hot press machine (CARVER, Model M, S/N 2000-3 62) to apply a controlled load and temperature.

### **3.3.2 Chemical testing and characterization**

#### **Characterization by Fourier Transformed Infrared Spectroscopy (FTIR)**

FTIR characterization was used in this work to analyse the chemical structure of the MCs obtained, in particular to confirm the presence of the unreacted NCO groups in the MCs core and to make a comparative (relative) evaluation of their quantity, among different syntheses. This characterization technique was also used to confirm the presence of other characteristic groups, to verify the presence of certain compounds in the shell. The FTIR equipment used was a Nicolet 5700 FTIR (Thermo Electron Corporation, USA), equipped with a Smart iTR™ Attenuated Total Reflectance (ATR) sampling accessory. Spectra were obtained at 8 cm<sup>-1</sup> resolution with a data collection of 16 scans.

#### **Characterization by Thermogravimetric Analysis (TGA)**

TGA was carried out to measure the mass loss of the MCs along a certain range of temperature under a controlled N<sub>2</sub> atmosphere, with the main objective of determining the core content or encapsulation capability of the MCs. TGA and FTIR together are complementary techniques to evaluate the encapsulation yield of the MCs. The analyses were performed in a nitrogen atmosphere, at a temperature increase rate of 10 °C min<sup>-1</sup> using a TGA HITACHI STA 7200.

## **4 Main studies: Results and discussion**

### **4.1 Study of the synthesis parameters**

Figure 4.1 shows the flow diagram related to the systematic experiments carried out with the goal of studying the role played by the varied synthesis parameters in the preparation of the MCs. Some of these studies and their related results are reported in chapters 4.1.1 to 4.1.4, while the others will be reported at the end of each group of synthesis in chapter 4.2.

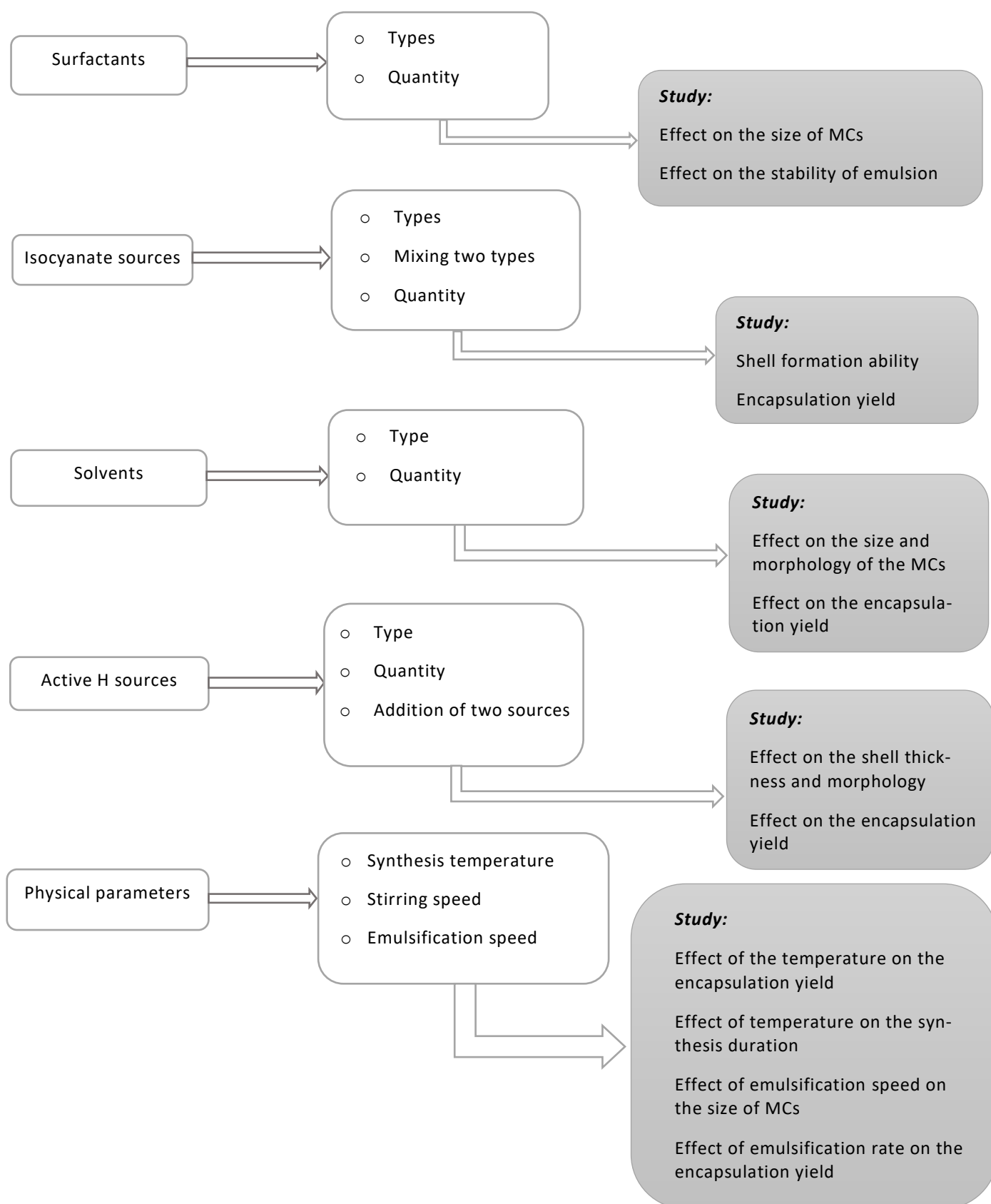


Figure 4.1 Schematic representation of the varied synthesis parameters, considering the different studies involved.

#### 4.1.1 Effect of concentration of surfactant on the droplets' size and emulsion stability

In this study, first, a solution of GA in Milli-Q water was prepared at different concentrations, then the mixture of Ongronat 2500 (ongronat) and IPDI was added to the aqueous solution and emulsification was performed by high shear mixing at 3200 rpm, by using an ULTRA –TURRAX, during 10 min at RT. The emulsion features were then evaluated by using an optical microscope and the size of the emulsion droplets was measured, being listed in Table 4.1. There is a large range of droplets' size for each synthesis, however a trend in terms of a decrease in the size of the droplets is observed, with the increase in the surfactant quantity.

Table 4.1 Effect of GA concentration on the stability of the emulsion and size of droplets

Synthesis No.	GA (wt%)	Amount of GA (gr)	Size of Droplets ( $\mu\text{m}$ )
IP-147	2	1.3	70-250
IP-131	5	3.3	50-220
IP-148	7	4.6	40-180
IP-149	10	6.6	30-150
IP-150	13	8.6	10-110

The same experiences were repeated by using DC 193 as a surfactant, instead of GA, however, the emulsion was stable only in a narrow range of surfactant concentration (from 2.5 to 3.5 wt%). So, it was not possible to study the effect of DC 193 concentration on the droplets' size. A loss in emulsion stability, for varied temperatures and surfactant concentration, was also observed for Tween 20, as shown in Figure 4.2. The reason can be the drastic change in the emulsion temperature due to improper work of the high shear mixer, as Tween -20 is quite sensitive to temperature changes. So, after several attempts this surfactant was removed from the list of primary materials.

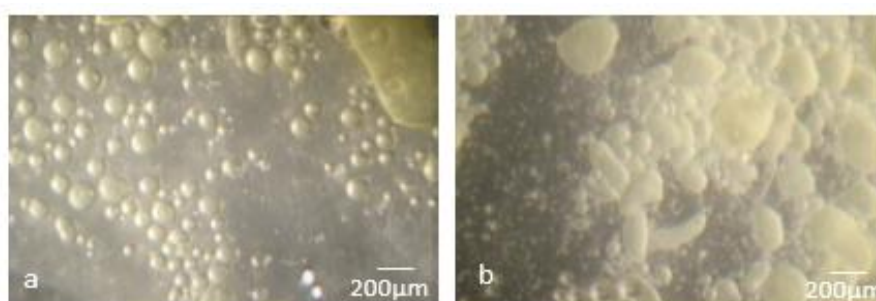


Figure 4.2 a) Instability in emulsion (droplet coalescence), after 3 mins of high shear stirring, using surfactant Tween -20 b) Droplet coalescence formed after 5 mins of high shear stirring, using surfactant DC 193.

## Conclusions

- This study revealed that by increasing the quantity of GA, the size of droplets tends to decrease, as shown in table 4.1.
- The stability of the emulsion and the shape of the droplets is not affected by GA concentration, when this ranges changes from 2 to 13 wt%. According to the literature, the concentration of GA can be increased up to 22 wt%, without any instability in emulsion formation (Yeganeh, 2016), but as it was difficult to measure smaller droplet sizes, the experiences were stopped by reaching 13 wt% of GA in this work.
- In the case of DC193, a stable emulsion with spherical droplets was obtained just in the narrow range of 2.5-3.5 wt%, when using the same quantity of aqueous phase and same type and quantity of organic phase.
- To complete the conclusion and according to observations during the whole syntheses in this work, the right quantity of GA, to obtain the required MCs size, will be slightly different when using different isocyanate compounds, so some fine tuning should be done when changing the type of organic phase.

### 4.1.2 Effect of variation of emulsification speed in the droplets' size

In this study, an aqueous solution of GA (5 wt%) was mixed with the organic phase (a mixture of Ongronat and IPDI). The emulsification was performed by high shear rate mixer (Ultra-Turrax) at different stirring speeds for 10 mins at RT. The resulting emulsion quality and the droplets' size were evaluated using optical microscope. Table 4.2 shows the synthesis's information and results of the size measurements and Figure 4.3 shows the optical photomicrographs related to these syntheses.

Table 4.2 Variation of droplets' size for different rotation speed in the emulsification process

Synthesis No.	Emulsification speed (rpm)	Size of droplets ( $\mu\text{m}$ )
IP-131	3200	35-220
IP-144	5000	18-160
IP-145	7200	10-90
IP-146	9000	6-70

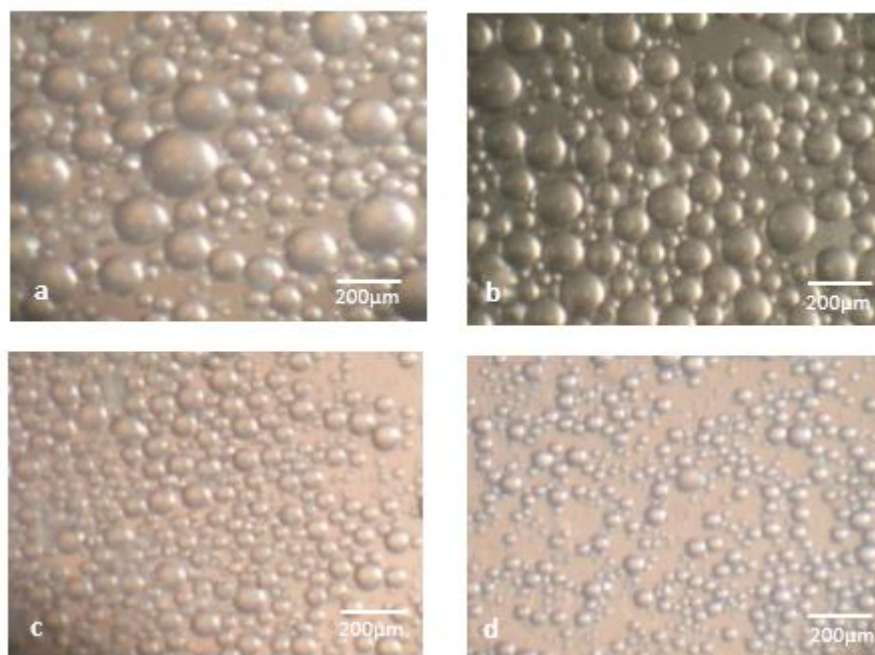


Figure 4.3 Effect of changing the emulsification rate on the size of droplets a) 3200 rpm, b) 5000 rpm, c) 7200 rpm, d) 9000 rpm

## Conclusions

- As shown in table 4.2, by increasing the emulsification speed, the average size of the droplets significantly decreases. Tsuda et al. have reported the same behaviour for a similar experiment (Tsuda, 2011). Thus, it is possible to control the MCs size by changing the emulsification speed.

The emulsion stability was obtained after 3 mins stirring. After a pause on the stirring process of 30 minutes the emulsion was still stable.

### 4.1.3 Effect of changing the synthesis temperature in the duration of the synthesis and efficiency of encapsulation

For performing this study, one of the synthesis with the best encapsulation efficiency was chosen to be repeated at different temperatures. The mixture of IPDI and Ongronat as an organic phase was added to the solution of 5 wt% GA in distilled water, 3200 rpm emulsification speed was used to prepare an emulsion, which was then transferred to a hot plate and stirred at 400 rpm by using a mechanical stirrer. The aqueous solution of 3-(2-Aminoethylamino) propyltrimethoxysilane (aminosilane) was added to the emulsion, dropwise. After 1hr, TEOS was also added to the emulsion, dropwise. This synthesis was repeated four times while the temperature was the only parameter being changed. Table 4.3 shows the synthesis's data and results on the synthesis duration and MCs size and. It should be noted that the

synthesis time reported in Table 4.3. was the one required for achieving mature, solid shells, except for the synthesis carried out at the lowest temperature, where 6 hr was still not long enough to exhibit a mature shell.

Table 4.3 Variation of synthesis time due to temperature change

Synthesis No.	Temperature(°C)	Time (hr)	Size of MCs (µm)
IP-130	40-50	6	20-100
IP-64	40-65	4.5	50-150
IP-73	60-70	4	50-180
IP-126	75-77	3.5	50-150

Figures 4.4-4.10 show the SEM photomicrographs of MCs obtained from these syntheses. As it is observed in these images, the MCs obtained from syntheses IP-64, IP-73 and IP-126 are not aggregated and have spherical shape with a core-shell morphology. While in the synthesis IP-130 after 6hr, MC's shell was still not mature enough to do filtration. The synthesis was stopped as it was not possible to proceed during the night, for safety reasons. SEM photomicrograph of these MCs (Figure 4.4) shows completely aggregated MCs, due to leaching or breaking of the shell during filtration, as it was expected.

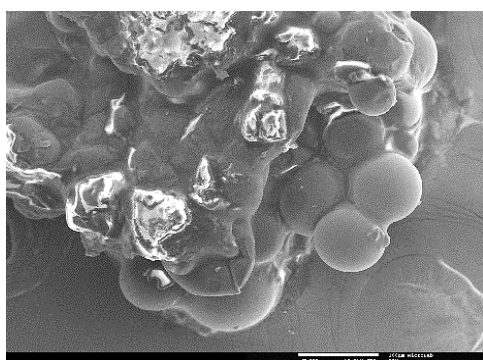


Figure 4.4 SEM photomicrograph, IP-130, Scalebar=100µm



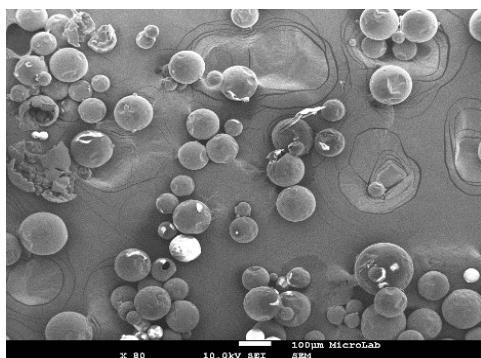


Figure 4.5 SEM photomicrograph, IP-64, Scalebar=100 $\mu$ m

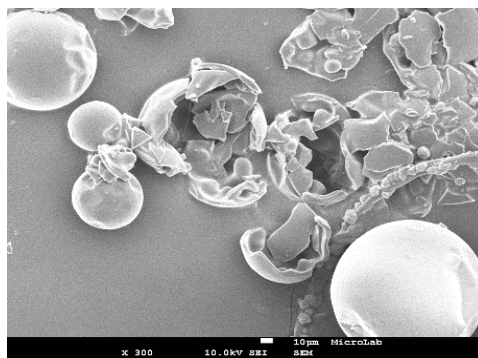


Figure 4.6 SEM photomicrograph, IP-64 Scalebar=10 $\mu$ m

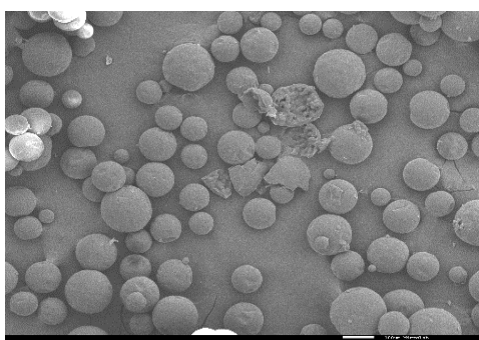


Figure 4.7 SEM photomicrograph, IP-73, Scalebar=100 $\mu$ m

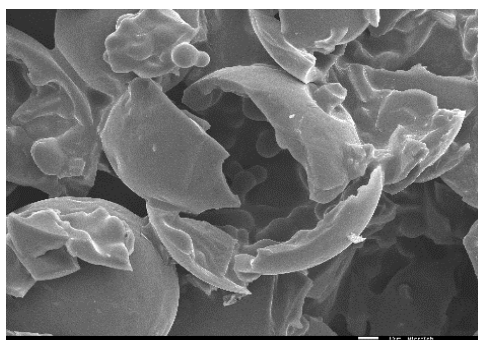


Figure 4.8 SEM photomicrograph, IP-73, Scalebar=10 $\mu$ m

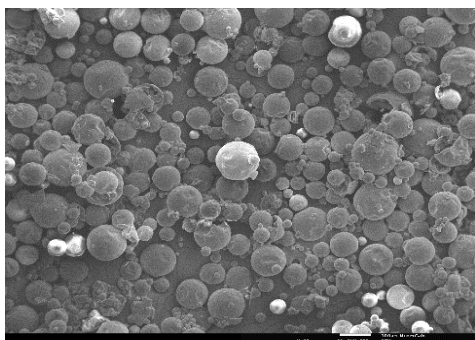


Figure 4.9 SEM photomicrograph, IP-126, Scalebar=100 $\mu$ m

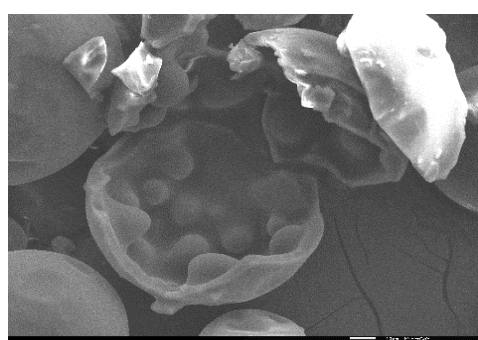


Figure 4.10 SEM photomicrograph, IP-126, Scalebar=10 $\mu$ m

Figure A1 in appendix-A shows the FTIR spectra of these MCs. The intense peak in the range of 2280-2260  $\text{cm}^{-1}$  is related to N=C=O stretch vibration bond, which shows the presence of unreacted NCO groups in the MCs, i.e. a successful encapsulation of IPDI. The peaks ascribed to the N-H stretching of the amine bonds at 3200-3400  $\text{cm}^{-1}$ , N-H bending at 1510  $\text{cm}^{-1}$ , carbonyl groups at 1700  $\text{cm}^{-1}$  (C=O from urethane) and at 1660-1690  $\text{cm}^{-1}$  (C=O from urea), C=C at 1522  $\text{cm}^{-1}$  and C-O-C at 1214  $\text{cm}^{-1}$  confirm the presence of urethane and urea linkages, i.e. an evidence that the shell is composed by polyurethane and polyurea. The presence of a peak at 1070  $\text{cm}^{-1}$ , typical of Si-O-Si asymmetric stretching vibrations, shows the presence of siloxane Si-O-Si moieties in the shell, derived from the silanes employed in the synthesis. Further calculation was carried out to estimate a relative measure of the encapsulation efficiency, by considering the peak area in the range of 1926 to 2444  $\text{cm}^{-1}$ , for -NCO, the peak area in the range of 1754

to  $1670\text{ cm}^{-1}$ , related to PU and/or PUa (carbonyl groups) and the peak area in the range of  $1090$  to  $1026\text{ cm}^{-1}$ , for Si-O-Si, as it is shown in Figure 4.11 The peaks area was calculated using OriginPro 8 software, and the relative encapsulation yield were calculated based on equation.7 as follows:

$$Y = \frac{Area_{NCO}}{Area_{PU+PUa} + Area_{Siloxane}} \quad \text{Eq.7}$$

where Y can be considered as a relative encapsulation yield, which represents an indirect measure of the encapsulation efficiency and  $Area_{NCO}$ ,  $Area_{PU+PUa}$  and  $Area_{Siloxane}$  represent the area related to the NCO, PU+PUa and siloxane related peaks, respectively.

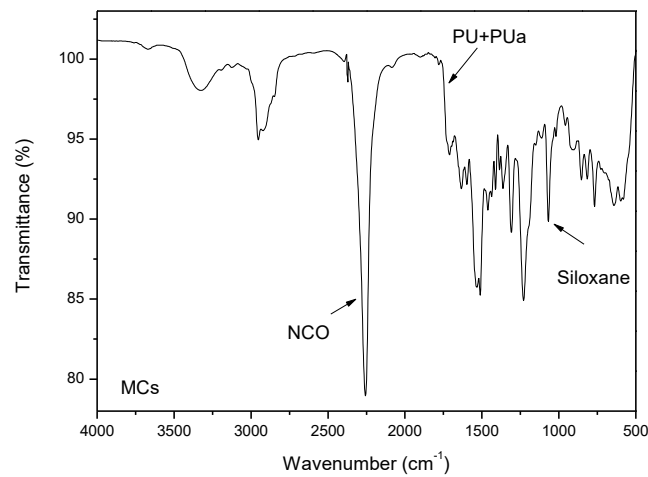


Figure 4.11 Typical FTIR spectrum of the MCs developed, showing the peaks involved in the area calculation for the relative encapsulation yield (Y) determination

The results obtained from the calculation of relative encapsulation yield (Y) are 5.7, 6.4, 4.12, 7.8 for IP-130, IP-64, IP-73 and IP-126 respectively, which are exhibiting a scattered behaviour, as the FTIR analyses were carried out after 45 or 30 days for some of the samples and after 5 or 10 days for others. These results suggest that the shell might be not fully dense or compact enough, so that, after the synthesis, part of the NCO groups might keep on reacting with the moisture of the outside environment, so the unexpected result can be related to the fact that, humidity was diffused throughout the MCs shells, consuming part of the NCO groups and therefore reducing the relative encapsulation yield. By repeating the SEM analyses (Figure 4.12), the shell thickness for MCs obtained from IP-73 was found to be much thicker, after 2 months, with a small core still remaining, corroborating such hypothesis.

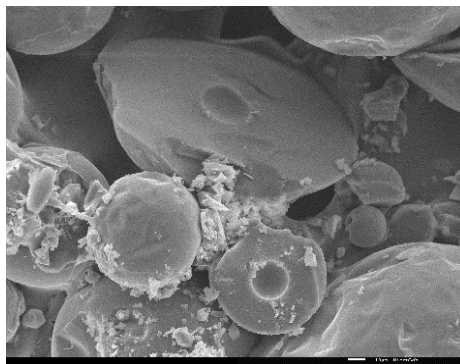


Figure 4.12 SEM photomicrograph, IP-73, Scalebar=10 $\mu$ m

## Conclusions

- As shown in Table 4.3, by increasing the temperature of the synthesis, the total duration of the synthesis, until a mature shell is formed, tends to decrease.
- A temperature range of 40-50 $^{\circ}$  C, is found not appropriate for the interfacial reaction to occur, within the studied timeframe. This range of temperature tends to slow down the polymerisation phenomenon and increase the reaction duration significantly.
- The size of the MCs is around 50 to 180  $\mu$ m, except for synthesis IP-130 (40-50 $^{\circ}$  C), where a significant reduction is observed. The low temperatures might facilitate the stability of the emulsion, avoiding droplet coalescence, or another reason could be the division of droplets to smaller one's due to the long-time stirring, while the shell was not still mature enough.

### 4.1.4 Effect of variation of mechanical stirring rate on the encapsulation efficiency

This study was carried out based on the same synthesis mentioned in chapter 4.1.3, but the temperature was fixed in the range of 60-65 $^{\circ}$  C for all syntheses, while stirring rate was changed to study the effect of this parameter. Table 4.4 shows data and some results related to these syntheses.

Table 4.4 Summary of results, due to stirring speed changing

Synthesis No.	Stirring speed (rpm)	Size of MCs ( $\mu$ m)	Synthesis Time (hr)	Y
IP-121	200	40-150	4	5.6
IP-74	300	50-150	4	4.14
IP-123	600	50-150	3	4.06

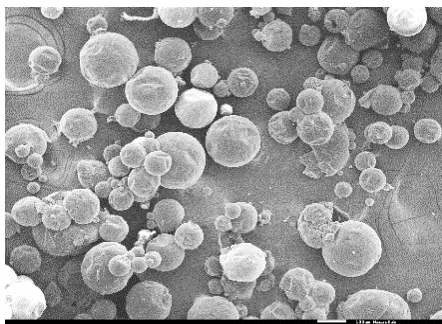


Figure 4.13 SEM photomicrograph, IP-121, Scalebar=100 $\mu$ m

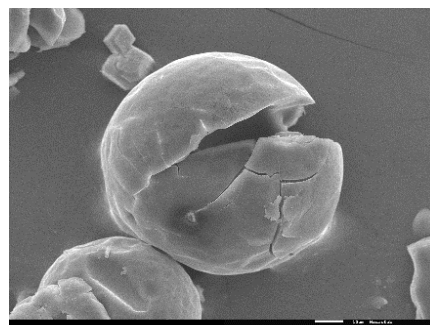


Figure 4.14 SEM photomicrograph, IP-121, Scalebar=10 $\mu$ m

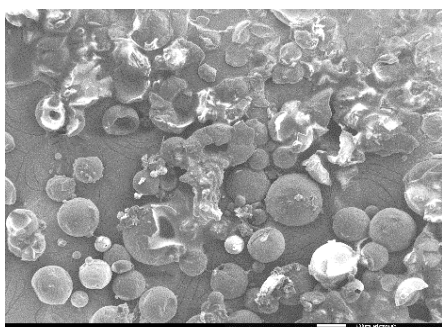


Figure 4.15 SEM photomicrograph, IP-74, Scalebar=100 $\mu$ m

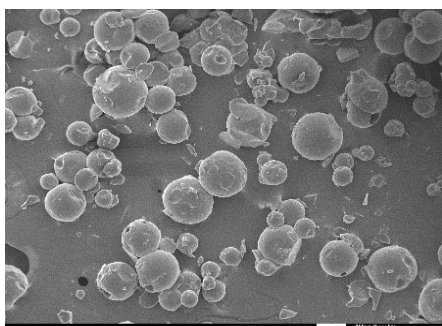


Figure 4.116 SEM photomicrograph, IP-123, Scalebar=100 $\mu$ m

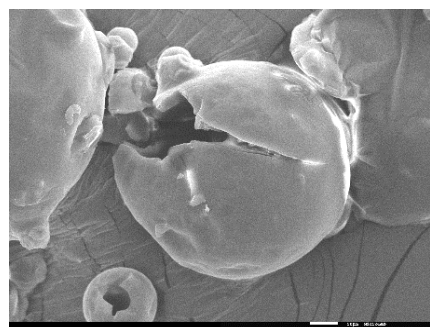


Figure 4.17 SEM photomicrograph, IP-123, Scalebar=10 $\mu$ m

Figures 4.13 to 4.17 show the SEM photomicrographs of the MCS obtained in this study. Evaluation by optical microscopy and SEM, show some degree of aggregation for MCs obtained from synthesis IP-121 and IP-74, which can be explained by low stirring rate (Figures 4.13 and 4.15). Figure A2 in Appendix -A shows the FTIR spectra of these samples. Again, the presence of an intense peak in the range of 2280-2260  $\text{cm}^{-1}$ , related to N=C=O stretch vibration bond confirmed the presence of unreacted NCO group in the MCs which means successful encapsulation of IPDI.

## Conclusions

- By increasing the stirring rate from 200 rpm to 600 rpm, the relative encapsulation yield was reduced from 5.6 to 4.1.

- By increasing the stirring rate, there is less aggregation of the MCs, so a compromise must be found, in terms of rotation speed, in order to reduce aggregation and increase encapsulation efficiency.

## 4.2 History of the syntheses

Several groups of synthesis were performed during this work, based on availability of primary material. At first the only available isocyanate compound, was Ongronat® 2500 and available surfactant was DC 193, thus several experiences were performed to achieve spherical shape MCs with intended size by changing the quantity of primary materials. The same experience was repeated by using GA, after this surfactant was available. This was followed by employing two different isocyanate compounds with different reactivity, in order to encapsulate less reactive group as a core and use the most reactive compound as a shell former. During these experiences, several active hydrogen sources were added to the aqueous phase to study their effect on the shell formation process, shell morphology and shell maturity. New syntheses campaigns were carried out by considering previous experience to encapsulate new materials. The total laboratory experiences took more than four months. The best syntheses were divided into twelve groups, according to the primary material used. Table B1 shows the history of those syntheses in more detail. Although it was possible to obtain spherical shape MCs with free NCO encapsulated within all groups, in the following chapters just the selected best results will be reported in more detail.

### 4.2.1 Group 1

This was the initial group of syntheses in this work, which were performed by using available primary materials, as shown in table 4.5.

**Objective:** The main objective of this series of syntheses was to learn and understand the microencapsulation process by micro emulsion and interfacial polymerization, as well as to identify the right quantity of each element of the synthesis e.g. surfactant, isocyanate compound, etc.

Table 4. 5 Selected syntheses from group 1

Synthesis No.	Organic Phase	Aqueous phase	Surfactant	Active H source	Temperature (°C)	Stirring rate (rpm)
IP-27	Ongronat	Water+EDA	DC 193	W+Glycerol	65-70	300
IP-33	Ongronat	Water	GA	None	65-70	400

The MCs of this study show a spherical shape, without any tendency to aggregation (Figures 4.18, 4.19 and 4.20). MCs obtained from IP-33 have a smoother surface when compared to those obtained from IP-

27, which can be justified by fast diffusion of EDA (short molecular chain) that destroys the stability of the emulsion, resulting in a coarse shell morphology, as it was discussed in more detail in chapter 2.4.1 (Zhang, 2009).

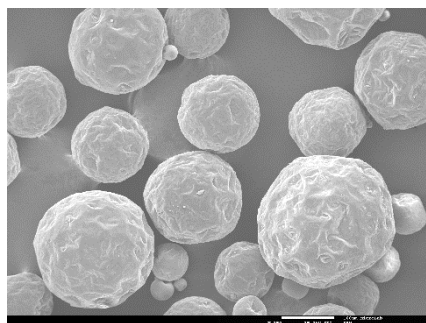


Figure 4.18 SEM photomicrograph of IP-27, Scalebar=100 $\mu$ m

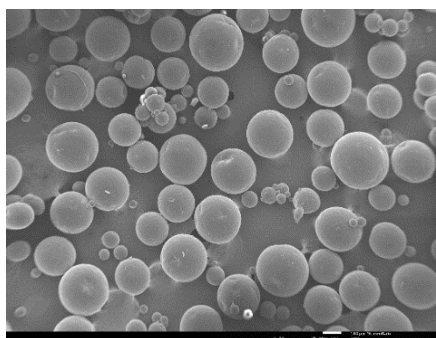


Figure 4.19 SEM photomicrograph of IP-33, Scalebar=100 $\mu$ m

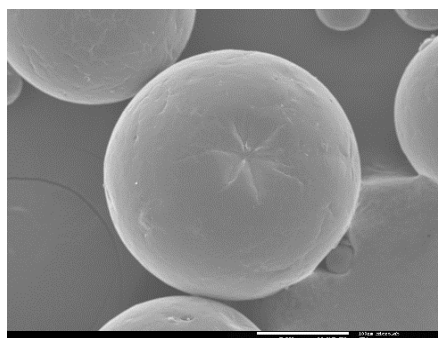


Figure 4.20 SEM photomicrograph of IP-33, Scalebar=100 $\mu$ m

The FTIR spectra in Figure A3 (appendix A) show an intense peak in the range of 2280-2260  $\text{cm}^{-1}$  related to N=C=O stretch vibration bond, which exhibits the presence of unreacted NCO group in the MCs, as well as a peak at 1533  $\text{cm}^{-1}$  from N-H bending, which derives for the presence of Ongronat, but also shows the formation of urethane and urea linkages, belonging to the shell. The sample prepared with EDA, as expected, has a more intense peak at 1533  $\text{cm}^{-1}$ . Also, there is a band peaked at ca. 1697  $\text{cm}^{-1}$  ascribed to the carbonyl groups of urethane and urea moieties, confirming that the formed shell is made of PU/PUa. On a first sight, the FTIR spectra of both samples are quite similar, but the band ascribed to the presence of NCO groups has some differences and the calculation of the relative encapsulation yield, carried out based on Eq-7, resulted in different values. Table 4.6 shows a summary of information, obtained from characterization by optical microscopy, SEM and FTIR.

Table 4.6 Group 1, summary of results

Synthesis No.	MCs Surface morphology	MCs size ( $\mu\text{m}$ )	Y
IP-27	Rough	40-300	18.35
IP-33	Smooth	40-400	29.21

## Conclusions

- The right quantity of DC 193 and GA as surfactants employed in this group was fixed at 2.8 wt% and 5 wt% respectively, in order to obtain a stable emulsion and to have the desired MC size distribution with spherical shape.
- Addition of EDA to the aqueous phase in IP-27, helped to form spherical MCs without any excess polymerization out of MCs. The fact can be explained by the fast formation of compact shell, due to fast diffusion of EDA through the membrane toward organic phase, which on the other hand leads to a rougher shell surface.

### 4.2.2 Group 2

The conclusion from the 1<sup>st</sup> group of synthesis and literature review related to encapsulation of isocyanate compounds, suggested that there might be an advantage of employing two isocyanate compounds with different reactivity, in order to encapsulate less reactive compound, while the most reactive one reacts prevalently with active hydrogen compounds, to form PU and/or PUa shell. In this sense, it is expected to achieve a core-shell MC morphology, instead of matrix type MCs (Yeganeh, 2016; Nguyen, 2014; Lu, 2011)

**Objective:** The objective of the 2<sup>nd</sup> group of syntheses was to achieve a core-shell morphology of the MCs, by using a lower reactivity isocyanate compound (IPDI) and a higher reactivity isocyanate compound (Ongronat).

Table 4.7 Primary materials used in the best syntheses of group 2

Synthesis No.	Organic phase	Aqueous phase	Surfactant	Active H source	Temperature (°C)	Stirring rate (rpm)
IP-64	Ongronat +IPDI	Water	GA	Aminosilane +TEOS	65-70	400
IP-66	Ongronat +IPDI	Water	GA	DETA	65-70	400

Figures 4.21 and 4.22, show the SEM photomicrographs related to IP-64. MCs are spherical and present a core-shell morphology, with the diameter ranging from 50 to 150  $\mu\text{m}$  and the shell surface has a smooth appearance (Figure 4.22).

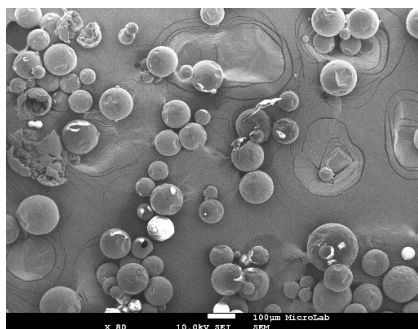


Figure 4.21 SEM photomicrograph of IP-64, Scalebar=100 $\mu\text{m}$

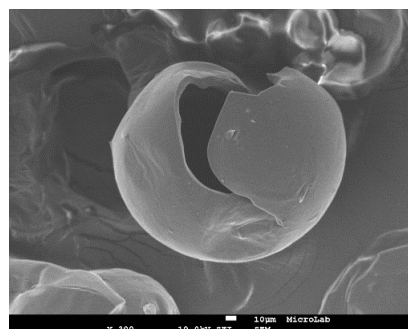


Figure 4.22 SEM photomicrograph of IP-64 Scalebar=10 $\mu\text{m}$

By optical microscopy (Figure 4.23), it was possible to follow what happens when a MC (just before the filtration step) is broken with the help of syringe needle, a significant amount of liquid core (isocyanate compound) is released from the MC.

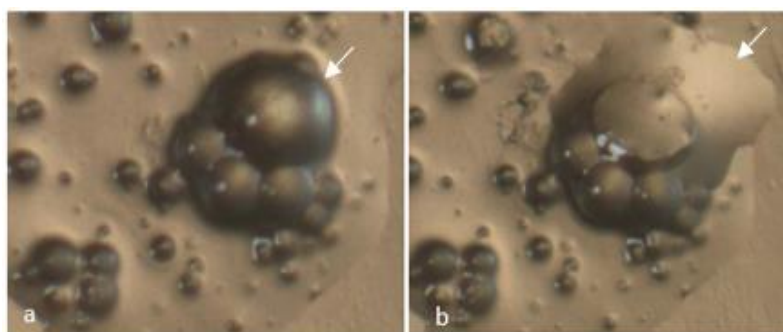


Figure 4.23 Optical microscope image a) MCs before tearing of shell by needle, b) The same image after breaking the shell

Regarding synthesis IP-66, where DETA was added as a hydrogen source, as previously discussed (in chapter 2.4.1), the long chain of DETA tends to slow down its diffusion towards the organic phase. Moreover,



a more cross-linked polymer is generated during reaction of MDI with DETA, which also may enhance the stability of the emulsion. The number of hydrophilic segments in amines plays an important role in the microstructure of the MCs (Zhang, 2009).

MCs from synthesis IP-66 present a larger size (80-180  $\mu\text{m}$ ) and there is no tendency to aggregation (Figure 4.24 and 4.25). Also, MCs from this synthesis appear to have a thinner shell than those from synthesis IP-64. The fact can be explained by shorter synthesis time due to higher reactivity of DETA and formation of branched or cross-linked polymer, when compared to the addition of aminosilane to the synthesis.

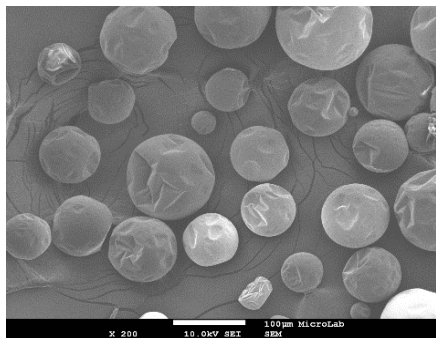


Figure 4.24 SEM photomicrograph of IP-66, Scalebar=100 $\mu\text{m}$

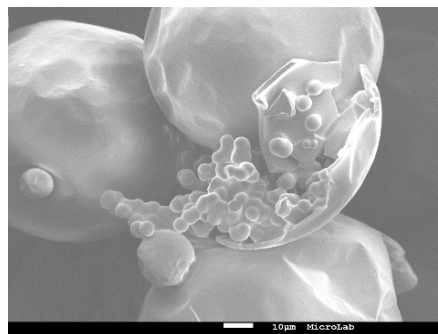


Figure 4.25 SEM photomicrograph of IP-66, Scalebar=10 $\mu\text{m}$

FTIR spectrum (Figure A4-appendix A) show the intense peak in the range of 2280-2260  $\text{cm}^{-1}$  related to N=C=O bond stretching vibration, which confirms the presence of unreacted NCO groups. The same calculation based on Eq-7 was used to obtain the relative encapsulation yields obtained for each synthesis. IP-66 exhibits a much larger relative encapsulation yield than IP-64 (Table 4.11).

TGA studies were performed for both MCs at a linear heating rate of 10  $^{\circ}\text{C}$  per min in nitrogen atmosphere, from RT to 600  $^{\circ}\text{C}$ . Table 4.8 represents general temperature ranges and related weight loss for isocyanate compounds, encapsulated by a PU and/or PUa shell. Generally, water and other solvents evaporation occurs at a first step. The next step is defined as the decomposition of encapsulated isocyanate and the last step is related to the shell decomposition which can be divided in two steps: decomposition of soft segments (derived from active hydrogen sources, chain extenders) and decomposition of hard segments. It should be stressed that there is an overlap resulting from the decomposition of isocyanate compounds (monomers and pre-polymers), PU and PUa material, so there is not exactly any border line to separate them. In particular there are references which mention that PU decomposition starts around 200  $^{\circ}\text{C}$  (Brochu, 2012), however the decomposition of isocyanate is also around this temperature (Yang, 2008; Li, 2011; Huan Yi, 2012). Also, it should be noted that the decomposition temperature range for encapsulated isocyanate compounds is slightly different from that of non-encapsulated ones, and such difference will depend on the shell thickness, composition and structure (Brochu, 2012; Koh, 2014).

Figure 4.26 shows the TGA results for IP-66 and IP-64. The two steps of weight loss, in the range of 220-260  $^{\circ}\text{C}$  and 260-310  $^{\circ}\text{C}$ , can be referred to decomposition of encapsulated isocyanate compounds. In fact,

the decomposition temperature for pure IPDI is reported in the range of 120-250 °C (Yang , 2008) but when encapsulated this temperature is slightly increased, which can be explained by protection of core contents by PU or PUa layers. However, shell decomposition is started around 310 °C and happens in two steps: a 1<sup>st</sup> step (310-370 °C) related to decomposition of soft segments and a 2<sup>nd</sup> step (above 370°C) related to decomposition of hard polymeric segments from PU and PUa parts of the shell (Koh, 2014). The same scenario with slightly different steps can be explained for IP-64. Tables 4.9 and 4.10 represent the related temperature ranges and mass loss for IP-66 and IP-64.

Table 4.8 Some of the temperature ranges and related phenomena, for TGA analyses

Temperature (°C)	Weight loss due to	Reference
≤ 100	Evaporation of solvent (with boiling point lower than 100°C) or water	(Koh, 2014)
120-250	Evaporation of IPDI	(Yang., 2008)
(145-204)-300	Evaporation of encapsulated IPDI	(Li, 2011;Huan Yi, 2012)
260–350	Decomposition of active H sources (chain extenders) or soft segments from the shell	(Koh, 2014)
360–490	Breakup of isocyanate hard domains of the MCs	(Koh, 2014)
200-650 (two steps)	Decomposition of PU	(Brochu, 2012)

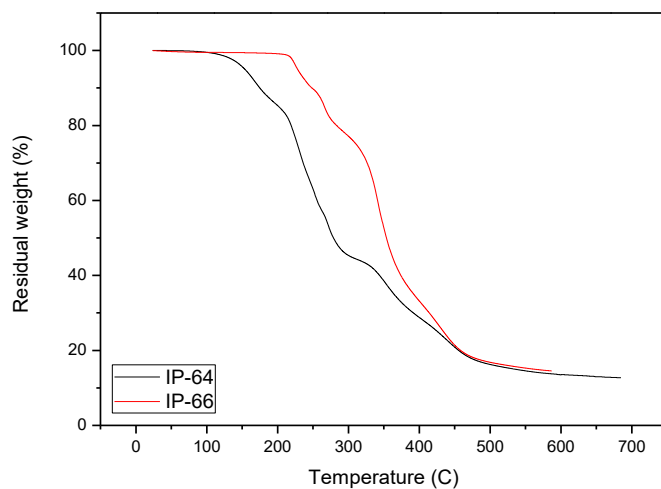


Figure 4.26 TGA for IP-64 & IP-66

Table 4.9 TGA results for IP-66

Steps	Water and/or solvent		Isocyanate compounds		Shell		Char (at 600°C)
	Temperature (°C)	Mass loss (%)	Temperature (°C)	Mass loss (%)	Temperature (°C)	Mass loss (%)	Mass (%)
1 <sup>st</sup>	100-214	1.4					
2 <sup>nd</sup>			214-249	9			
3 <sup>rd</sup>			249-317	15			
4 <sup>th</sup>					310-370	31	
5 <sup>th</sup>					370-470	22	
Total				1.4		24	

Table 4.10 TGA results for IP-64

Steps	Water and/or solvent		Isocyanate compounds		Shell		Char (at 600°C)
	Temperature (°C)	Mass loss (%)	Temperature (°C)	Mass loss (%)	Temperature (°C)	Mass loss (%)	Mass (%)
1 <sup>st</sup>	115-142	3					
2 <sup>nd</sup>			142-214	14			
3 <sup>rd</sup>					214-294	39	
4 <sup>th</sup>					294-343	6	
5 <sup>th</sup>					343-454	21	
Total				3		14	

Results from TGA analyses, in what regards encapsulated isocyanate compounds and MCs' shell, corroborate results from FTIR and SEM analyses. In fact, the amount of isocyanate (mass loss) is higher for IP-66, in conformity with the encapsulation relative yield calculated and the amount of shell material (mass loss) is lower for IP-66, in conformity with the thinner shells observed for IP-66. Table 4.11 shows the summary of results obtained from the characterization tests, which were performed to characterize these MCs.

Table 4.11 Group 2, Summary of results

Synthesis No.	MCs type	MCs size (µm)	Y	Core mass % from TGA
IP-64	Core-shell	50-150	6.47	14
IP-66	Core-shell	80-180	43.20	24

## Conclusions

- Obtaining core-shell MCs by using two different isocyanate compounds with different levels of reactivity is an important result obtained from this group of synthesis.
- IP-66 shows significantly higher encapsulation efficiency, which can be explained by the role of DETA in the final shell structure.
- Addition of different active hydrogen sources can affect size and shell structure of the MCs.

### 4.2.3 Group 3

Study effect of addition of 3-(Triethoxysilyl) propyl isocyanate(TPI) to the organic phase on the encapsulation efficiency.

**Objective:** In this group of syntheses (TPI) was added to the organic phase. As previously mentioned in Table 3.4, TPI contains double organic functionality, namely -NCO and ethoxy (OCH<sub>2</sub>CH<sub>3</sub> groups, which are hydrolysed, giving silanols) that can be used as a cross-linker and lead to the maturity of the shell, including a desired morphology and thickness of the shell. Synthesis IP-67 was the selected one from this group of synthesis.

Table 4.12 Primary material used in the best synthesis of group 3

Synthesis No.	Organic Phase	Aqueous phase	Surfactant	Active H source	Temperature (°C)	Stirring rate (rpm)
IP-67	Ongronat +IPDI+TPI	Water	GA	None	65-70	400

MCs from synthesis IP-67 exhibit, at the photomicrographs of Figures 4.27 to 4.29, a spherical shape with core-shell morphology and a thin shell, with some rough regions on the surface, probably due to the vacuum effect derived from the SEM operational procedure. Also, they are a little aggregated, but such aggregation could be easily eliminated by sonication. Evaluation of MCs by optical microscopy reveals a size distribution between 50 and 90 μm.

At the interface of the organic/aqueous phases the alkoxide groups (OCH<sub>2</sub>CH<sub>3</sub>) from TPI suffer hydrolyzation, forming silanols, which will react with the NCO groups, while the NCO groups from TPI will react with the OH groups from the aqueous phase. Also, the NCO groups from Ongronat prevalently tend to react with the aqueous phase, forming the shell material.

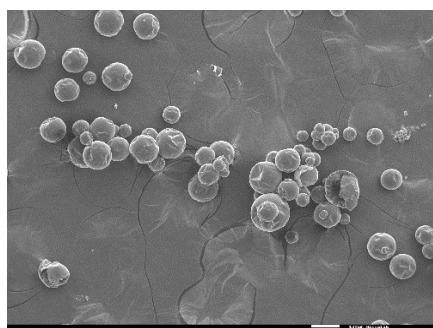


Figure 4.27 SEM photomicrograph of IP-67, Scalebar=100μm

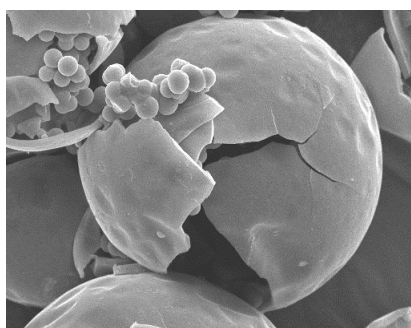


Figure 4.28 SEM photomicrograph of IP-67, Scalebar=10μm

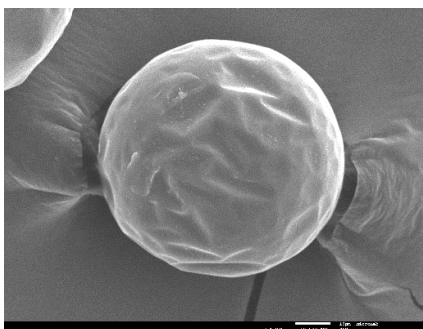


Figure 4.29 SEM photomicrograph of IP-67, Scalebar=10 $\mu$ m

As it can be observed from FTIR spectroscopy (Figure A5- Appendix-A), the intense peak in the range of 2280-2260  $\text{cm}^{-1}$  related to N=C=O stretch vibration bond, confirms the presence of unreacted NCO groups. Calculation based on Eq-7 was used to obtain the relative encapsulation yield. The summary of results is reported in Table 4.14.

As discussed before, mass loss of MCs, during TGA analyses, happens in several steps related to water and/or solvent loss, isocyanate core contents decomposition and shell decomposition. In Table 4.13 the different steps at the mass loss behaviour are represented according to the related TGA spectra in Figure 4.30.

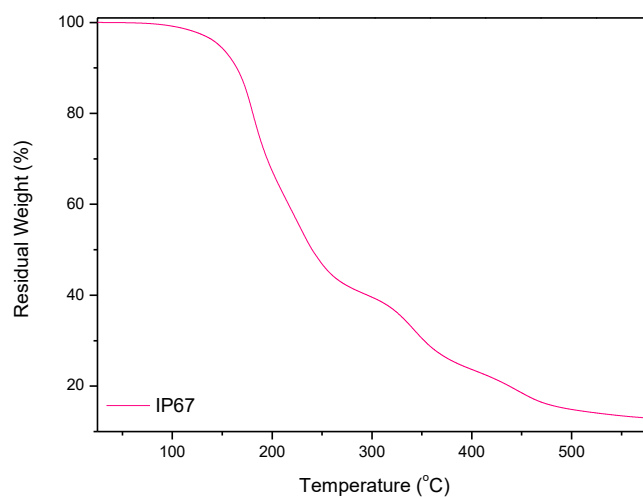


Figure 4.30 TGA for IP-67

Table 4.13 Summary of TGA results for IP-67

Steps	Water and/or solvent		Isocyanate compounds		Shell		Char (at 600°C)
	Temperature (°C)	Mass loss (%)	Temperature (°C)	Mass loss (%)	Temperature (°C)	Mass loss (%)	Mass (%)
1 <sup>st</sup>	70-130	2.5					
2 <sup>nd</sup>			130-186	20			
3 <sup>rd</sup>			186-207	10			
4 <sup>th</sup>			207-260	21			
5 <sup>th</sup>					260-322	7	
6 <sup>th</sup>					322-373	11	
7 <sup>th</sup>					373-440	11	
Total				2.5		51	

Table 4.14 Summary of synthesis results for IP-67

Synthesis No.	MCs type	MCs size (µm)	Y	Core mass % from TGA
IP-67	Core-shell	50-90	41.4	51

## Conclusions

- Microencapsulation of IPDI was performed successfully by addition of TPI to the organic phase without further addition of any other functional monomer to aqueous phase (besides water). This fact can be explained by the high reactivity of both functional groups of TPI. TPI appears to act as a coupling agent between the aqueous and the organic phase, in the sense that one of its end group reacts with the aqueous phase and the other end group reacts with the organic phase, assisting in the formation of the shell material, i.e. promoting crosslinking reactions within the shell.
- Significant microencapsulation efficiency, when compared with the last syntheses, is corroborated by both FTIR spectroscopy analysis and TGA.

#### 4.2.4 Group 4

After successful encapsulation of IPDI, in this group of syntheses several attempts were carried out, to encapsulate Ongronat. Several solvents and different active hydrogen sources were employed in this group as reported in Table B1.

**Objective:** The objective of this group of synthesis was defined as a microencapsulation of Ongronat by employing monomeric TDI, as higher reactivity isocyanate when compared with Ongronat. Table 4.15, shows the list of primary materials employed for the selected syntheses of this group.

Table 4.15 Primary material used in the best synthesis of group 4

Synthesis No.	Organic Phase	Aqueous phase	Surfactant	Temperature (°C)	Stirring rate (rpm)	Active H source
IP-83	Ongronat +TDI +n-Hexane	Water	GA	65-70	360	Aminosilane
IP-84	Ongronat +TDI +n-Hexane	Water	GA	65-70	400	DETA

MCs from IP-83 (Figures 4.31 and 4.32) have mostly spherical shape, with no tendency to aggregation. The size distribution of MCs is in the range of 70-200  $\mu\text{m}$ , with a shell thickness of ca. 10  $\mu\text{m}$ . As it is observed from SEM photomicrographs, internal surface of MC's shell looks smooth and the shell thickness seems to be uniform, when compared with previous cases. This fact can be due to the change of the solvent. n-Hexane was used in these syntheses, which can change the solubility of amine in the oil phase, as it was previously explained in chapter 2.4.1. The geometry of the PU shell has been reported to be primarily influenced by the solubility of the amine in the oil phase and can be tuned by the selection of the amine phase, oil phase, or the concentration of amine and isocyanate (Polenz, 2014). Moreover, the type of solvent influences the MCs formation by changing the interfacial tension of the medium (Ma, 2017).

Aminosilane, when incorporated into the aqueous phase tends to hydrolyse, forming silanol groups. Also, the amino groups tend to react with NCO groups at the interface of the aqueous/organic phases. The silanol groups, on the other hand, by polycondensation reactions, form siloxane moieties (FTIR peak assignment at ca. 1100  $\text{cm}^{-1}$ ), improving the mechanical strength and thermal resistance of the resulting shell, which will be a hybrid material based on PU/PUa and silica.

Figure 4.33 and 4.34 show the SEM photomicrograph of IP-84. The only difference between this synthesis and IP-83 was the type of active hydrogen source which is added to the synthesis. The obtained MCs from IP-84 (with DETA, instead of aminosilane) have spherical shape, the thickness of the shell in individual MCs looks uniform but, as it can be observed in Figure 4.33 and 4.34, the shell thickness varies approximately between 5 and 15  $\mu\text{m}$ , quite in line with the difference in the size of MCs. Smaller ones have higher active surface to volume (S/V) so, the interfacial reaction, for shell formation occurs significantly



faster than, in the case of the larger droplets, being the result a thinner shell. The successful encapsulation of Ongronat can be explained by reaction of amine groups of DETA with -NCO groups of TDI, and formation of a PUa shell.

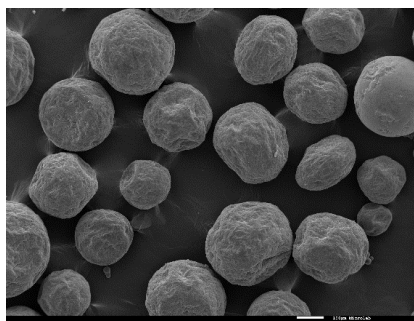


Figure 4.31 SEM photomicrograph of IP-83, Scalebar=100µm

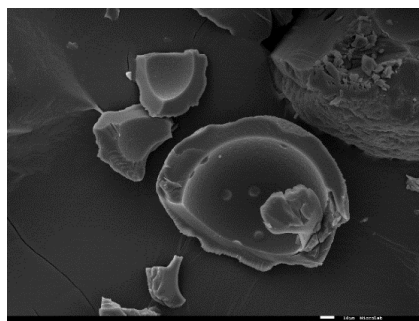


Figure 4.32 SEM photomicrograph of IP-83, Scalebar=10µm

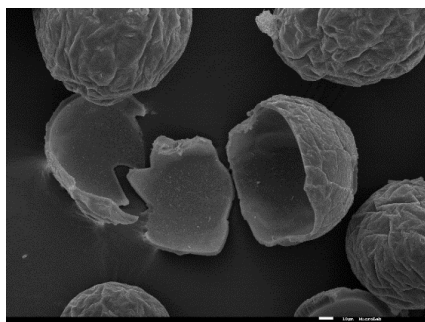


Figure 4.33 SEM photomicrograph of IP-84, Scalebar=10µm

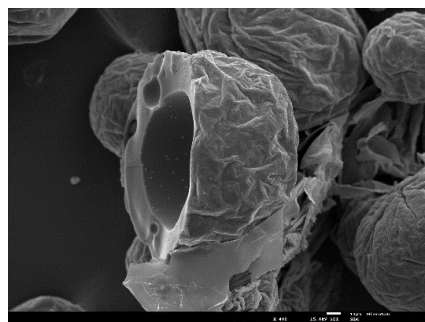


Figure 4.34 SEM photomicrograph of IP-84, Scalebar=10µm



Figure 4.35 SEM photomicrograph of IP-84, Scalebar=10µm

Again, the difference in surface morphology of the MC's shell, can be due to the difference in the partition coefficient ( $K_{ow}$ ) for aminosilane and DETA, as it was discussed in chapter 2.4.1.

FTIR spectra for IP-83 and IP-84 are shown in Figure A6 (Appendix-A) and confirm the presence of unreacted NCO, as there is an intense peak in the range of  $2280-2260\text{ cm}^{-1}$ . Calculations based on Eq.7, for

these two cases, revealed a significantly higher free NCO for IP-84, when compared with IP-83, as it is represented in Table 4.17.

Figure 4.36 shows the thermogram for synthesis IP-84. Table 4.16 lists some information extracted from it.

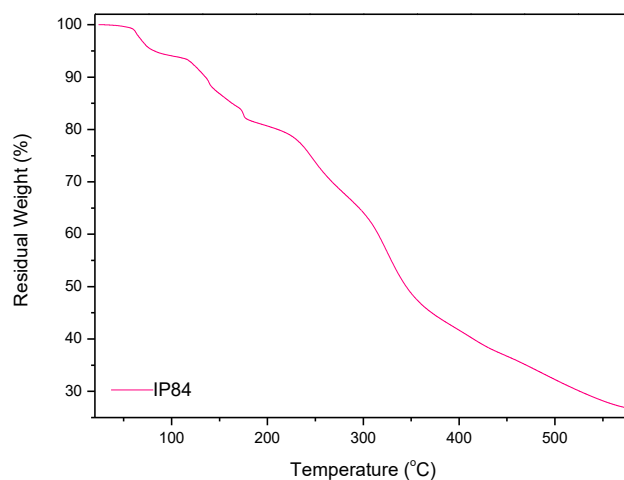


Figure 4.36 TGA for IP-84

Table 4.16 Summary of TGA results for IP-84

Steps	Water and/or solvent		Isocyanate compounds		Shell		Char (at 600°C)
	Temperature (°C)	Mass loss (%)	Temperature (°C)	Mass loss (%)	Temperature (°C)	Mass loss (%)	Mass (%)
1 <sup>st</sup>	60-118	7					
2 <sup>nd</sup>			118-177	11			
3 <sup>rd</sup>			177-236	4			
4 <sup>th</sup>			236-307	15			
5 <sup>th</sup>					307-351	18	
6 <sup>th</sup>					351-446	6	
7 <sup>th</sup>					446-529	11	
Total		7		30		35	26

Table 4.17 Summary of characterization results for IP-83 &amp; IP-84

Synthesis No.	MCs type	MCs size ( $\mu\text{m}$ )	Y	Core mass % from TGA
IP-83	Core-shell	70-200	5.47	-
IP-84	Core-shell	50-150	86.17	30

### Conclusions

- Successful encapsulation of Ongronat in TDI-derived shell was achieved, represented by these both syntheses, being the MCs obtained of core-shell type.
- DETA is proven to be a more effective active hydrogen source (chain extender) for the encapsulation of isocyanate species, when compared to aminosilane, probably due to the higher NH functionality, which results in higher reactivity and more cross-linking of the shell material.

After raising some experience on the encapsulation of isocyanate species, in particular on the use of different reactivity isocyanates to achieve core-shell MCs with desired properties, new experiments have been initiated with commercial isocyanate prepolymers, supplied by CIPADE. These materials are Suprasec 2234 and Desmodur RC, MDI and TDI prepolymers, respectively, and they are employed by CIPADE as cross-linkers to promote ultimate strength to the adhesive joint. These compounds are extremely reactive with active hydrogens, in order to be able to react within a very short period of time, when in contact with the base component (OH-rich) to produce a high strength joint in the footwear assembly. The first series of synthesis was done without addition of any solvent in the case of Desmodur RC and by addition of solvent in the case of Suprasec 2234, as its viscosity is significantly higher when compared to other isocyanate compounds. Further syntheses were performed by mixing of these two prepolymers and adding different types of solvents at different concentrations to control the reaction rate. Also, different active hydrogen sources were added to the aqueous phase, or in the case of TPI to the organic phase, to study the size and morphology of the MCs obtained. In the following chapters, the results of these series of syntheses will be presented.

#### 4.2.5 Group 5&6

**Objectives:** Microencapsulation of Suprasec 2234, MDI prepolymer, used by CIPADE as cross-linker of adhesive formulations. Due to the high reactivity of this prepolymer, several strategies were considered to control the reactions speed, such as carrying out the syntheses at low temperature, or adding different amines and polyols, with the main idea of increasing encapsulation efficiency and formation of an appropriate shell. The other objectives for these series of syntheses was finding the suitable solvent for dissolving the organic phase, as well as finding the minimum possible quantity for each solvent.

Table 4.18 Primary materials used in the selected syntheses of group 5&amp;6

Synthesis No.	Organic Phase	Aqueous phase	Surfactant	Active H source	Solvent	Temperature (°C)	Stirring rate (rpm)
IP-102	Suprasec 2234	Water	GA	DETA	Toluene	55-60	300
IP-91	Suprasec 2234	Water	GA	DETA	n-Hexane	55-60	400
IP-104	Suprasec 2234	Water	GA	1,6 Hex- anediol	Toluene	55-60	400
1P-117	Suprasec 2234	Water	GA	1,6 Hex- anediol	MEK	55-60	350
IP-114	Suprasec 2234+TPI	Water	GA	--	Toluene	55-60	400

Table 4.18 lists the materials which were employed in these groups of syntheses.

Inspection by optical microscopy and SEM were performed to evaluate MCs size and morphology. Table 4.19 lists physical features of the MCs and their relative encapsulation yield.

Table 4.19 Summary of characterization results for Group 5&amp;6

Synthesis No.	MCs size (µm)	Physical character of MCs	Y
IP-102	10-100	Tendency to aggregation	4.05
IP-91	70-200	Non-aggregated	1.43
IP-104	10-70	Tendency to aggregation	1.21
IP-117	50-250	Non-aggregated	2.03
IP-114	20-120	Some aggregated MCs	1.44

The SEM photomicrographs of IP-102 are shown in Figures 4.37 and 4.38, exhibiting a rough surface, which can be justified by inhomogeneous reaction kinetics (Kardar, 2015; Tatiya, 2016). It was not possible to break or open the MCs' shell, so that there is no information about the morphology of the MCs, which suggests either that the MCs are of core-shell morphology, where the shell is mechanically very strong, or that the MCs are of matrix-type morphology.

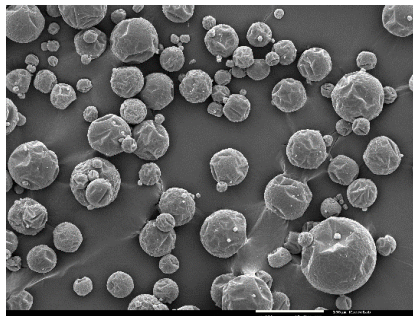


Figure 4.37 SEM photomicrograph of IP-102, Scalebar=100 $\mu$ m

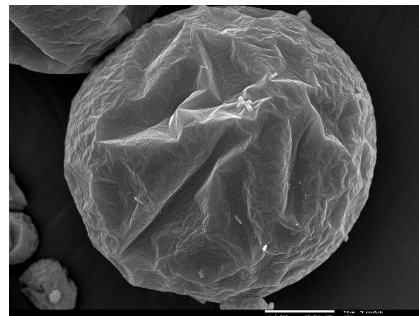


Figure 4.38 SEM photomicrograph of IP-102, Scalebar=10 $\mu$ m

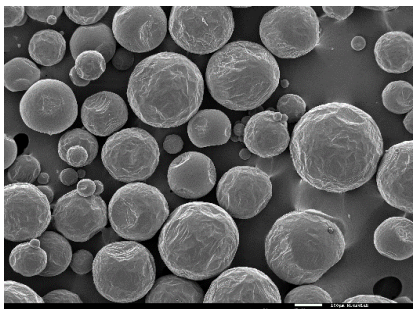


Figure 4.39 SEM photomicrograph of IP-91, Scalebar=100 $\mu$ m

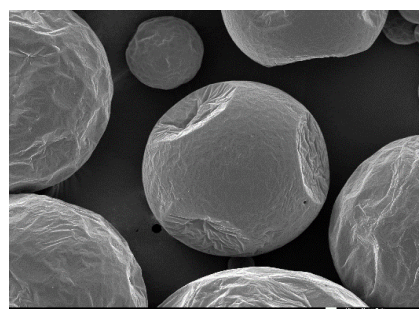


Figure 4.40 SEM photomicrograph of IP-91, Scalebar=10 $\mu$ m

Figures 4.39 and 4.40 show the SEM photomicrographs for IP-91. The primary materials and the synthesis parameters are the same as for IP-102, except for the type and quantity of solvent. The changes in the morphology of the MC's shell can be due to the different solvents employed in these two syntheses, while the significant changes in the MCs size can be due to the quantity of solvent added to the syntheses. Syntheses IP-104 and IP-117 were prepared with 1,6 Hexanediol added to the aqueous phase. The only difference between them was the type of solvent, which was employed, toluene for IP-104 and MEK for IP-117. There are no SEM images available for these two syntheses, but optical microscopy evaluation of IP-104 showed small spherical MCs in the range of 10-70  $\mu$ m but mostly in the range of 20-40  $\mu$ m, with tendency to aggregation. MCs obtained from IP-117, exhibited a shiny yellowish colour and spherical shape in the range of 50-250  $\mu$ m and without any tendency to aggregation.

In the last synthesis (IP-114) from this group TPI was added with the aim of increasing the microencapsulation efficiency, as it was observed in the case of IP-67. The outer surface of the MCs is found to be wrinkled, as it can be observed in Figures 4.41 and 4.42. The nonuniformity and wrinkles on the surface can be due to the fast formation of hard shell through the reaction of active hydrogen sources with highly reactive isocyanate compounds, followed by shrinking of the core through polymerization (Hano, 2017), Another reason is the inhomogeneous reaction kinetics, derived from the reaction of active sites in the shell with monomers of the core. (Kardar, 2015) A third hypothesis, less probable, could be some solvent

present in the core that is eliminated during SEM samples preparation and set-up procedure, leaving voids inside the MCs.

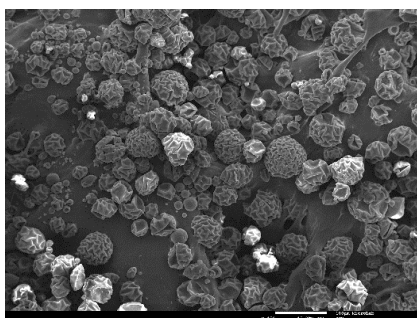


Figure 4.41 SEM photomicrograph of IP-114, Scalebar=100µm

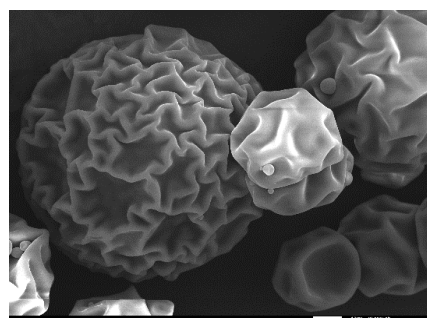


Figure 4.42 SEM photomicrograph of IP-114, Scalebar=10µm

Figure A7 (Appendix-A) shows normalized FTIR peaks of Suprasec 2234, as well as IP-91, IP-102, IP-104, IP-117 and IP-114. Again peaks located in the range of  $2280\text{-}2260\text{ cm}^{-1}$  are related to free (unreacted) -NCO in all MCs and Suprasec 2234. For Suprasec 2234 peaks located at  $1735\text{ cm}^{-1}$  are related to urethane. Further calculation was carried out to estimate encapsulation efficiency by considering the area at ( $1926\text{-}2444\text{ cm}^{-1}$ ) for NCO and the area at ( $1754\text{-}1670\text{ cm}^{-1}$ ) related to PU and/or PUa. Calculations to obtain relative encapsulation yield were performed based on these peaks and according to Eq.7. The results are listed in Table 4.19. The Y parameter also was calculated for Suprasec 2234 and  $Y_{\text{Suprasec}} = 11.65$  was obtained for this prepolymer.

## Conclusions

Several efforts were performed to encapsulate Suprasec 2234 by employing different solvents and different active hydrogen sources. As it was mentioned before, this was a hard task, because of the extremely high reactivity of Suprasec 2234, when compared to other isocyanate compounds, which were employed before in this work.

- FTIR results confirmed the successful encapsulation of Suprasec 2234, but only at a low level, when compared to other groups of syntheses. All the spectra of these syntheses exhibit a peak at  $2280\text{-}2260\text{ cm}^{-1}$  related to unreacted -NCO.
- The best encapsulation efficiency achieved was for IP-102, where DETA was added to the synthesis and toluene was employed as a solvent.
- Comparison between FTIR results for IP-91 versus IP-102 and IP-104 versus IP-117, reveals the effect of changing the solvent on the encapsulation efficiency, due to a change in the partition coefficient ( $K_{ow}$ ) when employing different types of solvent.

- Comparison between FTIR results for IP-102 versus IP-104 reveals the effect of changing the active hydrogen source on the encapsulation efficiency, due to a change in the partition coefficient ( $K_{ow}$ ), molecular structure and functionality.

#### 4.2.6 Groups 7, 8, 9, 10

**Objective:** Encapsulation of Desmodur RC (TDI prepolymer) as a highly reactive prepolymer.

In these groups of syntheses several efforts were performed to encapsulate Desmodur RC, by using different solvents and different hydrogen active sources. Table 4.20 shows the primary materials employed in selected syntheses from these groups.

Table 4.20 Primary materials used in syntheses of groups 7, 8, 9, 10

Synthesis No.	Organic Phase	Aqueous phase	Surfactant	Active H source	Solvent	T (°C)	Stirring rate (rpm)
IP-108	Desmodur+TPI	Water	GA	None	n-Hexane	55-60	300
IP-115	Desmodur+TPI	Water	GA	None	Toluene	55-60	400»300*
IP-122	Desmodur+TDI+TPI	Water	GA	None	MEK	55-60	300
IP-113	Desmodur (higher quantity) + TDI	Water	GA	1,6 Hexanediol	Toluene	55-60	350
IP-118	TDI (higher quantity) + Desmodur	Water	GA	1,6 Hexanediol	Toluene	55-60	350

\*Stirring rate was reduced, as it was observed some broken shell.

To encapsulate Desmodur RC, two strategies were employed according to the know-how built from last experiments. The first strategy was the addition of TPI to Desmodur RC, with the idea of incorporating NCO and silanol groups in the shell formation process, leading to siloxane rich regions within a PU/PUa shell. The second strategy was the addition of monomeric TDI to form shell of MCs. To recognize higher reactive isocyanate compound between Desmodur RC and monomeric TDI, the same quantity of polyol was added to a certain amount of both isocyanates at RT, although the reaction started first at monomeric TDI by changing the colour, but finally Desmodur RC transformed to bulky solid when monomeric TDI was still liquid. So, two syntheses were performed, first with the higher quantity of monomeric TDI (IP-118) and the other with the higher quantity of Desmodur RC (IP-113). FTIR was performed on the MCs from these syntheses to obtain more accurate information about the level of reactivity of these isocyanate compounds. There are no SEM photomicrographs available for this group of synthesis. MCs were characterized by optical microscopy and FTIR spectroscopy. Figure A8 (Appendix-A) shows FTIR spectra for all MCs of this group, as well as Desmodur RC. The same method was employed to calculate the relative encapsulation yield. The obtained results from FTIR and summary of all characterization results were presented in Table 4.21.

Table 4.21 Summary of characterization results for the selected MCs from Groups 7, 8, 9, 10

Synthesis No.	MCs size ( $\mu\text{m}$ )	Physical features of MCs	Y	Core mass % from TGA
IP-108	20-150	Non-aggregated	5.7	----
IP-115	20-100	Non-spherical + some broken shell	1.3	----
IP-122	20-80	Non-aggregated	2.6	----
IP-113	10-100	Non-aggregated	0.8	34.5
IP-118	70-150	Non-spherical + some broken shell	6.3	----

The relative amount of NCO to that of PU/PUa, was also calculated for Desmodur RC and monomeric TDI.

The results show  $Y_{\text{Desmodur}} = 0.4$  and  $Y_{\text{monomeric TDI}} = 22.8$ .

The TGA for MCs from IP-113, is shown in Figure 4.43. The extracted results from TGA were presented in Table 4.22.

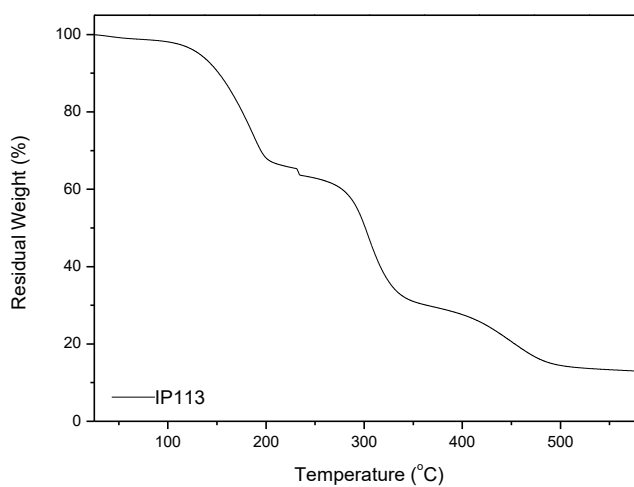


Figure 4.43 TGA for IP-113



Table 4.22-Summary of TGA results for IP-113

Steps	Water and/or solvent		Isocyanate compounds		Shell		Char (at 600°C)
	Temperature (°C)	Mass loss (%)	Temperature (°C)	Mass loss (%)	Temperature (°C)	Mass loss (%)	Mass (%)
1 <sup>st</sup>	50-134	5.5					
2 <sup>nd</sup>			134-198	26.5			
3 <sup>rd</sup>			198-281	8			
4 <sup>th</sup>					281-333	26.5	
5 <sup>th</sup>					333-400	6.5	
					400-492	12	
Total		5.5		34.5		45	13

### Conclusions

- FTIR results confirm the successful encapsulation of Desmodur RC, although in some cases with significantly low encapsulation efficiency. The fact can be justified by significantly low Y for Desmodur RC ( $Y_{\text{Desmodur}} = 0.4$ ), which means Desmodur has significantly low free NCO. The high Y for MCs when compared with  $Y_{\text{Desmodur}}$ , can be explained by the presence of free NCO from TPI and monomeric TDI, as the  $Y_{\text{Monomeric TDI}} = 22.8$ .
- Comparison between FTIR results for IP-108 *versus* IP-115, confirms the effect of changing the solvent on the encapsulation efficiency, due to partition coefficient ( $K_{\text{OW}}$ ) effects.
- Comparison between FTIR results for IP-113 *versus* IP-118, as well as  $Y_{\text{Monomeric TDI}}$  *versus*  $Y_{\text{Desmodur}}$  confirmed the higher reactivity of Desmodur RC when compared with monomeric TDI.

### 4.2.7 Group 11

**Objective:** Encapsulation of Suprasec 2234 (MDI prepolymer), assisted by Desmodur RC (supposed to be a more reactive prepolymer, because it derives from TDI).

In this group of syntheses, a mixture of Desmodur RC and Suprasec 2234 was employed, to take advantage of the different reactivity of these isocyanate compounds. It is expected that the most reactive one results in the formation of the PU/PUa shell, encapsulating the less reactive one. Several solvents, as well as different types of active hydrogen sources, were added to increase the encapsulation efficiency. Table 4.23 lists the primary materials employed in these series of syntheses.

Table 4.23 Primary materials used in the best syntheses of group 11

Synthesis No.	Organic Phase	Aqueous phase	Surfactant	Active H source	Solvent	Temperature (°C)	Stirring rate (rpm)
IP-88	Suprasec + Desmodur	Water	GA	DETA	n-Hexane	55-60	400
IP-90	Suprasec + Desmodur	Water	GA	None	n-Hexane	55-60	400
IP-105	Suprasec + Desmodur	Water	GA	Aminosilane	Toluene	55-60	400
IP-112	Suprasec + Desmodur	Water	GA	DETA	Toluene	55-60	250
IP-109	Suprasec + Desmodur	Water	GA	1,6 Hexanediol	Toluene	55-60	300
IP-119	Suprasec + Desmodur + TPI	Water	GA	None	MEK	55-60	350

MCs were characterized by optical microscopy, SEM and FTIR spectroscopy. Figures 4.44-4.53 reveal the MCs' morphology of some of these syntheses. As shown in Table 4.23, syntheses IP-88 and IP-90 were performed in the same synthesis conditions, but DETA was added to the IP-88. As it can be observed from SEM photomicrographs 4.45 and 4.47, the addition of DETA leads to a wrinkled shell surface, while MCs shell surface of IP-90 is completely smooth, which might be due to inhomogeneity in reaction kinetics, or simply because IP-88 has a core-shell morphology and the shell gets affected (collapses) when subject to the vacuum inside the SEM. The MCs achieved in this group of synthesis are so tough that it was not possible to break them using the tip of a needle. By changing the solvent from n-hexane in IP-88 to toluene in IP-112 again shell morphology has changed (Figures 4.48 and 4.49). One theory is that, due to higher diffusion coefficient in the case of toluene, there is more instability in the emulsion and more wrinkles on the shell surface are produced (Duan, 2016; Polenz, 2014). Another theory, is that such higher diffusion coefficient might promote a faster interfacial reaction, with formation of a thinner shell, that

isolates NCO groups from the OH and NH groups, stopping reaction. Such thinner shell tends to become even more affected by the vacuum produced at the microscope, collapsing in the form of wrinkles. Comparison between IP-109, prepared with 1,6 Hexanediol, and IP-112, prepared with DETA, also shows a change in the shell morphology, as it is represented in Figure 4.51 and Figure 4.48. It seems that IP-112 exhibits a thinner shell than IP-109, being therefore more deformed by vacuum conditions. In IP-119, TPI was added to the organic phase (Figures 4.52 and 4.53) and, in fact, the shell surface looks smoother with slightly shrunk regions, which can be explained by slight changes in homogeneity of reaction kinetics due to higher reactivity of TPI functional groups, the reason for inhomogeneity and the shrinkage of the shell has been explained before in pages 65 and 66.

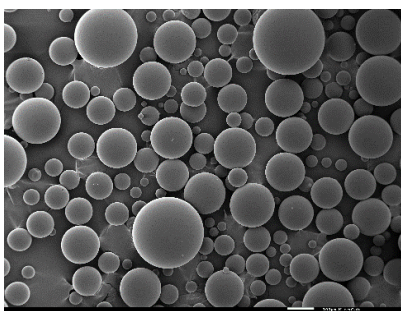


Figure 4.44 SEM photomicrograph of IP-90, Scalebar=100µm

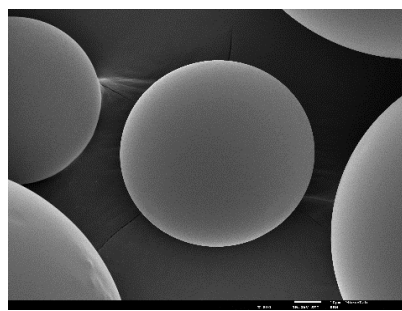


Figure 4.45 SEM photomicrograph of IP-90, Scalebar=10µm

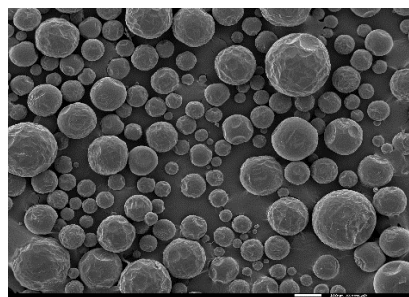


Figure 4.46 SEM photomicrograph of IP-88, Scalebar=100µm

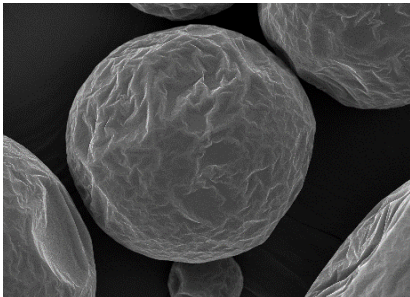


Figure 4.47 SEM photomicrograph of IP-88, Scalebar=10µm

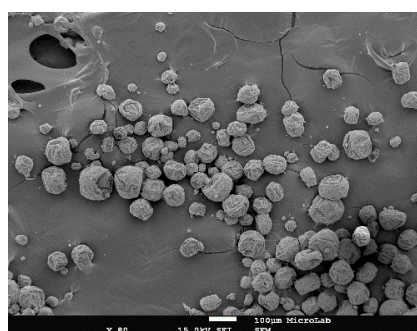


Figure 4.48 SEM photomicrograph of IP-112, Scalebar=100µm

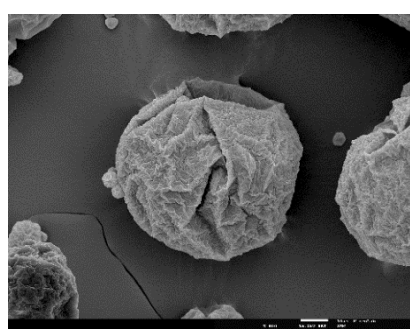


Figure 4.49 SEM photomicrograph of IP-112, Scalebar=10µm

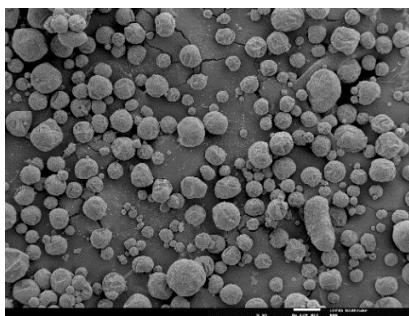


Figure 4.50 SEM photomicrograph of IP-109, Scalebar=100μm

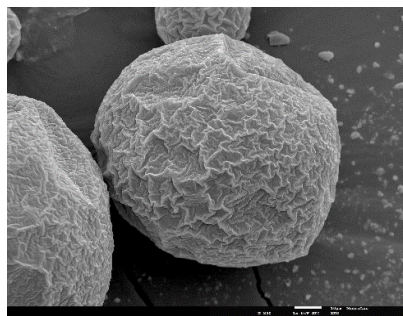


Figure 4.51 SEM photomicrograph of IP-109, Scalebar=10μm

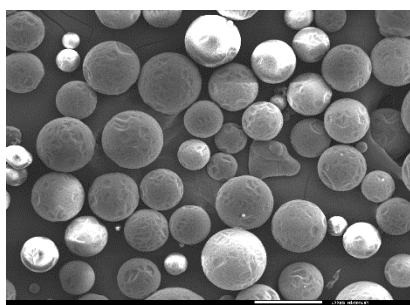


Figure 4.52 SEM photomicrograph of IP-119, Scalebar=100μm

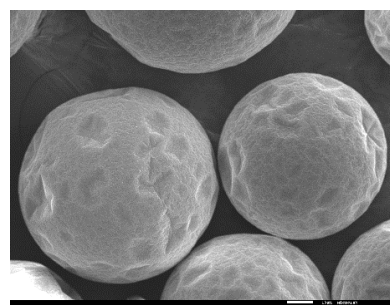


Figure 4.53 SEM photomicrograph of IP-119, Scalebar=10μm

The FTIR spectra for the MCs obtained from these series of syntheses are shown in Figures A9, A10 and A11 of Appendix A. For the sake of simplification these spectra were grouped according to the solvent used. It should be noted that  $Y_{\text{Desmodur}} = 0.4$  and  $Y_{\text{Suprasec}} = 11.65$ , as in this group of syntheses both pre-polymer were mixed together.

Figure A9 regarding IP-119, prepared with TPI, shows the presence of siloxane moieties, through the presence of a peak at ca.  $1100 \text{ cm}^{-1}$ , which is much more evident for this spectrum than for the other spectra, revealing that the MCs in this case are made of a hybrid material, based on PU/PUa and silica based material.

The peak assigned to NCO groups, in IP-88 spectrum (Figure A10, Appendix A) is more intense, compared to the carbonyl one from PU/PUa, than that of IP-90. This reveals that DETA improves the encapsulation efficiency ( $Y=0.65$  versus  $Y=0.47$ , shown in Table 4.26). As it can be observed in Figure A11, Appendix-A, aminosilane was shown to be not very efficient in NCO encapsulation. The NCO peak, for IP-105, is very weak, while, on the contrary, 1,6-hexanediol (IP-109) leads to higher encapsulation efficiency ( $Y=2.95$  for IP-109 versus  $Y=0.2$  for IP-105). The OH band, at ca.  $3400 \text{ cm}^{-1}$ , is also more intense for IP-109. In the case of IP-112 a value for  $Y$  at 0.61 was obtained from Eq. 7, being this result quite similar to that of IP-88, where the only difference was the solvent employed (n-Hexane for IP-88 and toluene for IP-112).

In Table 4.24 the summary of characterization results which were obtained from physical and chemical evaluation methods is presented.

Table 4.24 Summary of characterization results for Group 11

Synthesis No.	MCS size ( $\mu\text{m}$ )	Physical character of MCS	Y
IP-88	50-150	Non- aggregated	0.65
IP-90	70-200	Non- aggregated	0.47
IP-105	-----	Completely aggregated	0.2
IP-109	20-120	Low degree of aggregated	2.95
IP-112	10-100	Non-spherical and aggregated	0.61
IP-119	20-130	Non- aggregated	0.3

## Conclusions

- FTIR spectroscopy and the related calculus to obtain the relative encapsulation yield confirmed the encapsulation of isocyanate prepolymer (Suprasec), with a quiet low efficiency, especially for the synthesis with aminosilane, as active H source.
- Comparison between the FTIR results for IP-105 and IP-109 reveals that encapsulation efficiency clearly depends on the type of active H source employed, due to changing in the partition coefficient ( $K_{ow}$ ). The Y parameter, as a relative measure of encapsulation efficiency was found to be 0.2 (for IP-105 with aminosilane) and 2.95 (for IP-109 with 1,6-hexanediol).
- IP-91, with Suprasec 2234 being the only isocyanate compound, exhibits  $Y=1.43$ , while IP-88 with a combination of Suprasec 2234 and Desmodur RC (77wt%:23wt%), exhibits  $Y=0.65$ . So, one may conclude that Suprasec 2234 is the compound contributing to the shell formation in both cases, because  $Y_{Desmodur} = 0.4$  and  $Y_{Suprasec} = 11.65$ . This is somehow an unexpected result, since Desmodur, a TDI pre-polymer, has been employed as the most reactive compound.

### 4.3 Peeling strength test

As discussed before, in chapter 3.3.1, the peeling strength test was performed as an indirect way to evaluate the behaviour of the MCs in terms of adhesion capacity. This test involved the addition of selected MCs synthesized in this work, that contain a determined NCO groups content on the adhesive formulation base component (having OH groups free to react), this latter one supplied by CIPADE. This base component of name PEARLSTICK® 45-50/18, also called “Polyol” component in this work, has a small amount of OH groups that will react with the encapsulated NCO groups (upon the breaking or melting of the MCs), leading to the cross-linking of the adhesive material.

Experiences started by mixing 5 wt% of Ongronat (a known amount of NCO) with 95 wt% of the polyol component. The same ratio was considered for  $\frac{MCs}{Polyol}$  without considering the relative encapsulation yield of MCs obtained from FTIR results.

The selected MCs for performing these tests are those from IP-64 and IP-126, which contain encapsulated IPDI, from IP-84, which contains encapsulated Ongronat and from IP-118 and IP-122 that contain encapsulated TDI and /or Desmodur RC. The solution of 25 wt% PEARLSTICK® 45-50/18 in MEK was used as the polyol component. Ongronat was also mixed with the same quantity of polyol, as a reference test.

These tests were performed in seven steps: i) Weighing of the right quantity of polyol component and MCs or Ongronat, ii) Mixture with a glass rod, iii) Application of the mixture on the surface of a paper substrate, with a certain area, iv) Passing “adjustable wet film thickness applicator” to obtain a thin film of uniform thickness, v) Placement of another piece of paper substrate on top of the mixture, vi) Application of load and /or temperature during 15 minutes, vii) Separation (pulling apart) of both pieces of paper right after finishing the last step. Figures 4.54 to 4.57 show some of these steps, which were performed at the laboratory.



Figure 4.54 Addition of MCs to the polyol based component

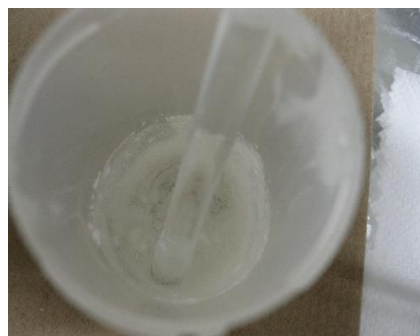


Figure 4.55 Step (ii) of peeling strength test



Figure 4.56 Steps (iii) & (iv) of peeling strength test



Figure 4.57 Step (vii) of peeling strength test, exhibiting mostly a structural type of failure of the adhesive joint

Table 4.25 summarizes the peeling strength testing conditions, as well as the results obtained for the first set of tests. The testing of other MCs prepared during this work is still on-going and was not included in this dissertation. It should be noted that MCs obtained from IP-84, were tested twice, i.e. right after being prepared and after three months from their synthesis, which is named as IP-84-2, in order to assess any change in the quality of the MCs over the time.

Table 4.25 Peeling strength test parameters and relative results (type of failure)

Test condition Mixture	Temperature (80° C)	Pressure (4 Kg.cm <sup>-2</sup> )	Temperature (80° C) + Pressure (4 Kg.cm <sup>-2</sup> )	Type of failure
Polyol	x			Adhesive
Polyol + Ongronat	x			Structural
Polyol + Ongronat			x	Structural
Polyol + IP-84	x			Adhesive
Polyol + IP-84		x		Structural
Polyol + IP-84			x	Structural
Polyol + IP-84-2	x			Adhesive
Polyol + IP-84-2		x		Structural
Polyol + IP-84-2			x	Structural-Cohesive
Polyol + IP-64			x	Structural-adhesive
Polyol + IP-126	x			Structural
Polyol + IP-126		x		Structural
Polyol + IP-126			x	Structural
Polyol + IP-118	x			Adhesive
Polyol + IP-118		x		Structural
Polyol + IP-118			x	Structural
Polyol + IP-122	x			Adhesive
Polyol + IP-122		x		Adhesive
Polyol + IP-122			x	Structural

## Conclusions

- The base component “Polyol” exhibits adhesion performance by itself, of the type of adhesive failure. It should be noted that cross-linking, by means of reaction with NCO groups, is critical for the desired adhesive performance and durability for the footwear industry.
- For all the samples assessed by the peeling strength test, there was an indirect evidence of free NCO groups, because structural failure, which is the desired type of failure, was achieved by means of pressure (load) exerted on the MCs, resulting on NCO release.
- NCO release from the MCs occurs mainly by pressure application and not by the effect of temperature. This was expected because the PU/PUa shell material is basically a thermoset polymer, i.e. does not melt at the test temperature, it only degrades at high temperatures, as it is visible at the



thermograms, obtained by TGA.

- The test carried out with IP-84 and IP-84-2, showed slightly worse results for IP-84-2, probably due to the gradual loss of core content of MCs over the time. This fact can be explained by reaction of encapsulated NCO species with the moisture that penetrates through the shell over time, which suggests that shells with less porosity than that of IP-84 should be developed.

## 5 Summary and main conclusions

The present work was defined as a part of the effort to encapsulate different chemical compounds of isocyanate (Ongronat, IPDI, TDI and highly reactive prepolymers) by micro emulsion technique combined with interfacial polymerization. New developed MCs contain isocyanate, which is covered (encapsulated) by a thin layer of PU/PUa, or hybrid material, in order to protect the isocyanate from reaction with surrounded (polyol rich) environment (in order to supply a monocomponent 1K adhesive system) and to protect the user from the toxicity of isocyanate compounds.

Initially Ongronat was successfully encapsulated by using DC 193 and GA as surfactants. In a second step, IPDI was successfully encapsulated by addition of Ongronat to the organic phase, as a higher reactivity isocyanate. The obtained MCs have core-shell morphology, with a higher encapsulation yield when compare with the first group. In a third step, Ongronat was successfully encapsulated by addition of monomeric TDI as a higher reactivity isocyanate compound. Different amines (EDA, DETA) and silanes (aminosilane, TEOS, TPI) were added to the syntheses. Among them, DETA and TPI were the ones leading to a higher relative encapsulation yield.

In a next phase of this work, it was possible to successfully encapsulate Desmodur RC and Suprasec 2234, which are highly reactive isocyanate prepolymers employed by CIPADE, the industrial partner of this work (ECOBOND Project).

Aiming at increasing the encapsulation efficiency, several studies were carried out to better understand the microencapsulation process and to optimize the synthesis parameters, such as emulsification rate, stirring speed, synthesis temperature and duration, surfactant concentration and type, among others.

Table 5.1 lists the best results which were obtained from more than 150 syntheses to encapsulate IPDI, Ongronat, Desmodur RC, monomeric TDI and Suprasec 2234.

Table 5.1 The best syntheses, according to the relative encapsulation yields achieved

Synthesis No.	Group	Encapsulated material	Addition organic phase	Active H source	Temperature (°C)	Stirring rate (rpm)	Y
IP-84	4	Ongronat	TDI + n-Hexane	DETA	65-70	400	87.2
IP-66	2	IPDI	Ongronat	DETA	65-70	400	43.2
IP-67	3	IPDI	Ongronat + TPI	-----	65-70	400	41.4
IP-33	1	Ongronat	----	-----	65-70	400	29.2
IP-118	8,9,10	TDI	Desmodur RC	1,6 Hexanediol	55-60	350	6.3
IP-108	8,9,10	Desmodur RC	TPI + n-Hexane	----	55-60	300	5.7
IP-102	5,6	Suprasec 2234	Toluene	DETA	55-60	300	4.1
IP-109	11	Suprasec 2234	Desmodur RC + Toluene	1,6 Hexanediol	55-60	300	3.0
IP-126	Study Temp.	IPDI	Ongronat	Aminosilane + TEOS	75-77	400	7.9
IP-121	Study rpm	IPDI	Ongronat	Aminosilane + TEOS	65-70	200	5.6

## 5.1 Main Conclusions

### 5.1.1 Conclusions related to primary materials

- Addition of another isocyanate compound with higher reactivity to the organic phase, improves the encapsulation efficiency, such as Ongronat to IPDI or TDI to Ongronat.
- From all the laboratory experiences, it is possible to conclude, for each isocyanate compound, the best combination in terms of active hydrogen source and solvent employed, being as follow:

Table 5.2 The best combination of active hydrogen source and solvent for each isocyanate compound in this work

Isocyanate compound	Active hydrogen source	Solvent
IPDI	DETA	None
Ongronat	DETA	n-Hexane
Suprasec 2234	DETA	Toluene
Desmodur RC	TPI	n-Hexane

- The reactivity of the isocyanate compounds employed in this work was realized to be as follow: Suprasec 2234 › Desmodur RC › monomeric TDI › Ongronat › IPDI.
- GA was a good performing surfactant in this work. Higher concentration of GA tends to decrease the MCs size.

### 5.1.2 Conclusions related to physical parameters of synthesis

- The performance of syntheses, at higher temperatures, i.e. in the temperature range of 75-77 °C improves the encapsulation efficiency, by reducing the synthesis duration. For example, in the case of Suprasec 2234 and Desmodur RC, the decrease of synthesis temperature from 60 °C to RT, implied an increase of the synthesis duration from 20 minutes to 4 hours, while a further decrease in temperature by using an ice bath, has stopped the reaction.
- Although the lower stirring rate improves the encapsulation efficiency, it was found to increase the synthesis duration, so the optimum range of 350-400 rpm can be considered as the best practical range.
- An increase in the emulsification rate leads to a decrease in the MCs size. In this work, an emulsification rate at 3200 rpm was employed.

### 5.2 Future work

- Development of MCs with more brittle shell, so they can fully release the isocyanate by the effect of loading (pressure): a few experiments have been done to synthesize MCs with brittle shells by addition of polystyrene (PS) solution in several solvents i.e. toluene, DCM, MEK, etc. (Group 12). Although the FTIR spectra of MCs confirmed the presence of PS, the shell strength and morphology did not show significant changes. More efforts will be necessary to optimize these syntheses.
- Development of MCs with thermal gates, so they can fully release the isocyanate by melting: a

few experiments were carried out to synthesize MCs with thermal gates by adding to the synthesis a solution of PCL in different solvents (Group 12), however, more efforts in this field should be done.

- Test of new promising active hydrogen sources, to improve the encapsulation efficiency of Suprasec 2234 and Desmodur RC: 1,4 Butanediol, TETA and 0.0 G PAMAM.
- Some of the MCs containing Suprasec and Desmodur were not possible to be broken by the tip of a needle. In this case, embedding them in resin as a mounting material, following by cutting the mounted sample by micro cutter might be done to better study their morphology.

## Bibliography

- (Aranais, 2012) F. Aranais, M. A. P. Liminana, M. S. Navarro and C. O. Barcelo, (2012). Developments in Microencapsulation Technology to Improve Adhesive Formulations. *The Journal of Adhesion*, Vol.88, 391–405, <http://dx.doi.org/10.1080/00218464.2012.660368>.
- (Arshady, 1998) R. Arshady, (1998). Preparation of microspheres and microcapsules by interfacial polycondensation techniques. *Journal of microencapsulation*, Vol.6, 13-28. doi:10.3109/02652048909019898
- (Avramenko, 2013) N. Avramenko, (2013). Encapsulation of flaxseed oil within modified. MSc dissertstion in food and bioproduct sciences, *Department of Food and Bioproduct Sciences. University of Saskatchewan, Canada*.
- (Azagheswari, 2015) Azagheswari, B. Kuriokase, S.Padma and S.P. Priya, (2015). A Review on Microcapsules. *Global Journal of Pharmacology*, Vol.9, 28-39. doi:DOI: 10.5829/idosi.gjp.2015.9.1.91110
- (Bayer, 2005) Bayer Material Science, (2005). *The Chemistry of Polyurethane Coatings*. Bayer Material Science Publication.
- (Brochu, 2012) A.B. Brochu, W. J. Chyan, W.M. Reichert, (2012). Microencapsulation of 2-octylcyanoacrylate tissue adhesive for self-healing acrylic bone cement. *Journal of Biomedical Materials Research - Part B Applied Biomaterials*, Vol.100, 1764-1772. doi:10.1002/jbm.b.32743
- (Carvalho, 2011) R. Carvalho, (2011). Supercritical Fluid Aided Microencapsulation of Dry Powders. PhD dissertation in chemical and biomedical engineering, Department of Chemical and Biomedical Engineering. *University of South Florida, USA*.
- (Ciriminna, 2011) R. Ciriminna, M. Sciortino, G. Alonzo, A. D. Schijver and M. Pagliaro, (2011). From Molecules to Systems: Sol-Gel Microencapsulation in Silica-Based Materials. *Chemical Reviews*, Vol.111, 765-789 doi:10.1021/cr100161x.
- (Credico, 2013) B. D. Credico and S.Turri, (2013). An efficient method for the output of new self-repairing materials through a reactive isocyanate encapsulation. *uropean Polymer Journal*, Vol.49, 2467-2476. doi:10.1016/j.eurpolymj.2013.02.006.
- (Duan, 2016) B. Duan, (2016). Microencapsulation via In Situ Polymerization. In *Handbook of Encapsulation and Controlled Release* by D.R. Karsa and R.A. Stephenson Published by Woodhead Publishing Limited, Abington Hall, Abington, Cambridge CB 1 6AH, England (pp. 308-314). Taylor & Francis Group, LLC.
- (Dubey, 2009) R. Dubey, (2009). Microencapsulation Technology and Applications Rama. *Defence Science Journal*, Vol.59, 82-95, doi.org/10.14429/dsj.59.1489.
- (ECOBOND, 2015) ECOBOND. (2015). Portugal 2020 Co-Promotion Project # 17930. "Development of new ecological, self-reactive, monocomponent adhesives Portugal.
- (Fan, 2017) J. Fan, X. Liu, (2017). Effect of solvent evaporation technique on the characteristics of curing agent microcapsules and the curing process. *Composites Science and Technology*, Vol. 138, 80-90. doi:http://dx.doi.org/10.1016/j.compscitech.2016.11.014.
- (Galgali, 2011) G. Galgali, E. Schlangen, S. V. D. Zwaag, (2011). Synthesis and characterization of silica microcapsules using a sustainable solvent system template. (Elsevier, Ed.) *Materials Research Bulletin*, Vol.46, 2445-2449. doi:10.1016/j.materresbull.2011.08.028.
- (Gogoi, 2014) R. Gogoi, M. S. Alam and R. K. Khanda, (2014). Effect of increasing NCO/OH molar ratio on the physicomechanical and thermal properties of isocyanate terminated polyurethane prepolymer. *International Journal of Basic and Applied Sciences*, Vol.2, 118-123. doi:10.14419/ijbas.v3i2.2416.

- (Haghighayegh, 2016) M. Haghighayegh, S. M. Mirabedini, H. Yeganeh. (2016). Microcapsules containing multi-functional reactive isocyanate- terminated polyurethane prepolymer as a healing agent. Part 1: synthesis and optimization of reaction conditions. *Journal of Master Science*. Vol.51, 3056-3068, doi:10.1007/s10853-015-9616-6.
- (Hano, 2017) N. Hano, M.Takafuji and H. Ihara (2017) One-pot preparation of polymer microspheres having wrinkled hard surfaces through self-assembly of silica nanoparticles, *Chemical Communications*, Vol.53,9147-9150, doi: 10.1039/C7CC05132H.
- (Hu, 2017) M. Hu, J. Guo, Y.Yu, L. Cao and Y. Xu, (2017). Research Advances of Microencapsulation and Its Prospects in the Petroleum Industry. *Materials*, Vol.4, pii:E369. doi:doi:10.3390/ma10040369
- (Huang, 2011) M. Huang and J.Yang, (2011). Facile microencapsulation of HDI for self-healing anticorrosion coatings. *Journal of Materials Chemistry*, Vol.48, 24959- 25506, doi:10.1039/c1jm10794a
- (Kardar, 2015) P. Kardar, (2015). Preparation of polyurethane microcapsules with different polyols component for encapsulation of isophorone diisocyanate healing agent. *Progress in Organic Coatings*, Vol.89 271-276. doi:10.1016/j.porgcoat.2015.09.009
- (Kaushiva, 1999) B. D.Kaushiva, (1999). Structure-Property Relationships of flexible polyurethane foams. PhD dissertation in chemical engineering, *Virginia Polytechnic Institute and State University*. USA
- (Koh, 2014) E.Koh, N. K. Kim, J. Shin and Y.W. Kim, (2014). Polyurethane Microcapsules for Self-Healing Paint Coatings. *RSC Advances* , Vol.4, 15830-15834, <http://dx.doi.org/10.1039/C3RA41454J>.
- (Langenberg, 2010) K. V. Langenberg, P. Warden, C. Adam and H.R. Milner (2010). The durability of isocyanate-based adhesives under service in Australian conditions(Literature Review). *Forest & Wood Products Australia Limited*.
- (Latnikova, 2012) A. Latnikova, (2012). Polymeric capsules for self-healing anticorrosion coatings. PhD dissertation in physical chemistry. Faculty of mathematics and natural sciences, *the University of Potsdam*. Germany
- (Li, 2011) J.Li, M.A.J. Mazumder, H.D.H. Stover , J.M. Sherly and A.P. Hitchcock, (2011). Polyurea microcapsules: Surface modification and capsule size control. *Journal of Polymer Science, Part A: Polymer Chemistry*, Vol.49, 3038-3047. doi:10.1002/pola.24740
- (Loureiro, 2016) M. D. J. V. Loureiro, (2016). Test and Development of Microcapsules for Rigid Polyurethane Foam. MSc dissertation in technological chemistry .Faculty of chemical and biomedical sciences, *University of Lisbon*. Portugal.
- (Loureiro, 2017) M. D.J.V. Loureiro, M. J. Lourenc, A. D. Schrijver, L. F. Santos, J. C. Bordado, and A. C. Marques, (2017). Amino-silica microcapsules as effective curing agents for polyurethane foams. *Master science*. Vol.52, 5380-5389, doi: 10.1007/s10853-017-0782-6.
- (Lu, 2011) S. Lu, J. Xing, Z. Zhang, G. Jia. (2011). Preparation and Characterization of Polyurea / Polyurethane Double-Shell Microcapsules Containing Butyl Stearate Through Interfacial Polymerization. *Journal of Applied Polymer Science*, Vol.121, 3377-3383. doi:10.1002/app.33994
- (Ma, 2017) Y. Ma, Y. Jiang, H. Tan, Y. Zhang and J. Gu, (2017). A Rapid and Efficient Route to Preparation of Isocyanate Microcapsules. *Polymers*, Vol.7, 24-27. doi:10.3390/polym9070274.
- (Madaan, 2014) V. Madaan, A. Chanana, M. K. Kataria and A. Bilandi, (2014). Emulsion technology and recent trends in emulsion application. *International Research Journal of Pharmacy*, Vol.5, 533-542.
- (Ming, 2016) Y. Ming, J. Hu, J. Xing, M. Wu and J. Qu. (2016). Preparation of polyurea/melamine formaldehyde double-layered self-healing microcapsules and investigation on core fraction. *Journal of Microencapsulation*. Vol.33,307-314, doi:10.1080/02652048.2016.1178352.

- (Nguyen, 2014) L.T.T. Nguyen, X. K. D. Hillewaere, R. F. A. Teixeira, O. V. D., Berg and F. E. D. Prez. (2014). Efficient microencapsulation of a liquid isocyanate with in situ shell functionalization. *Polymer Chemistry*, Vol.6, 1159-1170, doi:10.1039/C4PY01448K.
- (Nikkola, 2014) J.Nikkola, (2014). Microcapsule-protected actives reduce leaching. *European Coatings Journal*, Vol.4, 36-40.
- (Paiva,2015) R. M. M. D. Paiva, (2015). Development of a model to predict the mechanical properties of adhesives based on the formulation. Porto:PhD dissertation in mechanical engineering, department of mechanical engineering, *Porto university*.Portugal
- (Polenz,2014) I.Polenz, S.S. Datta and D.A, Weitz, (2014). Controlling the morphology of polyurea microcapsules using microfluidics. *Langmuir*,Vol.44, 13405-13410, DOI: 10.1021/la503234z.
- (Poncelet, 2013) Poncelet, C. Perignon and G. Ongmayeb. (2013). Interfacial polymerization versus cross-linking microencapsulation. *Bioencapsulation Innovations*, 6-11.
- (Ramos,2005) B. Z.Ramos, V. Soldi, E.L. Senna, R. Borsali, (2005). Use of Natural Monomer in the Synthesis of Nano- and Microparticles of Polyurethane by Suspension-Polyaddition Technique. *Macromoleculare Symposium*, Vol.229, 234-254. doi:10.1002/masy.200551129.
- (Saihi, 2005) D.Saihi, I. Vroman, S. Giraud, S. Bourbigot, (2005). Microencapsulation of ammonium phosphate with a polyurethane shell, Part I:Coacervation technique, *Reactive and Functional Polymers*, Elsevier Ltd, Vol.64, 127-138. doi:0.1016/j.reactfunctpolym.2005.05.004
- (Salaün, 2011) F. Salaün, G. Bedek, E. Devaux, D. Dupont, L. Gengembre. (2011). Microencapsulation of a cooling agent by interfacial polymerization: Influence of the parameters of encapsulation on poly(urethane-urea) microparticles characteristics. *Journal of membrane science*,Vol.370, 23-33. doi:10.1016/j.memsci.2010.11.033
- (Serineu, 2014) A. C. S.Serineu, (2014). Microcapsules Characterization for Polyurethane One Component Foam Systems. MSc dissertation in chemical engineering, Department of chemical engineering *Instituto superior tecnico Lisboa*.Portugal
- (Shukla, 2006) P. G.Shukla, S. K. Ghosh (2006). Microencapsulation of Liquid Active Agents. *Functional Coatings: Dr. S. K. Ghosh By Polymer Microencapsulation* (pp. 153-186). WILEY-VCH Verlag GmbH & Co. KGaA, Weinheim ISBN, doi: 10.1002/3527608478.ch5
- (Silva, 2017) A. C. M. Silva, A. D. Moghadam , P. Singh, P. K. Rohatgi, (2017). Self-healing composite coatings based on in situ micro – nanoencapsulation process for corrosion protection. *Journal of Coatings Technology and Research*.Vol.14, 1-29, doi:10.1007/s11998-016-9879-0
- (Silva, 2014) E. K. Silva, M. A. A. Meireles, (2014). Encapsulation of Food Compounds Using Supercritical Technologies: Applications of Supercritical Carbon Dioxide as an Antisolvent. *Food and Public Health*, Vol.4,247-258, doi:10.5923/j.fph.20140405.06.
- (Som, 2012) I. Som, K. Bhatia, M. Yasir, (2012). Status of surfactants as penetration enhancers in transdermal drug delivery. *Journal of Pharmacy and Bioallied Sciences*.Vol.1, 2-9, doi:10.4103/0975-7406.92724
- (Sondari, 2010) D. Sondari, A. A. Septevani, A. Randy, E. Triwulandari . (2010). Polyurethane microcapsule with glycerol as the polyol component for encapsulated self healing agent. *International Journal of Engineering and Technology*, Vol.2, 446-471.
- (Sun, 2015) D. Sun, J. An, G. Wu and J. Yang. (2015). Double-layered reactive microcapsules with excellent thermal and non-polar solvent resistance for self-healing coatings. *Journal of Materials Chemistry A*,Vol.3, 4435-4444. doi:10.1039/c4ta05339g.

- (Tan, 1991) H. S. Tan, H. K. Mahabadi, (1991). Interfacial polymerization encapsulation of a viscous pigment mix: emulsification conditions and particle size distribution. *J. Microencapsulation*, Vol.4, 525-536.
- (Tadros, 2013) T.F. Tadros, (2013). Emulsion Formation, Stability, and Rheology, pp. 1-75, Wiley-VCH Verlag GmbH & Co. KGaA. doi:10.1002/9783527647941.ch1.
- (Tatiya, 2016) P. D. Tatiya, R. K. Hedao, P. P. Mahulikar, and V. V. Gite, (2016). Designing of polyamidoamine-based polyurea microcapsules containing tung oil for anticorrosive coating applications. *Journal of Coatings Technology and Research*. Vol.13, 715-726, doi:10.1007/s11998-015-9780-2.
- (Tiwari, 2011) S. Tiwari and P. Verma, (2011). Microencapsulation technique by solvent evaporation method (Study of effect of process variables). *International journal of pharmacy & life sciences*, Vol.2, 998-1005.
- (Tsuda, 2011) N. Tsuda, M. Fuji, (2011). Preparation of self-bursting microcapsules by interfacial polymerization. *Advanced Powder Technology*, Vol.23, 724-730. doi:10.1016/j.apt.2011.09.005.
- (Yang, 2008) J. Yang, M. W. Keller, J. S. Moore, S. R. White and N. R. Sottos, (2008). Microencapsulation of Isocyanates for Self-Healing Polymers, *Macromolecules*, Vol.41, 9650-9655, doi: 10.1021/ma801718v.
- (Yi, 2012) H. Yi, Y. Yang, X. Gu, J. Huang and C. W. Huan, (2012). Multilayer composite microcapsule synthesized by Pickering emulsion templates and its application in self-healing coating. *Journal of Materials Chemistry A*, Vol.3, 13749-13757. doi:10.1039/x0xx00000x.
- (Zafar, 2012) F. Zafar, E. Sharmin, (2012). Polyurethane, Ch.1 Published by InTech. Croatia, <http://dx.doi.org/10.5772/51663>.
- (Zhang, 2009) H. Zhang, X. Wang, (2009). Synthesis and properties of microencapsulated n-octadecane with polyurea shells containing different soft segments for heat energy storage and thermal regulation. *Solar Energy Materials and Solar Cells*, Vol.93, 1366-1376. doi:10.1016/j.solmat.2009.02.021.





## Appendix A-FTIR spectrums

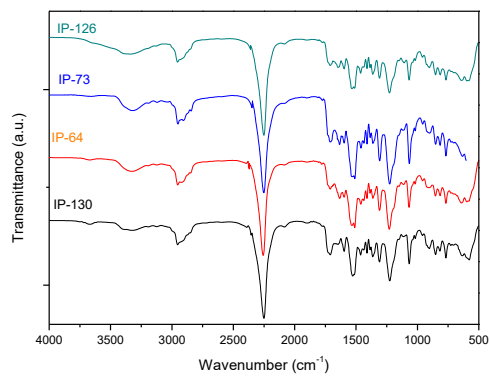


Figure A.1 FTIR for IP-130, 64, 73, 126

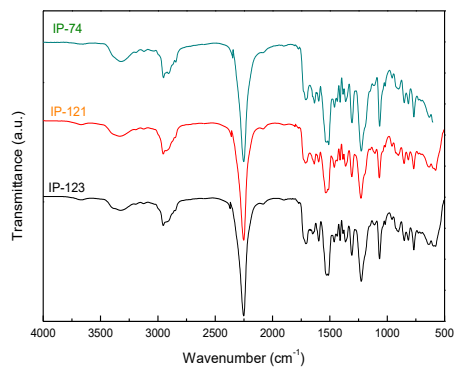


Figure A.2 FTIR for IP-74, 121, 123

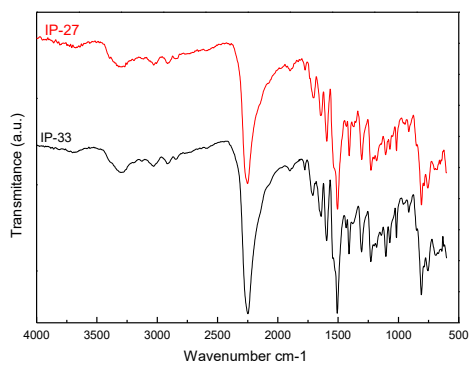


Figure A.3 FTIR for IP-27, 33

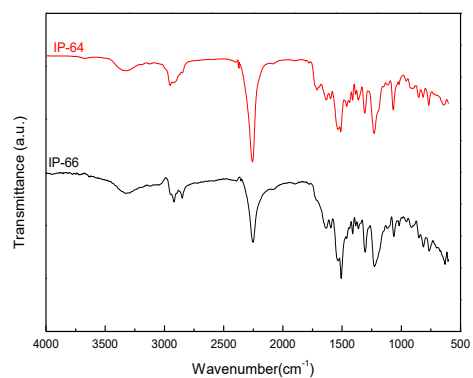


Figure A.4 FTIR for IP-64,66

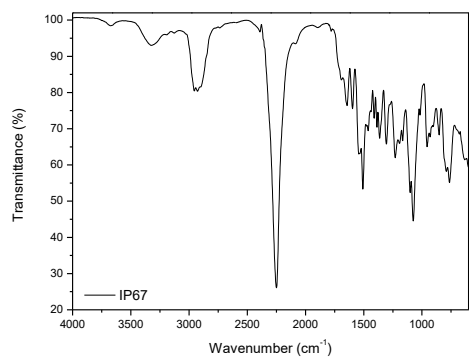


Figure A.5 FTIR for IP-67

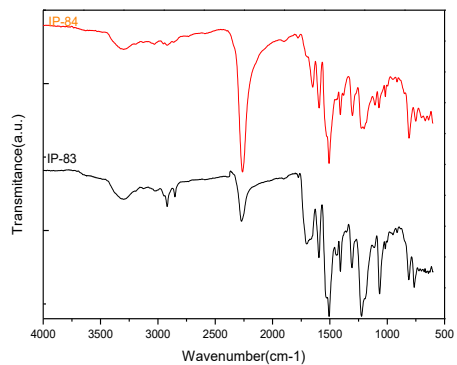


Figure A.6 FTIR for IP-83, 84

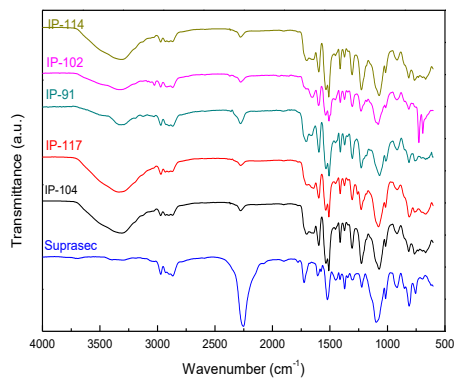


Figure A.7 FTIR for Suprasec 2234, IP-91, IP-102, IP-104, IP-117 & IP-114

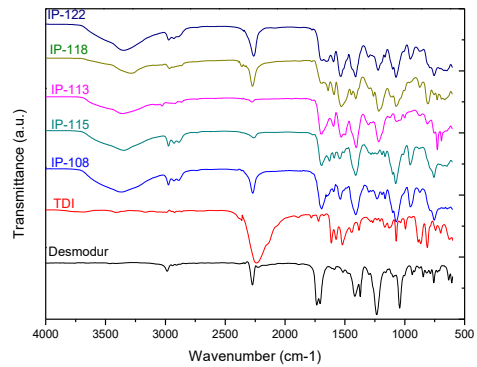


Figure A.8 FTIR for Desmodur RC, TDI, IP-108, IP-113, IP-115, IP-118 and IP-122

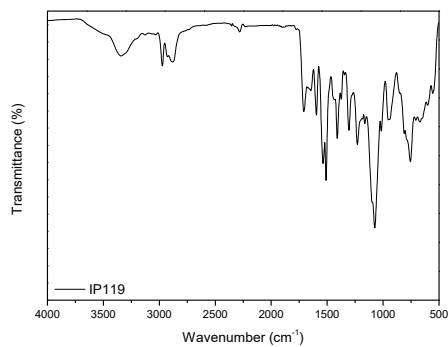


Figure A.9 FTIR for IP-119

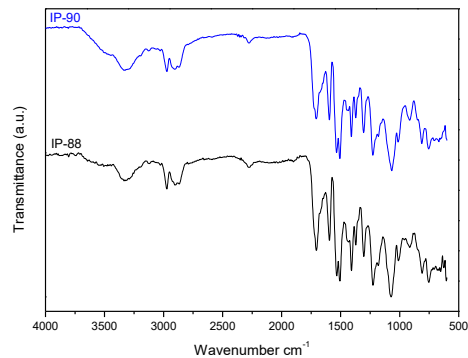


Figure A.10 FTIR for IP-88, IP-90

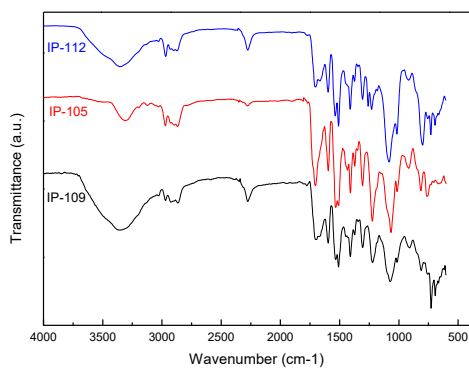


Figure A.11 FTIR for IP-105, IP-109 and IP-112

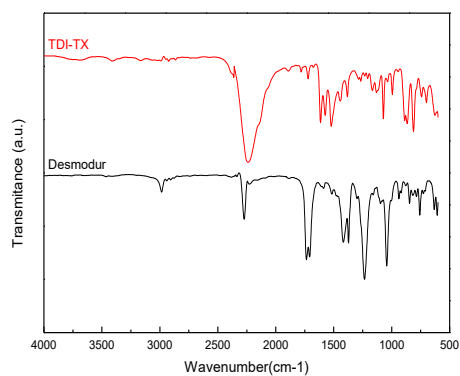


Figure A.12 FTIR for TDI-TX and Desmodur RC

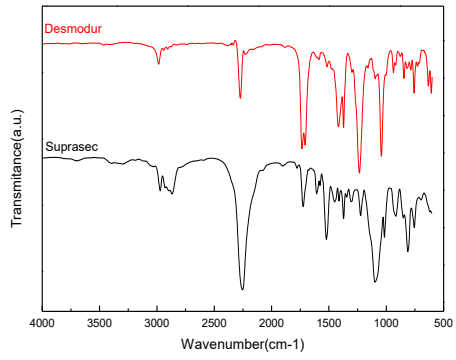


Figure A.13 FTIR for Desmodur RC and Suprasec 2234

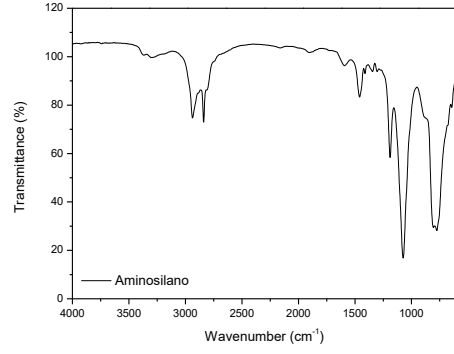


Figure A.14 FTIR for Aminosilane

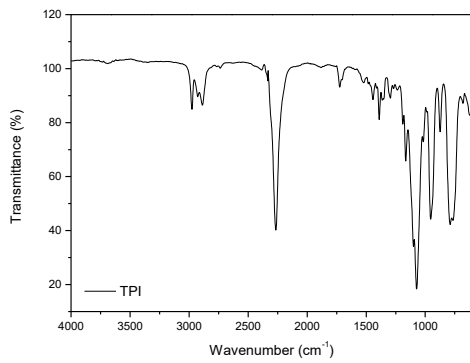


Figure A.15 FTIR for TPI

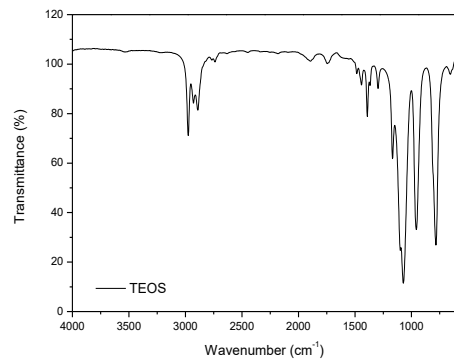


Figure A.16 FTIR for TEOS

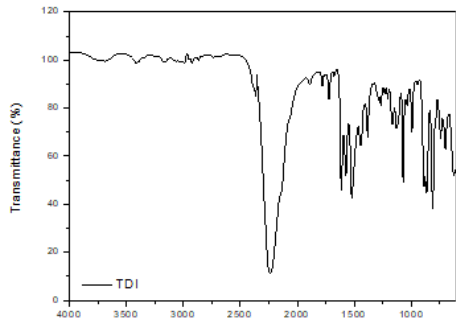


Figure A.17 FTIR for TDI-TX

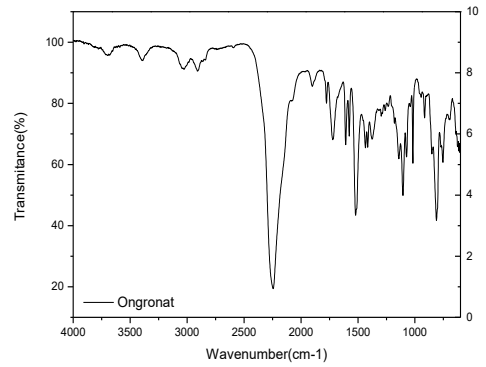


Figure A.18 FTIR for Ongronat

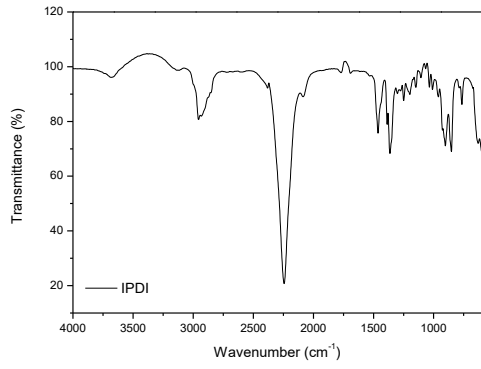


Figure A.19 FTIR for IPDI

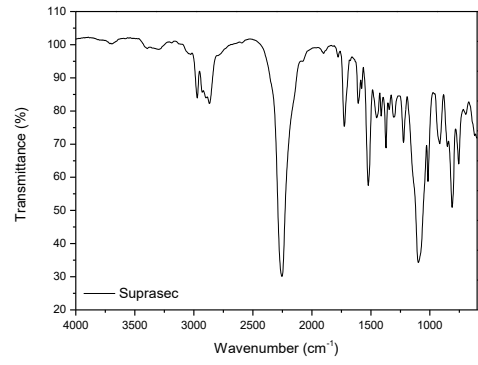


Figure A.20 FTIR for Suprasec 2234

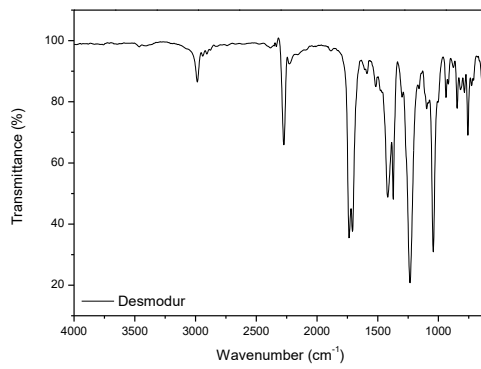


Figure A.21 FTIR for Desmodur RC

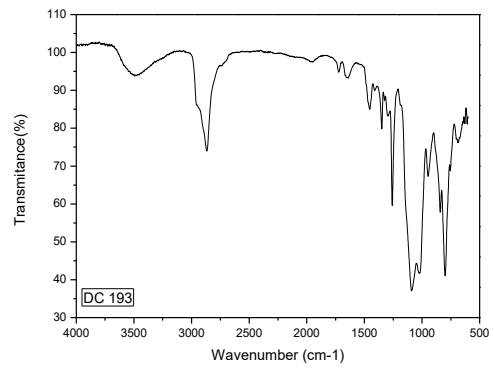


Figure A.22 FTIR for DC 193

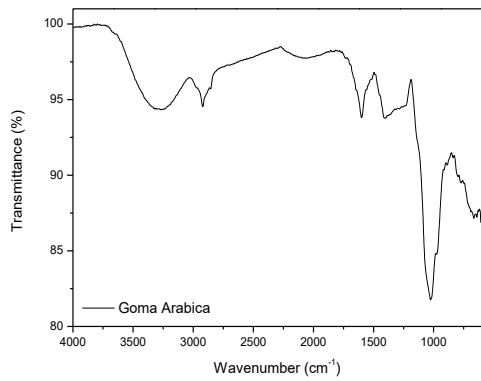


Figure A.23 FTIR for Gum Arabic

## Appendix B-History of the synthesis

Table B1-History of the syntheses

Synthesis Category	Organic Phase(s)	Aqueous Phase	Active H source	Solvent
Group1	Ongronat	Water +DC 193 Water +GA	EDA	None
Group 2	Ongronat + IPDI	Water +GA	Hexamethyldiamine Aminosilane EDA DETA Diethyl glycol Aminosilane +TEOS	None
Group 3	Ongronat + IPDI+TPI	Water +GA		
Group 4	Ongronat + TDI	Water +GA	Glycerol Aminosilane +TEOS DETA	Toluene n-Hexane
Group 5	Suprasec 2234	Water +GA Water +GA +Gela- tine	1,6 Hexanediol	Toluene n-Hexane Acetone MEK
Group 6	Suprasec 2234+TPI	Water +GA		Toluene
Group 7	Desmodur RC	Water +GA		
Group 8	Desmodur RC+TPI	Water +GA		
Group 9	Desmodur RC+TDI	Water +GA		Toluene MEK
Group 10	Desmodur RC+TDI+TPI	Water +GA		MEK
Group 11	Suprasec 2234+Desmodur RC+(TPI)	Water +GA	1,6 Hexanediol Aminosilane DETA Baysilon Gelatine	Toluene n-Hexane Acetone MEK
Group 12	Suprasec 2234+PS solution Suprasec 2234+PCL solu- tion	Water +GA		Toluene Acetone DCM MEK